In vitro Realisation of the Hydroxypropionyl-CoA/Acrylyl-CoA Cycle

Dissertation
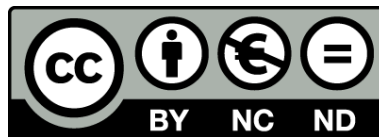
Zur
Erlangung des Doktorgrades
der Naturwissenschaften
(Dr. rer. nat.)

Dem Fachbereich Biologie
der Philipps-Universität Marburg
vorgelegt von

Richard McLean
aus Winnipeg, Manitoba, Kanada

Marburg/Lahn, Deutschland, 2022

Die Untersuchungen zur vorliegenden Arbeit wurden von Oktober 2017 bis April 2022 unter der Betreuung von Herrn Dr. Tobias Jürgen Erb in Marburg am Max-Planck-Institut für terrestrische Mikrobiologie in der Abteilung „Biochemistry and Synthetic Metabolism" durchgeführt.

Vom Fachbereich Biologie

der Philipps-Universität Marburg als Dissertation

angenommen am: 05.09.2022

Erstgutachter: Prof. Dr. Tobias Erb

Zweitgutachter: Prof. Dr. Lennart Randau

Weitere Mitglieder der Prüfungskommission:

Prof. Dr. Martin Thanbichler

Prof. Dr. Lars-Oliver Essen

Tag der mündlichen Prüfung: 14.10.2022

Erklärung

Ich versichere, dass ich meine Dissertation mit dem Titel „**In vitro Realisation of the Hydroxypropionyl-CoA/Acrylyl-CoA Cycle**" selbstständig ohne unerlaubte Hilfe angefertigt und mich dabei keiner anderen als der von mir ausdrücklich bezeichneten Quellen und Hilfsmittel bedient habe.

Diese Dissertation wurde in der jetzigen oder einer ähnlichen Form noch bei keiner anderen Hochschule eingereicht und hat noch keinen sonstigen Prüfungszwecken gedient.

Marburg, den 02. Mai 2022

Richard James McLean

*'**Isn't it a shame that with the tremendous amount of work you have done you haven't been able to get any results?**'*

Edison turned on me like a flash, and with a smile replied:

*'**Results! Why, man, I have gotten a lot of results! I know several thousand things that won't work.**'*

Edison, His Life and Inventions
Frank Lewis Dyer and Thomas Commerford Martin, 1910

Table of Contents

Summary

The birth of the industrial revolution initiated a significant shift in the global carbon cycle. In the intervening centuries, the production of anthropogenic atmospheric carbon rose dramatically and has resulted in a pronounced climactic shift. The rate of this change is accelerating, largely irreversible in the short-term, and is expected to have a profound negative impact on nearly every aspect of human life from culture and economics to mental and physical health. It is now generally recognised that past practices are unsustainable and that we must take immediate action if we are to ameliorate this problem. Global efforts to reduce carbon emissions have begun, and many novel technologies are currently being developed both to make manufacturing more efficient and to actively remove carbon from the atmosphere.

Despite these efforts, average atmospheric CO_2 concentrations have continued to rise, and the climate has continued to change. While a multitude of different methods will be required if we are to be successful in reducing global atmospheric carbon, an intriguing approach is generating designer organisms capable of fixing CO_2. Natural carbon fixation is the cornerstone of organic life, but there are potential improvements that could be made to generate more efficient carbon-fixing organisms. In addition to removing atmospheric CO_2, the carbon can potentially be funnelled into any number of value-added products.

In this work, we have pursued the artificial Hydroxypropionyl-CoA/Acrylyl-CoA Cycle in an in vitro system. We aim to demonstrate that the cycle is functional at ambient temperature and in the presence of oxygen making it an appealing candidate for future in vivo engineering efforts. In the first part, we investigate the oxidative portion of the cycle which involves the conversion of (2S)-methylmalonyl-CoA to malonyl-CoA. Originally this involved chemistry analogous to the TCA cycle, however due to difficulties with multiple steps of this pathway, we introduced a novel bypass that directly oxidises succinyl-CoA to the metabolically unusual fumaryl-CoA. This portion of the cycle also includes the first carbon-fixing reaction, the ATP-dependent carboxylation of acetyl-CoA.

In the second part, we evaluate the reductive portion of the cycle which involves the conversion of malonyl-CoA back to (2S)-methylmalonyl-CoA. This portion involves three reduction reactions and we explored two potential pathways going through either 3-hydroxypropionyl-CoA or β-alanyl-CoA. While both versions are functional, the lack of β-alanine-specific enzymes, especially a β-alanyl-CoA synthetase made the 3-hydroxypropionyl-CoA pathway more practical. In either case, this portion terminates with the reductive carboxylation of acrylyl-CoA to (2S)-methylmalonyl-CoA.

Finally, these pathways were combined to yield a continuous cycle. After flux through the cycle was achieved, we sought to resolve a variety of resultant issues including regeneration of ATP and NADPH, elimination of reactive oxygen species, protection from coenzyme B_{12} radical inactivation, regeneration of FAD-dependent enzymes, and the repair of chemically modified cofactors. The current HOPAC cycle was found to produce ~500 µM glycolate, or five CO_2-equivalents per molecule of acetyl-CoA.

Overall, in this work we established the HOPAC cycle, a new-to-nature synthetic CO_2-fixation pathway, in vitro and further optimised its functioning. This works provides another proof-of-principle for synthetic CO_2-fixation and opens the path for implementation of HOPAC in natural and synthetic cells in the future.

Zusammenfassung

Mit dem Beginn der industriellen Revolution hat sich der globale Kohlenstoffkreislauf erheblich verändert. In den dazwischen liegenden Jahrhunderten stieg die Produktion von anthropogenem atmosphärischem Kohlenstoff dramatisch an und hat zu einer ausgeprägten klimatischen Veränderung geführt. Dieser Wandel beschleunigt sich, ist kurzfristig weitgehend unumkehrbar und wird voraussichtlich tiefgreifende negative Auswirkungen auf nahezu alle Aspekte des menschlichen Lebens haben, von der Kultur über die Wirtschaft bis hin zur geistigen und körperlichen Gesundheit. Es ist inzwischen allgemein anerkannt, dass die bisherigen Praktiken nicht nachhaltig sind und dass wir unverzüglich Maßnahmen ergreifen müssen, wenn wir dieses Problem verringern wollen. Es wurden weltweite Anstrengungen zur Verringerung der Kohlenstoffemissionen unternommen, und es werden derzeit viele neue Technologien entwickelt, um die Produktion effizienter zu gestalten und Kohlenstoff aktiv aus der Atmosphäre zu entfernen.

Trotz dieser Bemühungen ist die durchschnittliche CO_2-Konzentration in der Atmosphäre weiter angestiegen, und das Klima hat sich weiter verändert. Wenn wir den globalen atmosphärischen Kohlenstoffgehalt erfolgreich reduzieren wollen, ist eine Vielzahl verschiedener Methoden erforderlich. Ein interessanter Ansatz ist die Entwicklung von Designerorganismen, die CO_2 binden können. Die natürliche Kohlenstoffbindung ist der Eckpfeiler des organischen Lebens, aber es gibt potenzielle Verbesserungen, die vorgenommen werden könnten, um effizientere kohlenstoffbindende Organismen zu erzeugen. Neben der Beseitigung von atmosphärischem CO_2 kann der Kohlenstoff potenziell in eine beliebige Anzahl von Produkten mit Mehrwert umgewandelt werden.

In dieser Arbeit haben wir den künstlichen Hydroxypropionyl-CoA/Acrylyl-CoA-Zyklus in einem In-vitro-System untersucht. Wir wollen zeigen, dass der Zyklus bei Umgebungstemperatur und in Gegenwart von Sauerstoff funktioniert, was ihn zu einem attraktiven Kandidaten für künftige In-vivo-Entwicklungen macht. Im ersten Teil untersuchen wir den oxidativen Teil des Zyklus, der die Umwandlung von (2S)-Methylmalonyl-CoA in Malonyl-CoA beinhaltet. Ursprünglich geschah dies analog zum TCA-Zyklus, doch aufgrund von Schwierigkeiten mit mehreren Schritten dieses Weges haben wir einen neuartigen Bypass eingeführt, der Succinyl-CoA direkt zu dem metabolisch ungewöhnlichen Fumaryl-CoA oxidiert. Dieser Teil des Zyklus umfasst auch die erste kohlenstoffbindende Reaktion, die ATP-abhängige Carboxylierung von Acetyl-CoA.

Im zweiten Teil bewerten wir den reduktiven Teil des Zyklus, der die Rückumwandlung von Malonyl-CoA in (2S)-Methylmalonyl-CoA beinhaltet. Dieser Teil umfasst drei Reduktionsreaktionen, und wir haben zwei mögliche Wege untersucht, die entweder über 3-Hydroxypropionyl-CoA oder β-Alanyl-CoA verlaufen. Beide Varianten sind zwar funktionell, aber das Fehlen von β-Alanin-spezifischen Enzymen, insbesondere einer β-Alanyl-CoA-Synthetase, machte den 3-Hydroxypropionyl-CoA-Weg praktischer. In jedem Fall endet dieser Abschnitt mit der reduktiven Carboxylierung von Acrylyl-CoA zu (2S)-Methylmalonyl-CoA.

Schließlich wurden diese Wege kombiniert, um einen kontinuierlichen Zyklus zu erhalten. Nachdem der Fluss durch den Zyklus erreicht war, versuchten wir, eine Reihe von daraus resultierenden Problemen zu lösen, darunter die Regeneration von ATP und NADPH, die Beseitigung reaktiver Sauerstoffspezies, den Schutz vor der radikalen Inaktivierung von Coenzym B_{12}, die Regeneration von FAD-abhängigen Enzymen

und die Reparatur chemisch veränderter Cofaktoren. Der aktuelle HOPAC-Zyklus produziert ~500 µM Glykolat oder fünf CO_2-Äquivalente pro Acetyl-CoA-Molekül.

Insgesamt haben wir in dieser Arbeit den HOPAC-Zyklus, einen in der Natur neuartigen synthetischen CO_2-Fixierungsweg, in vitro etabliert und seine Funktionsweise weiter optimiert. Damit haben wir einen weiteren Grundsatzbeweis für die synthetische CO_2-Fixierung erbracht und den Weg für die künftige Implementierung von HOPAC in natürlichen und synthetischen Zellen geebnet.

Publications

Schwander, T., **McLean, R.**, Zarzycki, J., & Erb, T. J. (2018). Structural basis for substrate specificity of methylsuccinyl-CoA dehydrogenase, an unusual member of the acyl-CoA dehydrogenase family. Journal of Biological Chemistry, 293(5), 1702-1712.

Burgener, S., Luo, S., **McLean, R.**, Miller, T. E., & Erb, T. J. (2020). A roadmap towards integrated catalytic systems of the future. Nature Catalysis, 3(3), 186-192.

Miller, T. E., Beneyton, T., Schwander, T., Diehl, C., Girault, M., **McLean, R.**, Chotel, T., Claus, P., Cortina, N. C., Baret, J. C., & Erb, T. J. (2020). Light-powered CO2 fixation in a chloroplast mimic with natural and synthetic parts. Science, 368(6491), 649-654.

McLean, R. & Erb, T. J. et al. (2022) In vitro Realisation of the Hydroxypropionyl-CoA/Acrylyl-CoA Cycle. In Preparation.

1. Introduction

1.1. Global Atmospheric Carbon

The global carbon cycle is a complex network of carbon-containing reactions including the dissolution and outgassing of carbon from oceans, dissipation into the atmosphere, retention in soils and seafloor sediments, sequestration in limestone and its derivatives, fixation by autotrophs, cellular respiration, and decomposition of detritus (Battin, 2009). The cycle operates slowly and is relatively static over million-year time frames in the absence of large-scale perturbations (Berner, 2003).

The mid-eighteenth century marked the beginning of the industrial revolution and initiated the period of the most dramatic change our species has ever caused on this planet. As technology improved, the demand for fossil fuels escalated, leading to a precipitous increase in the production of waste carbon dioxide. CO_2 is a compound that contributes to the greenhouse effect, a process whereby radiatively active gases in the atmosphere such as methane, water vapour, and halocarbons absorb long-wave radiation and emit it back to the surface. The global mean temperature of Earth is expected to be ~255K without the greenhouse effect (Kaushika, 2016), making it essential for modern terrestrial life, but as greenhouse gases accumulate in the atmosphere, the effect is magnified causing a rise in the global mean temperature. At the onset of the revolution, atmospheric CO_2 was ~280 ppm, currently, atmospheric CO_2 has reached ~420 ppm (Mauna Loa, 2022), the highest level in millions of years (Pagini, 2010). It is well understood that atmospheric CO_2 contributes to planetary warming, and the annual anthropogenic CO_2 emissions have reached 37.4 ± 2.9 $GtCO_2$ (Friedlingstein, 2022). Currently, nearly half of anthropogenic carbon is retained in the atmosphere (Canadell, 2007).

There are a variety of knock-on effects from global warming including deglaciation (Liu, 2019), permafrost melt (Farquharson, 2019), rising sea levels (Nerem, 2018) as well as acidification and deoxygenation of oceans (Heinze, 2021), loss of biodiversity which has triggered the beginning of the sixth mass extinction (Bello, 2015), and a significant loss of population genetic diversity of remaining species (Leigh, 2019). In addition to these generally undesirable effects, there are also multiple positive feedback loops inherent to global warming including feedback from loss of ice albedo (Riihelä, 2021), ocean and atmospheric heat transport feedback (Mahlstein, 2011; Alexeev, 2013), loss of sequestered CO_2 from melting permafrost (Kypke, 2021), and water vapour feedback (Sherwood, 2018). The cumulative effect of these feedback loops emphasises the long-term compound impact our current actions will have on long term trends. As of the twenty-first session of the Conference of the Parties in Paris in 2015, 196 international parties have

agreed to take steps to limit global warming to 2.0°C above the pre-industrial average temperature, with ambitions to limit warming to 1.5°C (Horowitz, 2016).

Largely in response to the restrictive effect of the COVID-19 pandemic, global CO_2 emissions decreased by about 2.6 $GtCO_2eq$ in 2020, an unprecedented reduction (Le Quéré, 2021). In spite of this surpassing even our most ambitious goals for the year, we are still on track for a global mean temperature increase of 2.7°C by the end of the century, overshooting our modest goal of 2.0°C (Zhongming, 2021). This taken with the trend of CO_2 emissions rebounding after historic drops (Li, 2021) underlines the severity of the problem faced. Now more than ever, we require an all-hands-on-deck approach to decrease carbon emissions and sequester atmospheric carbon on a mass scale.

While a multitude of different methods will be required if we are to be successful in reducing global atmospheric carbon, an intriguing approach is developing designer organisms capable of enhanced CO_2 fixation. In addition to removing atmospheric CO_2, the carbon can potentially be funnelled into synthetic pathways to produce any number of value-added products. Natural carbon fixation is the cornerstone of organic life, but there are potential improvements that could be made to generate more efficient carbon-fixing organisms.

Natural metabolic cycles capable of assimilating inorganic carbon have been identified in all domains of life and in very diverse environments. Creating synthetic pathways involves recombining natural pathways, incorporating reactions from non-autotrophic species, and/or engineering enzymes to perform novel reactions. When designing cycles, factors such as the oxygen sensitivity of certain enzymes, or their reliance on extreme temperatures must be taken into account when examining the feasibility of their use in engineered systems. A cycle that is only functional at 95°C or in strict anoxic conditions is unlikely to be of much use in an engineered plant, for example. In the next sections, I will discuss several natural and synthetic carbon fixation cycles. First, I will discuss natural cycles, and delineate oxygen sensitivity from oxygen tolerance as well as thermal dependence. I will then discuss several synthetic cycles and highlight the HOPAC cycle which is the focus of this work.

1.2.   Natural Carbon Fixing Cycles

1.2.1. Oxygen-Sensitive Carbon Fixation

1.2.1.1.   *Dicarboxylate/4-Hydroxybutyrate Cycle*

The Dicarboxylate/4-Hydroxybutyrate Cycle (DC4HBC), (Huber, 2008) fixes two molecules of CO_2 and generates one molecule of acetyl-CoA (Figure. 1.1.). In the first fixation, acetyl-CoA is reductively

carboxylated by pyruvate synthase (EC 1.2.7.1) to pyruvate and CoA at the expense of two reduced ferredoxin, effectively limiting this cycle to anaerobic conditions. The second fixation is performed by PEP carboxylase (EC 4.1.1.31) converting phosphoenolpyruvate and bicarbonate to oxaloacetate.
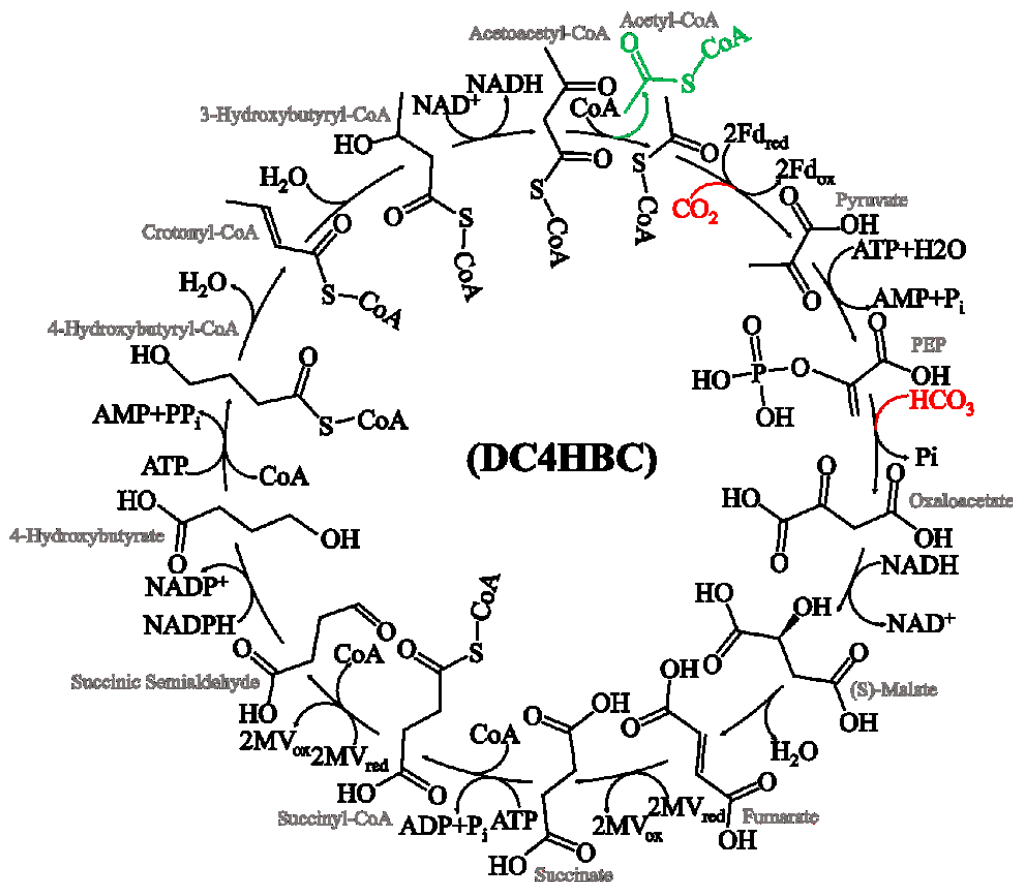
Figure. 1.1. The Dicarboxylate/4-Hydroxybutyrate Cycle, an oxygen-sensitive cycle that fixes two molecules of CO_2 and produces acetyl-CoA. Adapted from Huber, 2008.

1.2.1.2.   Reductive Tricarboxylic Acid Cycle

The Reductive Tricarboxylic Acid Cycle (RTCAC, Arnon-Buchanan cycle), (Evans, 1966) fixes one molecule of CO_2 and one molecule of bicarbonate and generates one molecule of acetyl-CoA (Figure. 1.2.). The first fixation utilises 2-oxoglutarate synthase (EC 1.2.7.3) which converts succinyl-CoA and CO_2 to 2-oxoglutarate and CoA at the expense of two reduced ferredoxin, effectively limiting this cycle to anaerobic conditions. The second fixation is performed by isocitrate dehydrogenase (EC 1.1.1.41/42) which reductively carboxylates 2-oxoglutarate to isocitrate at the expense of NAD(P)H.
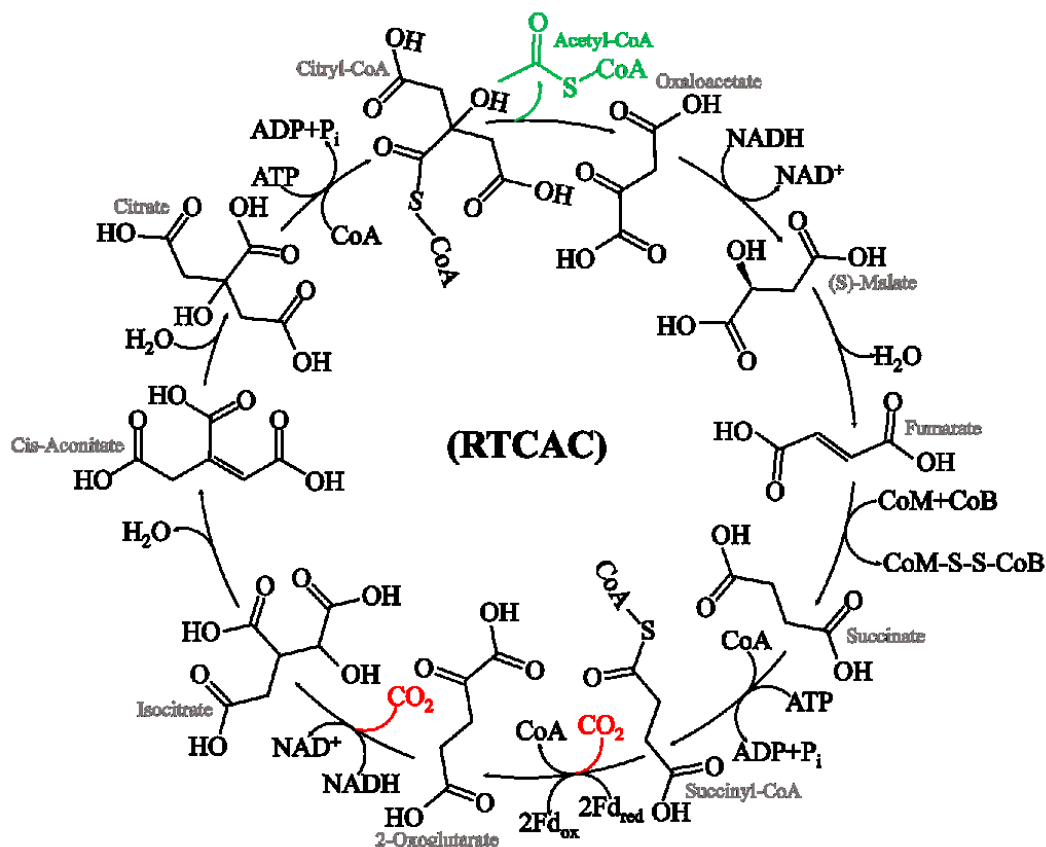
Figure. 1.2. The Reductive Tricarboxylic Acid Cycle, an oxygen-sensitive cycle that fixes CO_2 and bicarbonate and produces acetyl-CoA. Adapted from Hügler, 2005.

1.2.1.3.   Reductive Acetyl-CoA Pathway

The Reductive Acetyl-CoA Pathway (RACP, Wood-Ljungdahl Pathway), (Ljungdhal, 1986) fixes one molecule of CO_2, one molecule of formate, generates one molecule of acetyl-CoA (Figure. 1.3.), and is the most energetically efficient carbon fixation pathway known (Song, 2020). In the first fixation, tetrahydrofolate is formylated by Formate:tetrahydrofolate ligase (EC 6.3.4.3) generating 10-Formyltetrahydrofolate at the expense of ATP. In the second fixation, CO-methylating acetyl-CoA synthase (EC 2.3.1.169) synthesises acetyl-CoA from CO, CoA, and a methyl-Co(III) corrinoid Fe-S protein. This cycle utilises reduced ferredoxin and iron-sulfur centers rendering it sensitive to oxygen.
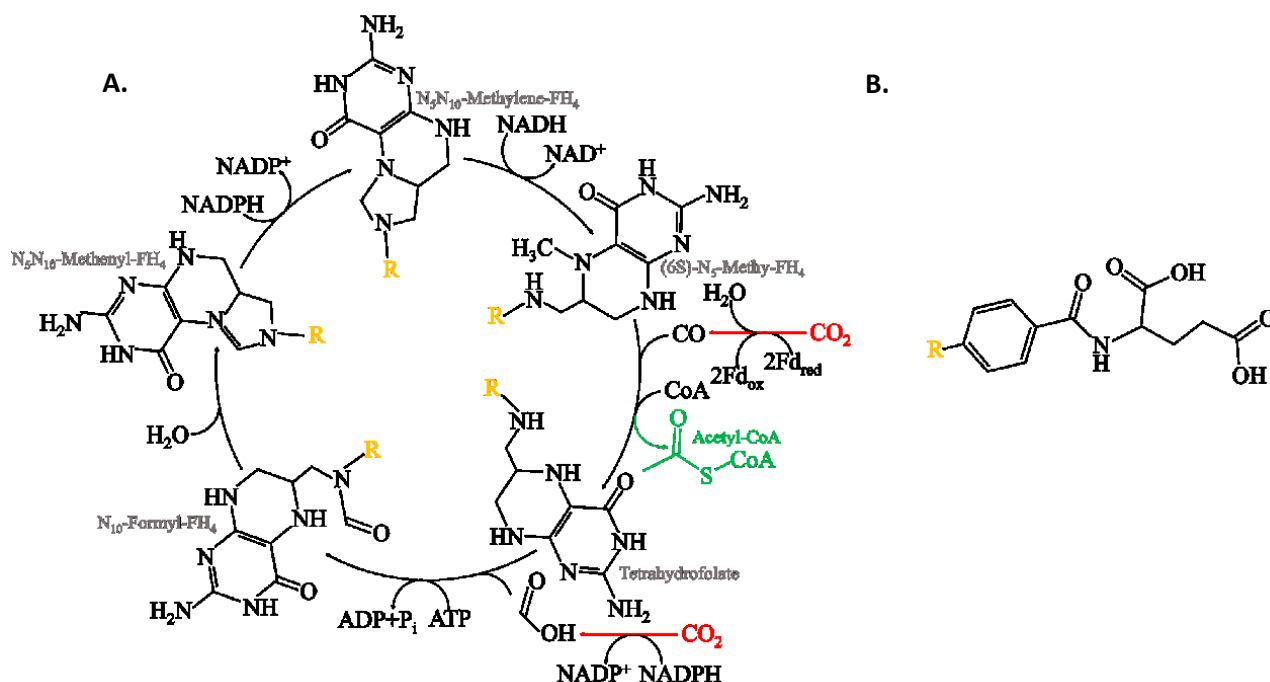
Figure. 1.3. **A.** The Reductive Acetyl-CoA Pathway, the most energetically efficient carbon fixing pathway. The cycle fixes CO_2 and generates acetyl-CoA. **B.** The unmodified P-Aminobenzoyl-L-Glutamate designated by a yellow R in the first panel.

1.2.2. Oxygen-Tolerant Carbon Fixation

1.2.2.1. 3-Hydroxypropionate/4-Hydroxybutyrate Cycle

The 3-Hydroxypropionate/4-Hydroxybutyrate Cycle (3HP/4HBC), (Berg, 2007) fixes two molecules of bicarbonate, generates one molecule of acetyl-CoA (Figure. 1.4.), and is the most energetically efficient aerobic cycle known (Könneke, 2014). In the first fixation, propionyl-CoA carboxylase (EC 6.4.1.3) converts propionyl-CoA and bicarbonate to (2S)-methylmalonyl-CoA at the expense of ATP. In the second fixation, a similar reaction performed by acetyl-CoA carboxylase (EC 6.4.1.2) converts acetyl-CoA and bicarbonate to malonyl-CoA at the expense of ATP. This cycle is oxygen tolerant and has been found in mesophilic *Thaumarchaeota*.
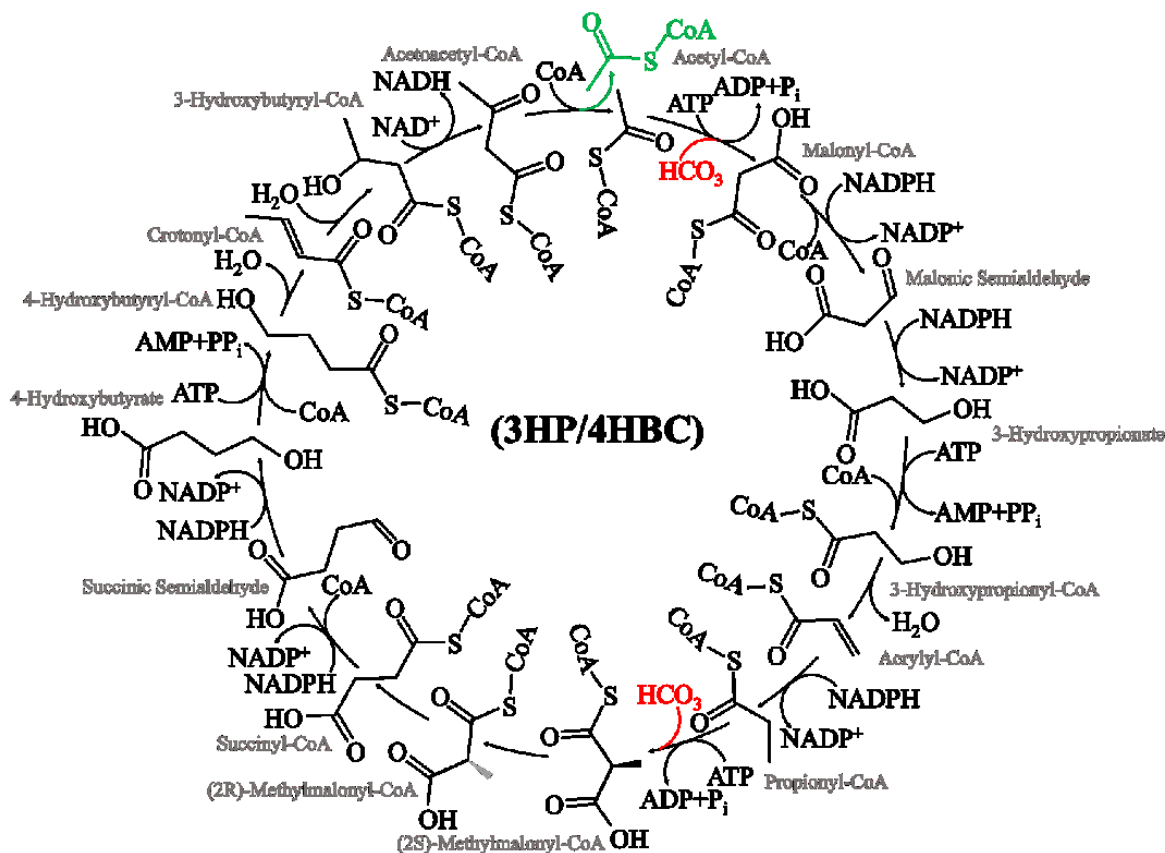
Figure. 1.4. The 3-Hydroxypropionate/4-Hydroxybutyrate Cycle, the most energetically efficient oxygen-tolerant cycle, fixes bicarbonate and generates acetyl-CoA. Adapted from Berg, 2007.

1.2.2.2.   3-hydroxypropionate Bicycle

The 3-hydroxypropionate Bicycle (3HPB), (Zarzycki, 2009) utilises the same carboxylation reactions as 3HP/4HBC and as such, fixes two molecules of bicarbonate (Figure. 1.5.). The subsequent chemistry diverges however, and the product is one molecule of pyruvate. Like the 3HP/4HBC, none of the reactions are oxygen sensitive, however the cycle thus far has only been identified in the thermophilic *Chloroflexaceae*.
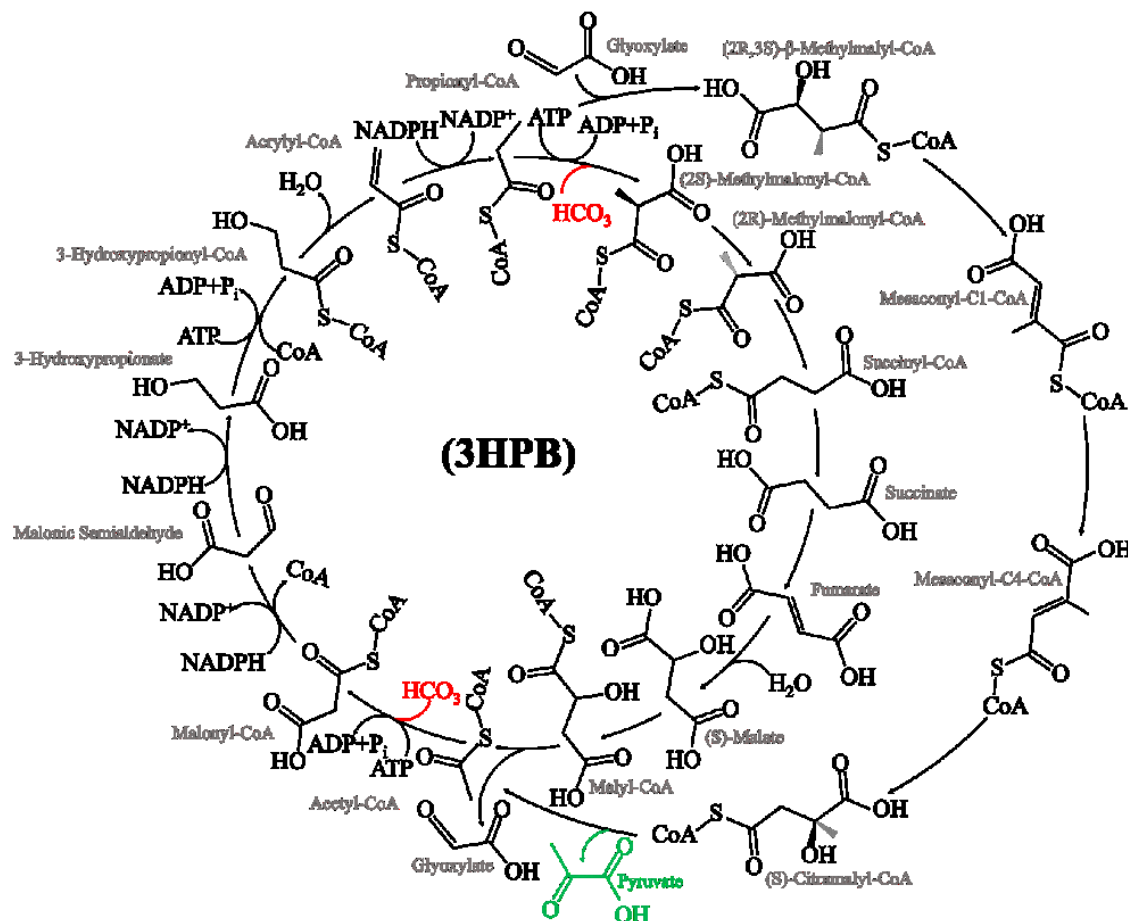
Figure. 1.5. The 3-hydroxypropionate Bicycle, an oxygen-tolerant duel cycle that fixes bicarbonate and generates glyoxylate in the first cycle, then converts the glyoxylate to pyruvate in the second cycle. Adapted from Zarzycki, 2009.

1.2.2.3.   Reductive Pentose Phosphate Cycle

The Reductive Pentose Phosphate Cycle (RPPC, Calvin-Benson-Bassham Cycle), (Bassham, 1960) is by far the most common, making use of ribulose-1,5-bisphosphate carboxylase/oxygenase (RuBisCO) (Figure. 1.6.) which has been proposed to be the most common enzyme in the world (Ellis, 1979)
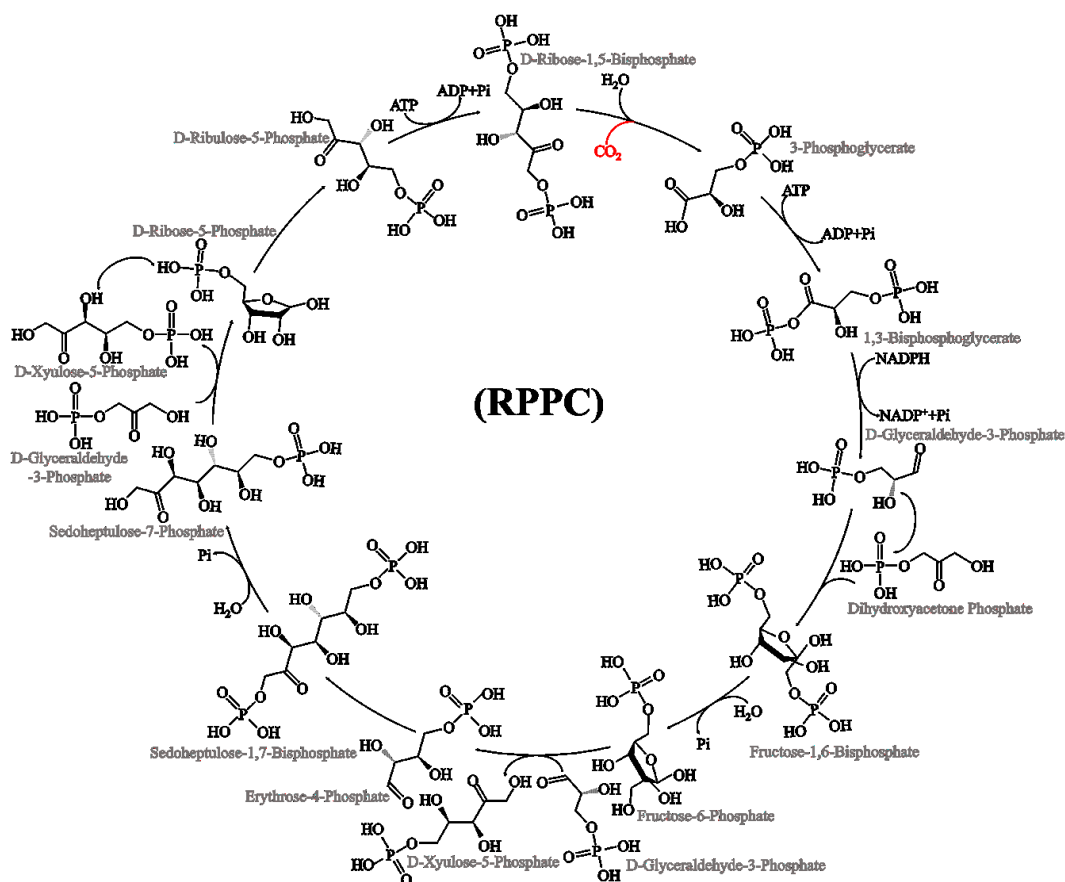
Figure. 1.6. The Reductive Pentose Phosphate Cycle, which utilises RuBisCO, the most prevalent enzyme on the planet. While oxygen-tolerant, it is inhibited by O_2, and has a side activity on O_2.

In spite of its prevalence in the global ecosystem, there are multiple drawbacks to using RuBisCO in terms of optimal carbon fixation. First, it is an average enzyme with regard to reaction rate (Bathellier, 2018) and is outperformed by several other carboxylating enzymes including many reductive carboxylases and PEP carboxylase. Second, RuBisCO is competitively inhibited by O_2 (Tamiya, 1949), thought to be an evolutionary relic from a time with lower atmospheric O_2 concentration. Finally, as the name implies, RuBisCO not only performs carboxylation, but is also capable of performing oxygenation in the presence of molecular O_2 (Benson, 1951). The result of oxygenation is the generation of 2-phosphoglycolate, a toxic byproduct. 2-phosphoglycolate must then be metabolised in photorespiration (Figure. 1.7.) which results in the loss of a fixed CO_2, NH_3, and additional energy expenditure.

Figure. 1.7. Photorespiration. When RuBisCO performs oxygenation, 2-phosphoglycolate is generated and must be recycled. Photorespiration serves this purpose at the expense of ATP and previously fixed CO_2 and ammonia.

Although the RPPC cycle is limited by RuBisCO, RTCAC, RAPC, and DC4HBC are oxygen sensitive while 3HPB has only been identified in thermophiles. This relegates most known naturally occurring carbon fixation cycles to relatively extreme environments allowing the Calvin Benson Cycle to dominate. 3HP/4HBC is the exception to this being both oxygen tolerant and found in mesophilic *Thaumarchaeota. Thaumarchaeota* are a wildly successful phylum of archaea found in both terrestrial (Lu, 2017) and marine environments ranging from mountain lakes (Auguet, 2013) to the deepest depths of the ocean (Zhong, 2020). The pervasive nature of this phylum might hint at the potential utility of other aerobic, mesophilic cycles.

1.3. Synthetic Carbon Fixation

In recent years, efforts to design and realise synthetic carbon fixing cycles exploiting natural and engineered enzymes have begun. The field is still very much in its youth, but the following early successes

demonstrate that novel pathways exploring chemistries unutilised by evolution can be fruitful and are worth pursuing.

1.3.1. The Crotonyl-CoA/Ethylmalonyl-CoA/Hydroxybutyryl-CoA Cycle

The crotonyl-CoA/ethylmalonyl-CoA/hydroxybutyryl-CoA (CETCH) cycle (Schwander, 2016) utilises two reductive carboxylation steps performed by crotonyl-CoA carboxylase/reductase (Ccr) (EC 1.3.1.85) and generates one molecule of glyoxylate (Figure. 1.8.). First, crotonyl-CoA is carboxylated to (2S)-ethylmalonyl-CoA at the expense of NADPH, second, acrylyl-CoA is carboxylated to (2S)-methylmalonyl-CoA oxidising another NADPH. This cycle is oxygen tolerant and mesophilic. The cycle combines chemistry converting (2S)-methylmalonyl-CoA to crotonyl-CoA from 3HP/4HBC and chemistry linking crotonyl-CoA to propionyl-CoA from the ethylmalonyl-CoA pathway (Erb, 2007) with an engineered propionyl-CoA oxidase which converts propionyl-CoA to acrylyl-CoA which is then carboxylated to close the cycle.
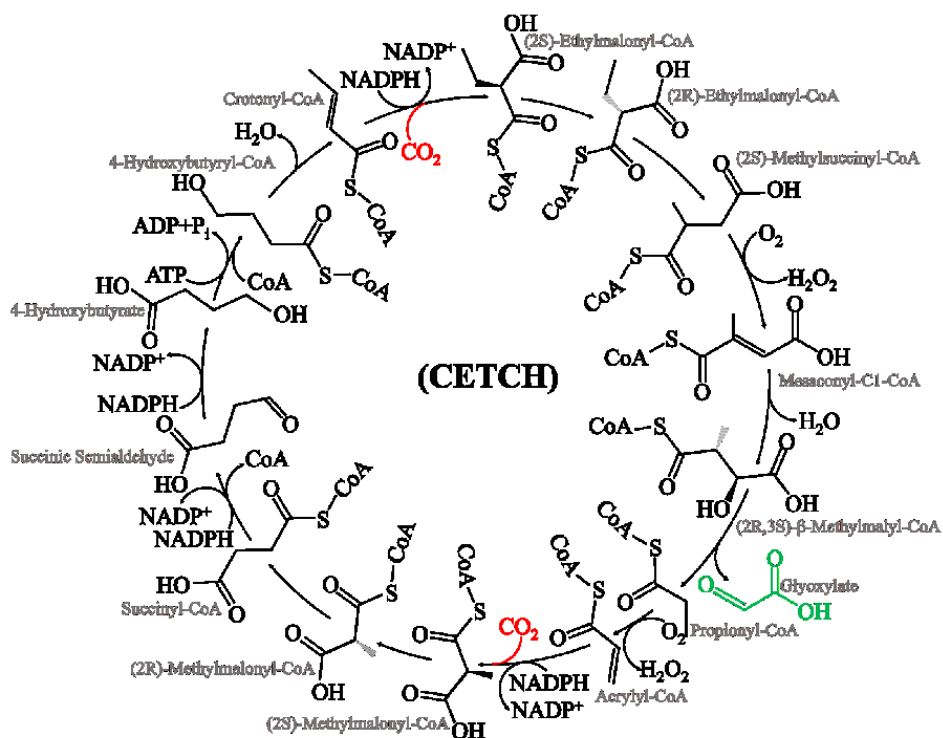
Figure. 1.8. The crotonyl-CoA/ethylmalonyl-CoA/hydroxybutyryl-CoA cycle, an oxygen-tolerant synthetic cycle that fixes CO_2 and generates glyoxylate. Adapted from Schwander, 2016.

1.3.2. The Reductive Glyoxylate/Pyruvate Synthesis Cycle and Malyl-CoA-Glycerate Pathway

The reductive glyoxylate and pyruvate synthesis (rGPS) cycle and the malyl-CoA-glycerate (MCG) pathway (Luo, 2022) fixes one molecule of CO_2 and one molecule of bicarbonate generating one molecule of acetyl-

CoA (Figure. 1.9.). In the first fixation, phosphoenolpyruvate carboxylase (EC 4.1.1.31) generates oxaloacetate from PEP and bicarbonate. In the second fixation, crotonyl-CoA is reductively carboxylated by Ccr to (2S)-ethylmalonyl-CoA at the expense of NADPH. This cycle is oxygen tolerant and mesophilic. The cycle combines chemistry linking acetyl-CoA to mesaconyl-C1-CoA from the ethylmalonyl-CoA pathway, mesaconyl-C1-CoA to acetyl-CoA and pyruvate from 3HBP, and pyruvate to (S)-malate from DC4HBC with the synthesis of (S)-malyl-CoA and cleavage to glyoxylate and acetyl-CoA, closing the cycle.
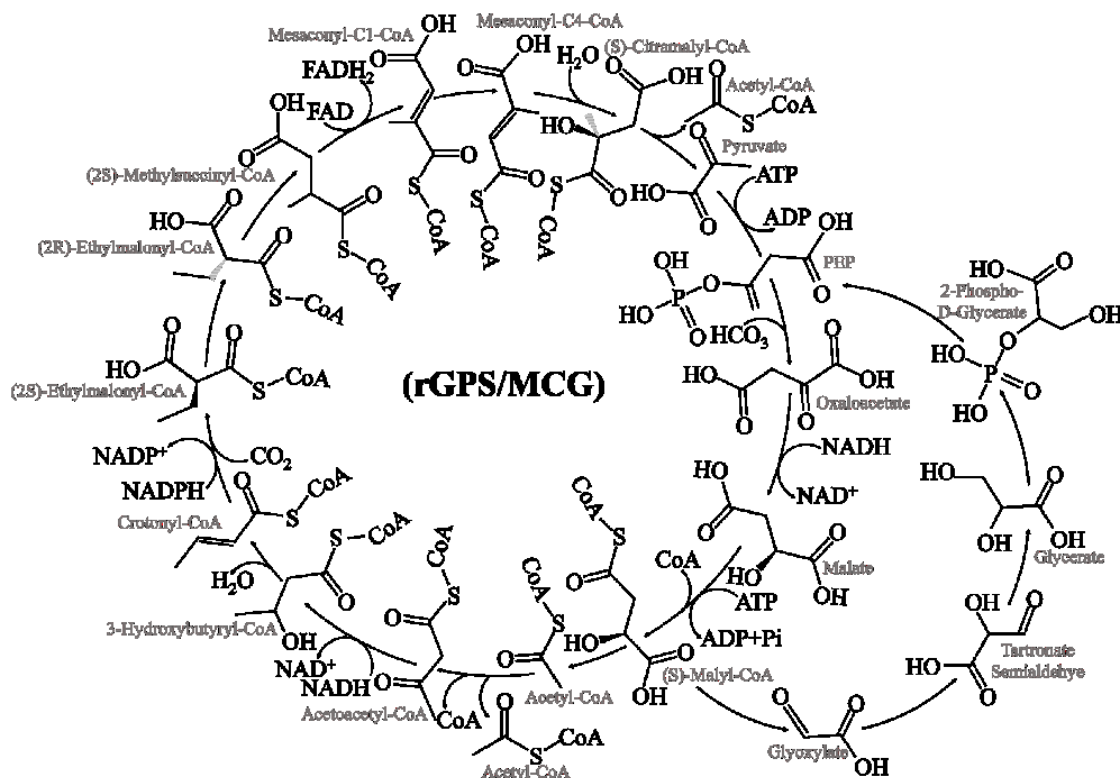
Figure. 1.9. The reductive glyoxylate/pyruvate synthesis cycle and the malyl-CoA-glycerate pathway, an oxygen-tolerant synthetic cycle that fixes CO_2 and bicarbonate and generates acetyl-CoA. Adapted from Luo, 2022.

1.3.3. The Tartronyl-CoA Pathway

The tartronyl-CoA (TaCo) pathway (Scheffen, 2021) fixes one molecule of bicarbonate while rescuing one molecule of 2-phophoglycolate and producing one molecule of 3-phosphoglycerate (Figure. 1.10.). This pathway serves the same purpose as photorespiration, but impressively manages to fix carbon rather than release previously fixed CO_2 and ammonia. The fixation step is the ATP-dependent carboxylation of glycolyl-CoA to (S)-tartronyl-CoA by glycolyl-CoA carboxylase, an engineered propionyl-CoA carboxylase (EC 6.4.1.3). While this pathway was designed with RuBisCO in mind, it is also of particular interest to the

CETCH and HOPAC cycles. Both cycles produce glyoxylate which can be reduced to glycolate and made useful by this pathway.
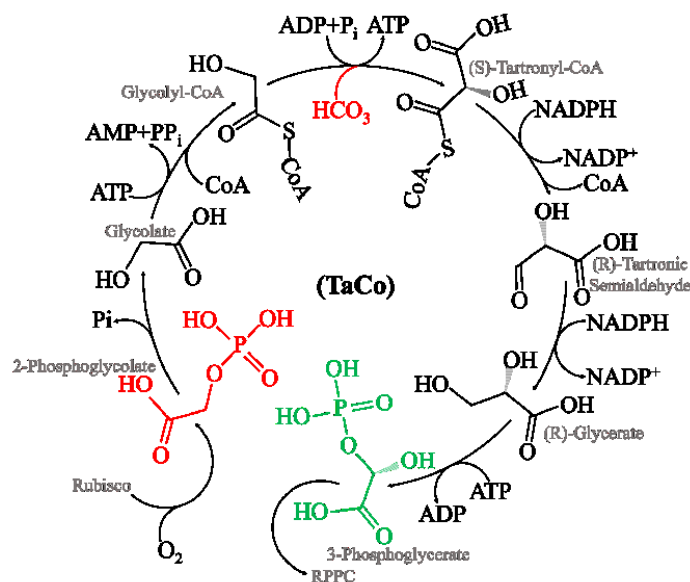
Figure. 1.10. The tartronyl-CoA pathway, an alternative to photorespiration that recycles 2-phosphoglycolate but fixes bicarbonate rather than losing CO_2 and ammonia. Adapted from Scheffen, 2021.

1.4. The HOPAC Cycle

1.4.1. Original HOPAC

In this study, we have built upon the foundational work of Schwander, 2018a and realised the **H**ydr**o**xy**p**ropionyl-CoA/**A**crylyl-**C**oA (HOPAC) Cycle (Figure. 1.11.). First conceived in Schwander, 2016, The cycle was inspired by the 3HPB of *Chloroflexus aurantiacus* and motivated by the reductive carboxylation reaction of crotonyl-CoA reductase. This is a valuable reaction as it proceeds in a single step. The alternative is to reduce acrylyl-CoA to propionyl-CoA followed by the ATP dependent carboxylation of propionyl-CoA to (2S)-methylmalonyl-CoA, resulting in a less energy efficient path of metabolism. The rest of the cycle was devised by metabolic retrosynthesis, evaluating possible reactions for thermodynamic feasibility, availability of enzymes, and aerotolerance. While the 3HPB has been partially implemented in vivo (Mattozzi et al., 2013), the cycle was limited to the native pathway design using the thermophilic enzymes from *C. aurantiacus*. For our cycle, we have broadened the constraints allowing for mesophilic enzymes from a variety of different species as well as for alternative reaction paths.
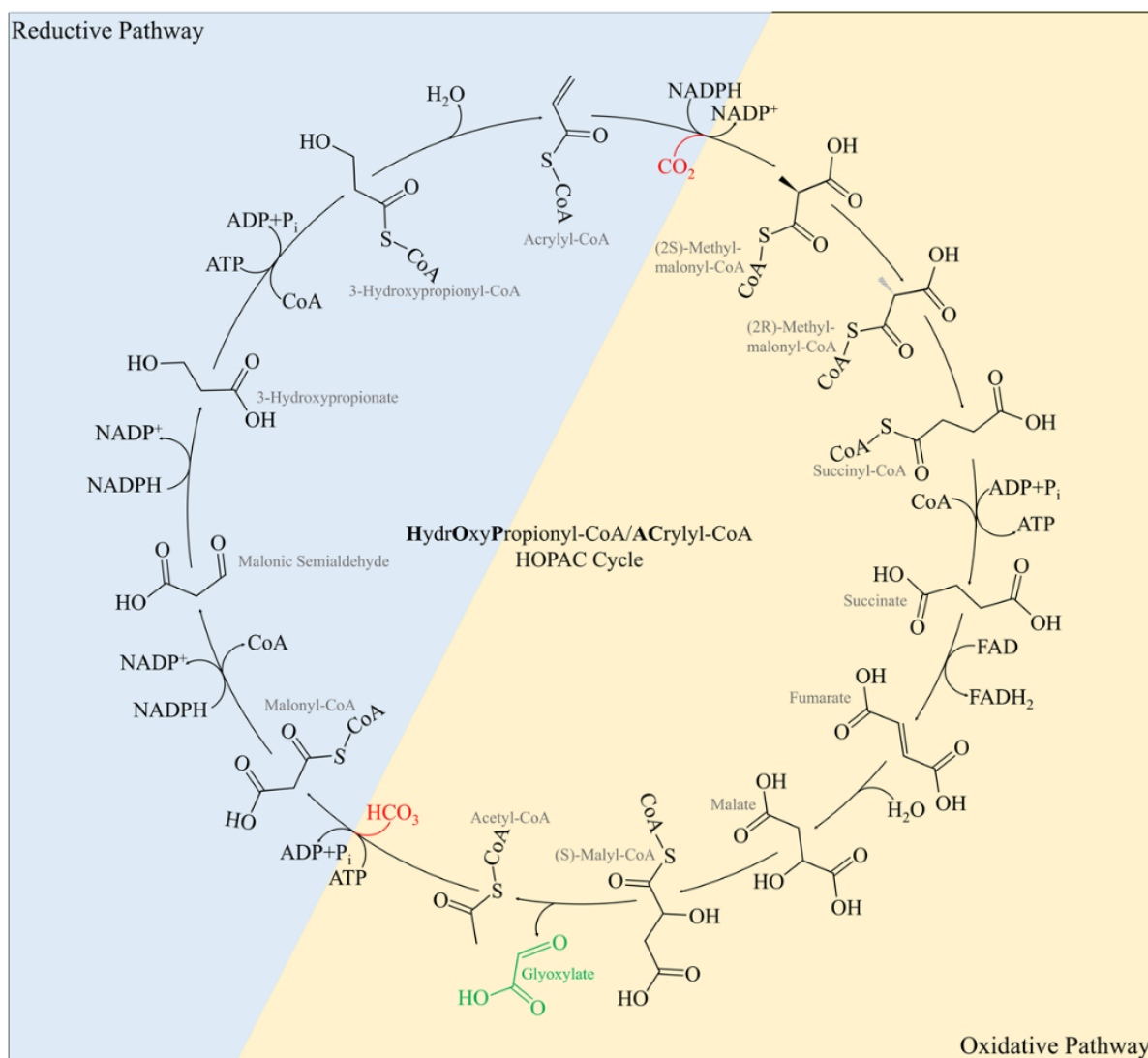
Figure. 1.11. Hydroxypropionyl-CoA/Acrylyl-CoA, an oxygen-tolerant synthetic cycle that fixes CO_2 and bicarbonate and generates glyoxylate. Adapted from Schwander, 2016.

1.4.2. Retrosynthesis from Acrylyl-CoA

Acrylyl-CoA can be generated by the dehydration of lactoyl-CoA (EC 4.2.1.54) or 3-hydroxypropionyl-CoA (EC 4.2.1.116) or the deamination of β-alanyl-CoA (EC 4.3.1.6). Lactoyl-CoA and β-alanyl-CoA are only produced by transferases, although in principle, synthetases could be engineered. 3-hydroxypropionyl-CoA can be produced by a synthetase (EC 6.2.1.36), or by the reduction of 3-oxopropionyl-CoA (Ploux, 1988). In principle, 3-oxopropionyl-CoA can be produced by a carboxylic acid reductase from malonyl-CoA at the expense of ATP and NADPH, but this activity has never been detected. The only reaction for the production of 3-hydroxypropionate valuable to this path is the reduction of malonic semialdehyde at the

expense of NAD(P)H (EC 1.1.1.59/1.1.1.298). Malonic semialdehyde can be produced by the transamination of β-alanine (EC 2.6.1.18/2.6.1.19/2.6.1.55/2.6.1.120) and the reduction of malonyl-CoA releasing CoA (EC 1.2.1.75). Conveniently, malonyl-CoA can be generated by the carboxylation of acetyl-CoA, increasing the carbon-fixing capacity of the cycle (Figure. 1.12.).
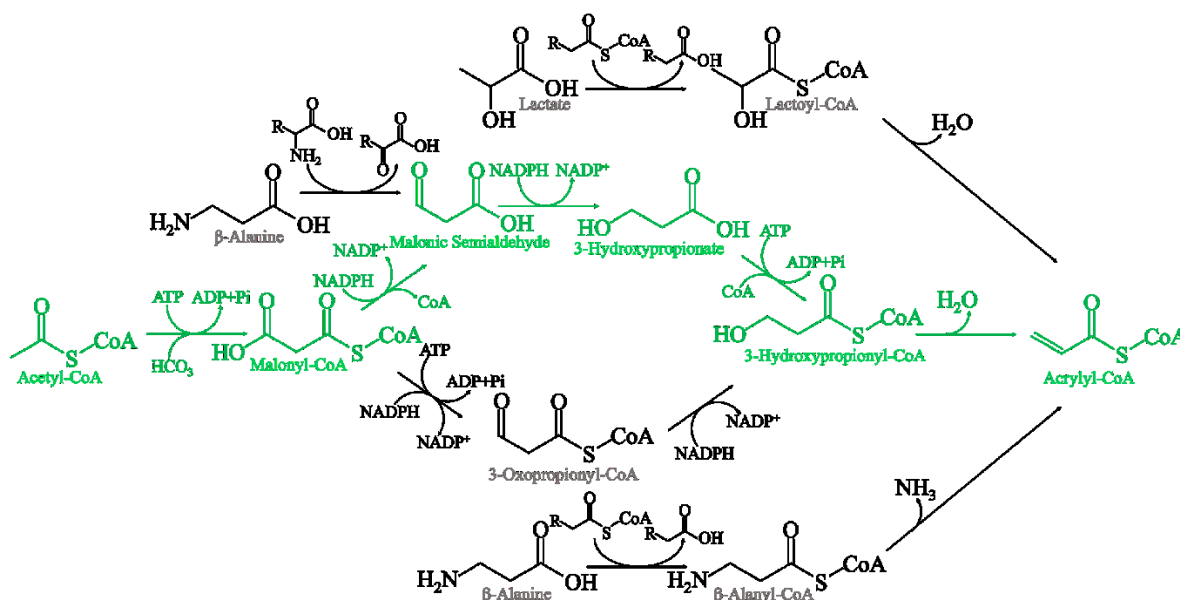
Figure. 1.12. Metabolic retrosynthesis from acrylyl-CoA. Exploring multiple pathways to generate acrylyl-CoA with previously characterised enzymes. Compounds highlighted in green were selected for implementation in the HOPAC cycle.

1.4.3. Synthesis from (2S)-Methylmalonyl-CoA

Further to this, if we can connect (2S)-methylmalonyl-CoA to acetyl-CoA, the cycle will be closed (Figure. 1.13.). There is little that can be done with (2S)-methylmalonyl-CoA apart from hydrolysis to methylmalonate (EC 3.1.2.17) and isomerisation to (2R)-methylmalonyl-CoA (EC 5.1.99.1). Methylmalonate can be ligated to CoA generating (2R)-methylmalonyl-CoA, but this is at the expense of ATP, a wasteful path to achieve the same chemistry. (2R)-methylmalonyl-CoA is isomerised again, this time to succinyl-CoA (EC 5.4.99.2).

Succinyl-CoA can be converted to succinate and CoA (EC 3.1.2.3/6.2.1.4/6.2.1.5) or reduced to succinic semialdehyde (EC 1.2.1.76). Succinic semialdehyde can be transaminated (EC 2.6.1.19/ 2.6.1.96) to 4-Aminobutyrate or reduced to 4-Hydroxybutyrate (EC 1.1.1.61). There is little that can be done with 4-aminobutyrate, but 4-hydroxybutyrate can be ligate to CoA generating 4-Hydroxybutyryl-CoA at the expense of ATP (EC 6.2.1.40/6.2.1.56). 4-Hydroxybutyryl-CoA can be dehydrated to crotonyl-CoA (EC

4.2.1.120) or alternatively to vinylacetyl-CoA, which is then isomerised to crotonyl-CoA (EC 5.3.3.3). Crotonyl-CoA can be reduced to Butanoyl-CoA (EC 1.3.1.44/1.3.1.86) and isomerised to 2-Methylpropanoyl-CoA (EC 5.4.99.13) which is ultimately a dead end, or carboxylated to (2S)-ethylmalonyl-CoA (EC 6.4.1.3) at the expense of ATP. Alternatively, crotonyl-CoA can be reductively carboxylated to (2S)-ethylmalonyl-CoA (1.3.1.85), saving an ATP. Another route hydrates crotonyl-CoA to 3-hydroxybutyryl-CoA (EC 4.2.1.150) which is oxidised to acetoacetyl-CoA (EC 1.1.1.157) and cleaved to two molecules of acetyl-CoA (EC 2.3.1.16) which closes the cycle. Taken with the previously selected reductive path, however, this collapses into the 3HP/4HBC cycle, apart from the reductive carboxylation of acrylyl-CoA. Unfortunately, this reductive carboxylation would not be feasible for this pathway because crotonyl-CoA would likely also be carboxylated.

The chemistry following (2S)-ethylmalonyl-CoA is relatively constrained, first it is isomerised to (2R)-ethylmalonyl-CoA (EC 5.1.99.1), and again to (2S)-methylsuccinyl-CoA (EC 5.4.99.63), then oxidised to mesaconyl-C1-CoA (EC 1.3.8.12). Mesaconyl-C1-CoA can be hydrated to (2R,3S)-β-methylmalyl-CoA or isomerised to mesaconyl-C4-CoA (EC 5.4.1.3). (2R,3S)-β-methylmalyl-CoA can be cleaved to glyoxylate and propionyl-CoA (EC 4.1.3.24) which can be oxidised to acrylyl-CoA (Schwander, 2016). While this closes the cycle, it simply reforms the CETCH cycle by eliminating the sequence from acetyl-CoA to acrylyl-CoA. Mesaconyl-C4-CoA, on the other hand, can be hydrated to (S)-citramalyl-CoA (EC 4.2.1.153) which can then be cleaved to pyruvate and acetyl-CoA (EC 4.1.3.25), again closing the cycle.

Instead of reduction, succinyl-CoA can be cleaved to succinate (EC 3.1.2.3/6.2.1.4/6.2.1.5). There are a variety of reactions succinate can be involved in, the most pertinent to our purposes is the oxidation of succinate to fumarate (EC 1.3.5.1/ 1.3.5.4), followed by hydration to (S)-malate (EC 4.2.1.2). (S)-malate can be oxidised to oxaloacetate (EC 1.1.5.4), which can then be cleaved to oxalate and acetate (EC 3.7.1.1), and the acetate can be ligated to CoA at the expense of ATP generating acetyl-CoA (EC 6.2.1.1/ 6.2.1.13) and closing the cycle. Alternatively, (S)-malate can be ligated to CoA at the expense of ATP (EC 6.2.1.9) and cleaved to glyoxylate and acetyl-CoA (EC 4.1.3.24), once again closing the cycle.

Figure. 1.13. Metabolic synthesis from (2S)-methylsuccinyl-CoA. Pathways that terminated in acetyl-CoA were sought after. Compounds highlighted in green were selected for implementation in the HOPAC cycle.

While the pathway that runs from succinic semialdehyde to (2R,3S)-β-methylmalyl-CoA is intriguing, it ultimately collapses into the CETCH cycle. The similar pathway that runs from succinic semialdehyde to (S)-citramalyl-CoA is appealing because it contains three carboxylation reactions and generates the C3 compound pyruvate, however it requires 19 reactions which is cumbersome in vitro.

The pathway that runs from succinate to oxaloacetate produces the C2 oxalate as a product. It is difficult to convert oxalate to anything useful. The most straight-forward method is to ligate oxalate to CoA at the expense of ATP (EC 6.2.1.8), then to reduce oxalyl-CoA to glyoxylate and CoA at the expense of NADPH (EC 1.2.1.17). Since this is the same product as the pathway that runs from succinate to (S)-malyl-CoA without the additional ATP and NADPH requirement, this is not a desirable route. The pathways highlighted in green in Figures. 1.12. and 1.13. were selected to unite into the HOPAC cycle. These reactions are by no means exhaustive, especially if engineered enzymes are utilised, but this is a plausible sequence of reactions that are oxygen tolerant, have mesophilic homologs, and are thermodynamically feasible. The net reaction is:

$$CO_2 + HCO_3^- + 2ATP + 3NADPH + FAD = glyoxylate + 2ADP + 3NADP^+ + FADH_2$$
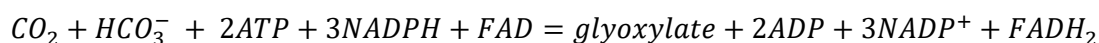
The cycle is notably similar to the 3-hydroxypropionate bicycle from *Chloroflexus aurantiacus* except, as a result of the reductive carboxylation of acrylyl-CoA it is more energy efficient, and we have persued a set of mesophillic enzymes to realise the cycle.

1.5. Aims of this Thesis

The general aim of this thesis was to evaluate the Hydroxypropionyl-CoA/Acrylyl-CoA cycle and potential variants for their ability to fix CO_2. The cycle was designed around the reductive carboxylation of acrylyl-CoA, a side-activity of the highly efficient crotonyl-CoA carboxylase/reductase (Ccr). The project aims to show that the cycle is feasible in vitro and may be a good candidate for future in vivo work.

1.5.1. The Oxidative Pathway of the HOPAC Cycle

Chapter 2 set out to investigate the feasibility of the oxidative half of the cycle, converting the product of Ccr, (2S)-methylmalonyl-CoA to acetyl-CoA, the substrate of the second carboxylation reaction. In the initial version of the HOPAC cycle, succinyl-CoA was converted to (S)-malate in a series of reactions analogous to those found in the TCA cycle. Multiple variants of this series of reactions were explored, but all were problematic in vitro. To circumvent this problem, we designed a bypass set of reactions that saw the direct oxidation of succinyl-CoA to the unusual metabolite fumaryl-CoA, which is then hydrated to (S)-

malyl-CoA. Finally, (S)-malyl-CoA is cleaved into acetyl-CoA, releasing glyoxylate, the C2 product of the cycle.

1.5.2. The Reductive Pathway of the HOPAC Cycle

Chapter 3 set out to investigate the feasibility of the reductive half of the cycle, converting acetyl-CoA to (2S)-methylmalonyl-CoA and closing the cycle. In the initial version of the HOPAC cycle, 3-hydroxypropionate was ligated to CoA generating 3-hydroxypropionyl-CoA by a hydroxypropionyl-CoA synthetase (Hps). Because we had stability issues with this enzyme, we explored a propionyl-CoA synthetase that performed this reaction as well as the following hydration and reduction generating propionyl-CoA. As an alternative, we explored a bypass that utilised β-alanine in largely analogous chemistry. Ultimately, we were able to identify a highly active Hps and used it to demonstrate that the initial version of the reductive half of the cycle worked best.

1.5.3. Uniting the HOPAC

Chapters 4 and 5 aim to investigate the entire HOPAC as a cohesive unit. We began by implementing various regeneration systems that will be required when the two pathways are united into a single, continuous cycle. In the individual pathways, one molecule of NADPH is required for each reductive step in the cycle and one molecule of ATP is required for each ATP-dependent step per molecule of acetyl-CoA added. When the cycle is united, and each molecule of acetyl-CoA can, in principle, traverse the cycle endlessly until the enzymes or intermediates degrade, far more cofactors are required than are practical to add to solution. We investigated options for the regeneration of ATP, NADPH, FAD, and coenzyme B12, as well as the decomposition of reactive oxygen species. After combining the pathways, we interrogated the systems capacity to incorporate ^{13}C from $^{13}CO_2$ and ^{13}C-bicarbonate and produce glyoxylate, the C2 product of the cycle.

2. The Oxidative Pathway

For the sake of simplicity, the HOPAC was arbitrarily divided into two pathways linking the carboxylation reactions. The first, referred to here as the Oxidative Pathway, contains the only oxidation reaction of the cycle as well as the intervening reactions. The second, referred to in Chapter 3 as the Reductive pathway, contains three reduction reactions. In these chapters, I will outline the required reactions for each pathway and the enzymes that have been found to perform them under our desired conditions. I then combine those reactions to investigate the feasibility of different versions of each pathway.

2.1. Isomerisation of (2S)-Methylmalonyl-CoA to Succinyl-CoA

In all versions of the oxidative pathway, (2S)-methylmalonyl-CoA is converted to (2R)-methylmalonyl-CoA by methylmalonyl-CoA epimerase (Epi) (EC 5.1.99.1), which is then isomerised to succinyl-CoA by methylmalonyl-CoA mutase (Mcm) (EC 5.4.99.2) (Figure. 2.1.A.). Mcm and Epi are nearly ubiquitous in life, with the exception of plants. Many Mcms are found in heterodimers such as in *M. extorquens* (Korotkova, 2002). To simplify our system, we opted for the relatively uncomplicated homodimer from *C. sphaeroides* which was found to have an activity of 450 Umg^{-1} and a Km of 19 µM (Figure. 2.1.B.). Both enzymes produce at high concentrations, stored well, and were highly active so we did not utilise alternatives.
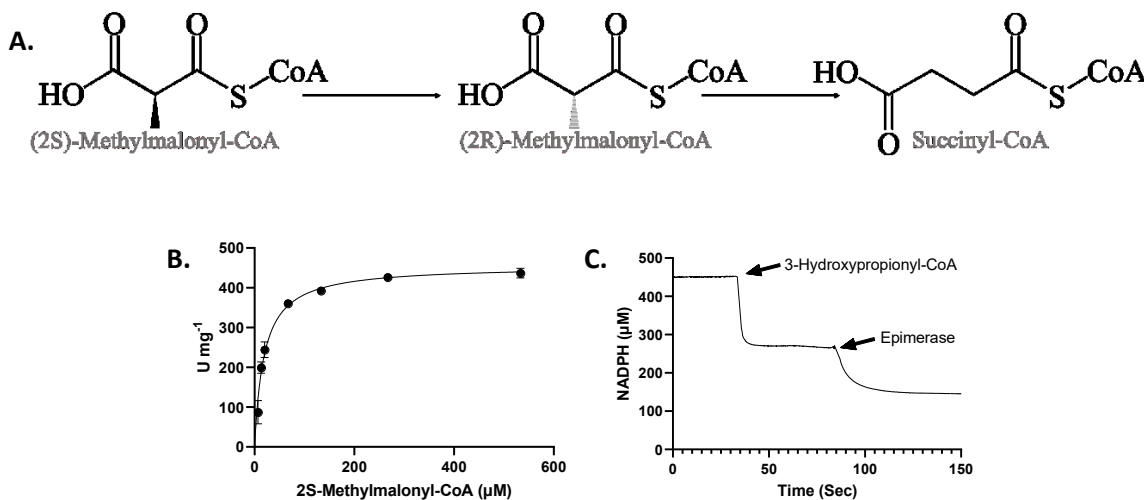
Figure. 2.1. **A.** Isomerisation of (2S)-methylmalonyl-CoA to (2R)-methylmalonyl-CoA and then to succinyl-CoA. **B.** Michaelis–Menten kinetics for Mcm from *C. sphaeroides*. (2R)-methylmalonyl-CoA was isomerised to succinyl-CoA which was reduced by succinyl-CoA reductase, the resulting oxidation of NADPH was monitored in real time at 360 nm. Assay described in Chapter 8.3.3. **C.** Activity plot of Epi from *C. sphaeroides*. 3-hydroxypropionyl-CoA was converted to (2S)-methylmalonyl-CoA by Ech and Ccr which

accounts for the initial oxidation of NADPH. Epi was added allowing for conversion of (2S)- to (2R)-methylmalonyl-CoA which was then isomerised to succinyl-CoA and reduced by succinyl-CoA reductase accounting for the second oxidation of NADPH.

2.2. Conversion of Succinyl-CoA to (S)-Malyl-CoA

In the initial design of the HOPAC cycle, the conversion of succinyl-CoA to (S)-malyl-CoA proceeded through succinate, fumarate, and (S)-malate. The oxidation of succinate to fumarate was performed by succinate dehydrogenase (Sdh) (EC 1.3.5.1), and the hydration of fumarate to (S)-malate was performed by fumarase (Fum). There are many options for these enzymes as they are present in the TCA cycle and can be found in all domains of life, in multiple forms in the case of fumarase. There are, however, multiple avenues for the cleavage of succinyl-CoA to succinate and CoA and the religation of (S)-malate to CoA generating (S)-malyl-CoA.

Alternatively, we explored a path that retained the thioester bond by directly oxidising succinyl-CoA to fumaryl-CoA exploiting a side-activity of methylsuccinyl-CoA dehydrogenase (Mcd) and the subsequent hydration of fumaryl-CoA to (S)-malyl-CoA by a side-activity of mesaconyl-C1-CoA hydratase (Mch).

2.2.1. Cleavage and Religation Path

2.2.1.1 Cleavage of Succinyl-CoA to Succinate and CoA

We investigated three options for the cleavage of succinyl-CoA to succinate. First, a transferase directly transferring the CoA from the succinyl moiety of succinyl-CoA to (S)-malate (Smt) (EC 2.8.3.22), second, the NTP regenerating cleavage of succinyl-CoA synthetase (Scs) (EC 6.2.1.4/6.2.1.5), and finally, the thioester squandering succinyl-CoA hydrolase (Sch) (EC 3.1.2.3) (Figure. 2.2.).

In the first case, there are enzymes available. Indeed, an Smt is the option employed by *Chloroflexus aurantiacus* in the 3HPB (Friedmann, 2006). This is an appealing option because it will simultaneously generate the (S)-malyl-CoA required three steps later in the cycle. Although it is a viable option, it does cause a complication in vitro. The transferase requires (S)-malate, but (S)-malate won't be generated until the succinate is liberated, oxidised, and then hydrated, so one of the reactants will always be missing. This can be overcome by the simultaneous addition of succinate, fumarate, and/or (S)-malate, but it complicates the comparison of different versions of the cycle.
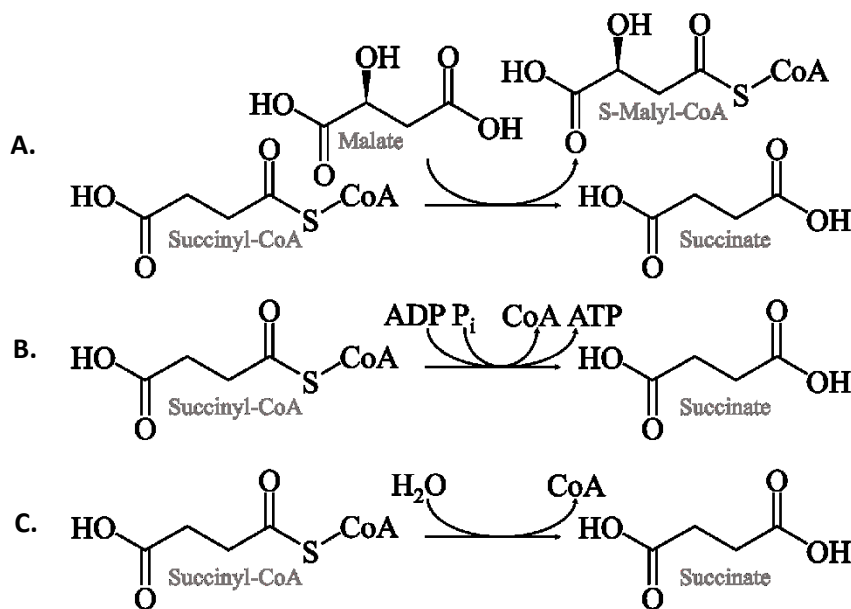
Figure. 2.2. Three potential reactions for the cleavage of succinyl-CoA. **A.** Smt, transfer of CoA from the succinyl moiety to (S)-malate generating succinate and (S)-malyl-CoA. **B.** Scs, ATP synthesis coupled to the cleavage of succinyl-CoA generating succinate and CoA. **C.** Sch, hydrolysis of succinyl-CoA generating succinate and CoA without recycling ATP.

The second case also seems like a viable option because the NTP generating cleavage of succinyl-CoA to succinate is present in the TCA cycle. There is a complication however, namely that there are multiple ATP dependent reactions in the cycle. Typically, we try to maintain a high ATP:ADP/AMP ratio to help drive the cycle forward. If Scs is used, this practice is counterproductive and may prevent the reaction from occurring outright. While this balance is maintained through a complex metabolism in vivo, it is difficult to maintain in vitro. If the balance shifts too far in the direction of ADP, other ATP-dependent reactions will be inhibited or halted, but if the balance shifts too far in the direction of ATP, cleavage of succinyl-CoA becomes difficult, and any that is cleaved will be rapidly religated. Nevertheless, there are many Scs available, we selected the Scs from *E. coli*.

The final option is to simply hydrolyse the thioester bond (Figure. 2.3.). Succinyl-CoA is by far the most labile acyl-CoA present in the cycle and the cycle might function, albeit extremely slowly, with no enzyme to cleave this bond. While the spontaneous rate of hydrolysis is impractical, acyl-CoA hydrolases exist which can expediate the process. The benefit to this option is that high concentrations of ATP can be maintained, helping to drive ATP-dependent reactions without concern that the cleavage of succinyl-CoA will be reversed. While this is preferable in this regard, there are two concerns: first that the ATP will not

be recovered as in the case of a synthetase (making the cycle less energy efficient), and second, potential promiscuity of the hydrolase causing the loss of various other intermediates. Succinyl-CoA hydrolases have been reported in both *Mus musculus* and *Sus scrofa* (Gergely, 1952; Westin, 2005) and we selected the *M. musculus* homolog to determine how feasible this option is. A secondary activity was found on fumaryl-CoA, however this is not a problem because fumaryl-CoA is not present in this version of the cycle. A potential issue though, is a significant activity on malyl-CoA. Sch is used in concert with (S)-malyl-CoA ligase (EC 6.2.1.9) which could lead to a futile cycle that wastes ATP.
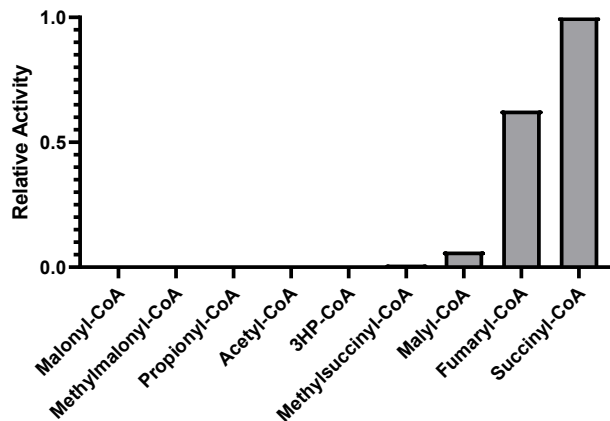
Figure. 2.3. Substrate specificity of *M. musculus* Sch. Fumaryl-CoA is not present in the version of the HOPAC cycle that utilises Sch but malyl-CoA is. Assay described in Chapter 8.3.9.

2.2.1.2. Oxidation of Succinate to Fumarate

Two enzymes exist that oxidise succinate to fumarate, succinate dehydrogenase (Sdh) (EC 1.3.5.1) (Figure. 2.4.A.) and fumarate reductase (Frd) (EC 1.3.1.6). Unfortunately, soluble Frd perform the irreversible reduction of fumarate to succinate (Leys, 1999) and are not appropriate for this purpose. Membrane Frd are closely related to Sdh and are nearly interchangeable in most respects (Lancaster, 1999). They perform the oxidation of succinate to fumarate after which, electrons are passed through a series of FAD and iron-sulfur centers before being accepted by ubiquinone or molecular oxygen (Figure. 2.4.).

Both Sdh and Fdr are heterotetrameric, membrane-bound enzymes. Proteins of this nature are often complicated to employ, and these are no exception. Although methods to purify the full complexes have been developed (Kita, 1989), they are typically comparatively complicated as the protein must be isolated from purified membranes and made soluble, and these methods often require storage of the purified enzyme in a detergent such as Lubrol PX which is undesirable in multi-enzyme applications.

As an alternative, we purified the soluble domains to determine if they were capable of the oxidation in the absence of their transmembrane counterparts. The active site of Sdh is found in the SdhA domain, which also contains an FAD, SdhB contains three iron-sulfur clusters. We generated a construct containing SdhA alone, and one containing both SdhA and SdhB (SdhAB). Both constructs were soluble and found to be active, with 230 mU/mg and 590 mU/mg respectively (Figure. 2.4.A. and B.).

As a secondary approach, we purified photosynthetic vesicles from *Cereibacter sphaeroides* (Kim, 2017) which were previously found to contain Sdh (Zeng, 2007). Because they are found in their native, membrane-bound state, we anticipated that this might be a valuable approach. This proved to be problematic however, because a multitude of other proteins copurified, and it was difficult to know how much Sdh was present resulting in undesirable batch-to-batch variability.
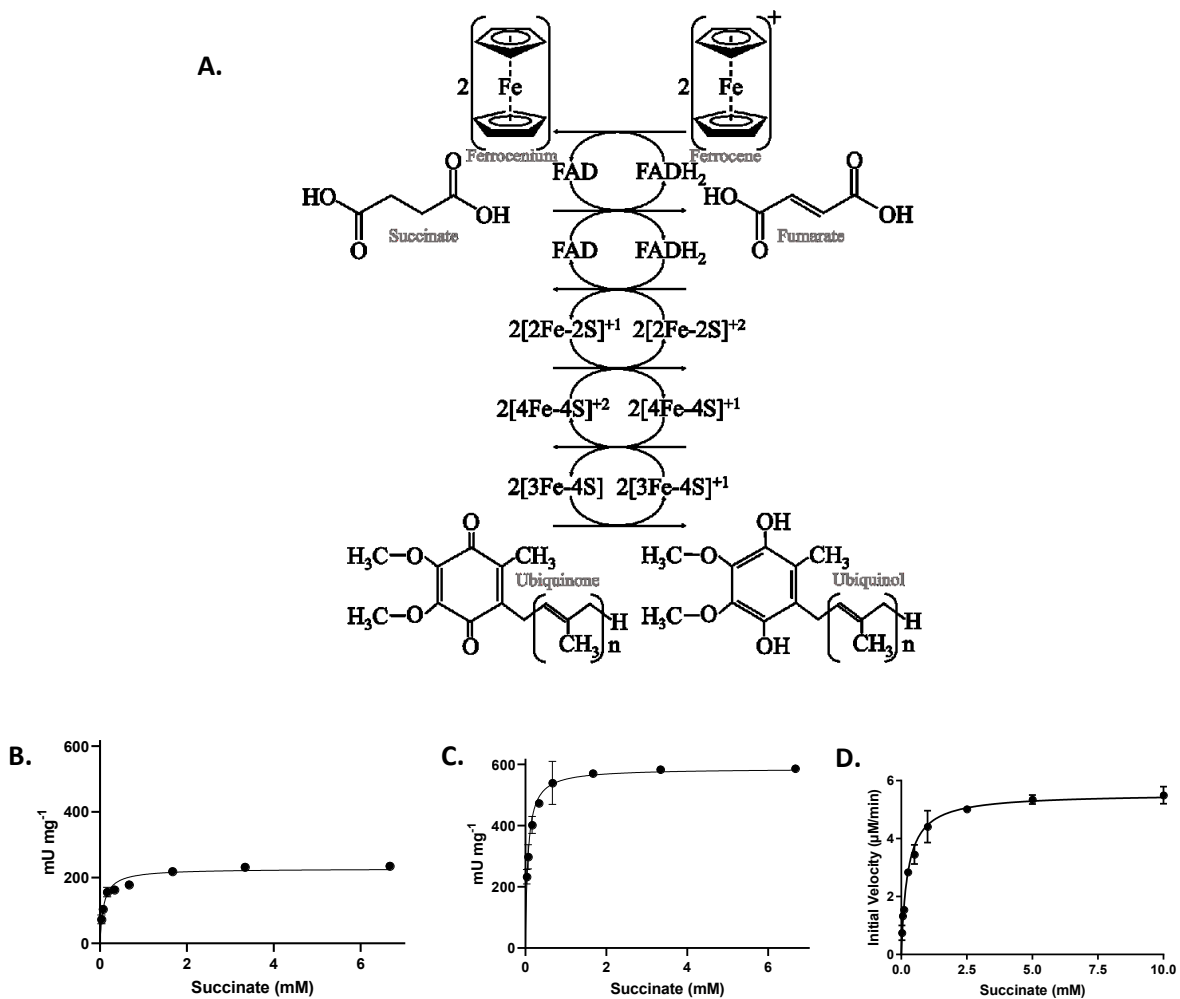
Figure. 2.4. **A.** Oxidation of succinate to fumarate and the resultant electron transfer to ubiquinone or ferrocenium. **B.** Michaelis–Menten kinetics of SdhA from *E. coli*. **C.** SdhAB from *E. coli*. **D.** SdhABCD in

vesicles from *C. sphaeroides*. Sdh oxidised succinate and subsequently reduced ferrocenium to ferrocene which was monitored at 300 nm. Assay described in Chapter 8.3.5.

2.2.2.3. Hydration of Fumarate to (S)-Malate

The hydration of fumarate to (S)-malate (Figure. 2.5.A.) by fumarate hydratase (EC 4.2.1.2) is another fundamental reaction found in the citric acid cycle. We selected the three canonical fumarases from *E. coli* ASKA collection (Kitagawa, 2005) (FumA, FumB, and FumC) as well as YggD and YdhZ, recently determined to be FumD and FumE respectively (Sévin, 2017).

All five enzymes were determined to have fumarase activity. However, FumA and FumB were oxygen sensitive, FumD precipitated, and FumE had activity much lower than FumC, which was found to have an activity of 640 Umg^{-1} and a Km of 0.18 mM on fumarate and an activity of 430 Umg^{-1} with a Km of 0.43 mM on (S)-malate (Figure. 2.5.B. and C.).
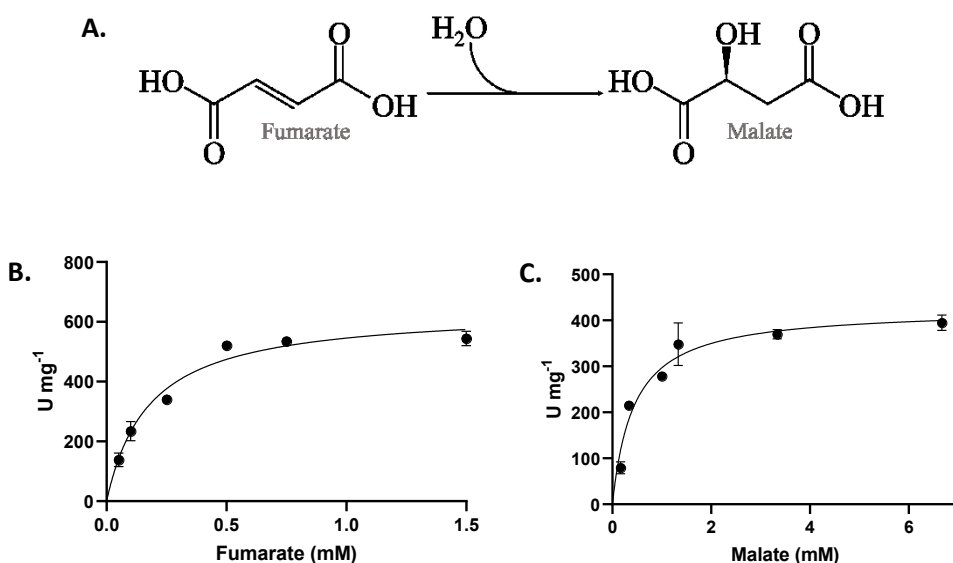
Figure. 2.5. **A.** Hydration of fumarate to (S)-malate. Michaelis–Menten kinetics of FumC from *E. coli*. **B.** Fumarate. **C.** Malate. Loss of the alkene bond was monitored in real time at 290 nm. Assay described in Chapter 8.3.8.

2.2.2.4. Ligation of (S)-Malate and CoA to (S)-Malyl-CoA

The method used to ligate (S)-malate to CoA is dependent on which method was used to cleave succinyl-CoA. Of course, if Smt is used, one of the products is (S)-malyl-CoA, so no additional enzymes are required. On the other hand, if Scs, Sch, or spontaneous hydrolysis are utilised, a malyl-CoA synthetase (Mcs) is required (Figure. 2.6.). To explore these options, we used the Mcs from *M. extorquens*. When used in

conjunction with Scs, one ATP is produced and one is consumed whereas when Sch is used, it is at a net loss of one ATP.
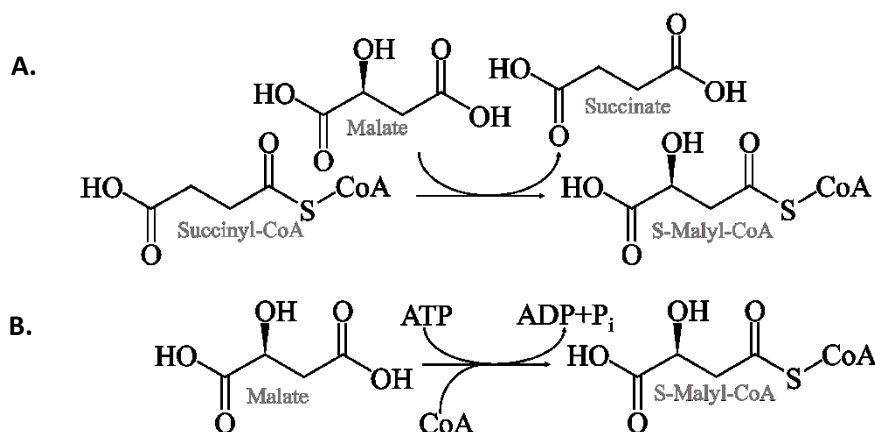
Figure. 2.6. Production of (S)-malyl-CoA. **A.** Transfer of acyl-CoA thioester bond from succinyl-CoA to (S)-malate. **B.** ATP-dependent ligation of (S)-malate to CoA.

2.2.2. Fumaryl-CoA Bypass

2.2.2.1. Oxidation of Succinyl-CoA to Fumaryl-CoA

The oxidation of succinyl-CoA to fumaryl-CoA (Figure. 2.7.) is not found in any known metabolism. In hopes of finding a significant succinyl-CoA oxidation activity, we first investigated the glutaryl-CoA dehydrogenase (Gcd) (EC 1.3.99.32) from *Desulfococcous multivorans* in hopes that the shift from the C_5 glutaryl- to C_4 succinyl-CoA would be accommodated. Unfortunately, no activity was detected.

Next, we opted for the methylsuccinyl-CoA dehydrogenase (Mcd) (EC 1.3.8.12), again exploiting a C_5 activity in hopes of accommodating succinyl-CoA. We began with the Mcd from *Cereibacter sphaeroides* because it has previously been mutated from a dehydrogenase to an oxidase which could be desirable for this cycle. In this case, activity was detected, however it was low. We next performed a homolog screen in hopes of finding a homolog with higher succinyl-CoA oxidation activity. This proved to be more successful with the homolog from *Pseudomonas migulae* performing best with an activity of 5.2 Umg^{-1} and a Km of 80 μM. The investigation into Mcd succinyl-CoA oxidation is discussed in greater detail in Chapter 6.
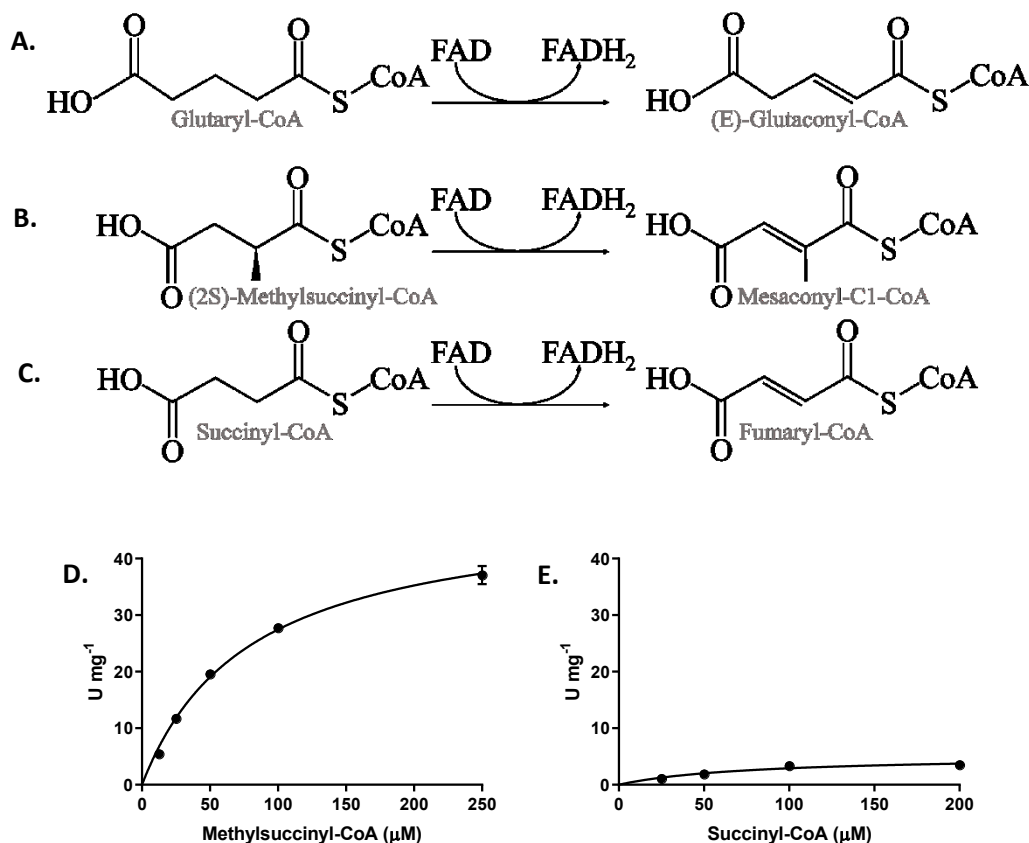
Figure. 2.7. Oxidation of **A.** Glutaryl-CoA to (E)-glutaconyl-CoA, **B.** Methylsuccinyl-CoA to mesaconyl-C1-CoA, and **C.** Succinyl-CoA to fumaryl-CoA. Michaelis–Menten kinetics of Mcd from *P. migulae* on **D.** (2S)-methylsuccinyl-CoA and **E.** Succinyl-CoA. Mcd was added and the reduction of ferrocenium to ferrocene was monitored in real time at 300 nm. Assay described in Chapter 8.3.5.

2.2.2.2. Hydration of Fumaryl-CoA to (S)-Malyl-CoA

Because fumaryl-CoA is not a known natural metabolite, fumaryl-CoA hydrating enzymes are also unknown. To resolve this issue, we focused on candidate enzymes with potential side activities towards fumaryl-CoA. Mesaconyl-C1-CoA and fumaryl-CoA are structurally similar apart from the presence of a methyl group at the C2 carbon, much like the difference between succinyl and methylsuccinyl-CoA. Following the success with Mcd, we tested the Mesaconyl-C1-CoA Hydratase (Mch) (EC 4.2.1.148) from *C. sphaeroides* which naturally hydrates mesaconyl-C1-CoA to (2R,3S)-β-methylmalyl-CoA (Figure. 2.8.A.). This enzyme was found to be a capable hydratase for our purposes with an activity of 1.7×10^3 Umg^{-1} and a Km of 280 μM on fumaryl-CoA, an activity of 18 Umg^{-1} and a Km of 80 μM on (S)-malyl-CoA, and an activity of 59 Umg^{-1} and Km of 210 μM on (2R,3S)-β-methylmalyl-CoA (Figure. 2.8.B. and C.).
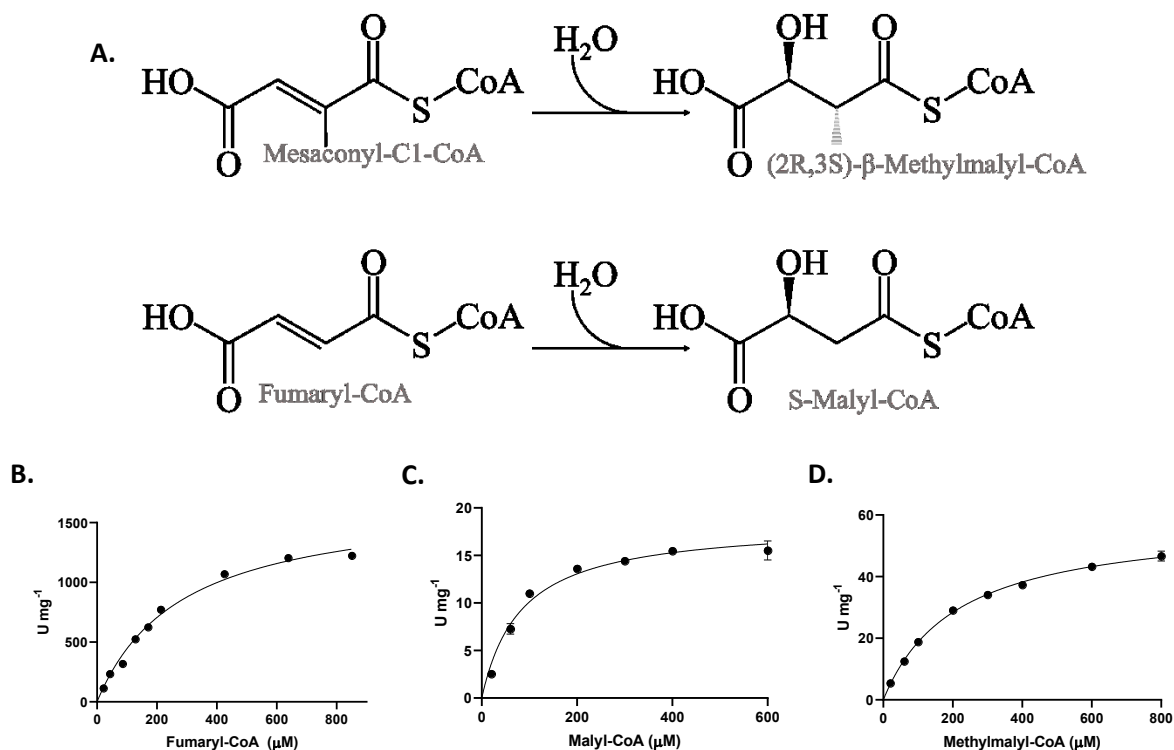
Figure. 2.8. **A.** Hydration of mesaconyl-C1-CoA (methylfumaryl-CoA) to (2R,3S)-β-methylmalyl-CoA. Hydration of fumaryl-CoA to (S)-malyl-CoA. Michaelis–Menten kinetics of Mch from *C. sphaeroides* on **B.** Fumaryl-CoA. **C.** (S)-malyl-CoA. **D.** (2R,3S)-β-Methylmalyl-CoA. Mch was added and loss or gain of the alkene bond was monitored in real time at 290 nm. Assay described in Chapter 8.3.7.

2.3. Cleavage of (S)-Malyl-CoA to Glyoxylate and Acetyl-CoA

The terminal step of the cycle cleaves (S)-malyl-CoA to acetyl-CoA and releases the C2 product glyoxylate (Figure. 2.9.A.). This reaction is performed by (S)-malyl-CoA lyase (Mcl) (EC 4.1.3.24). The lyase from *C. sphaeroides* has an activity of 6.3 Umg^{-1} and a Km of 40 μM on (S)-malyl-CoA and an activity of 9.7 Umg-1 and Km of 110 μM on (2R,3S)-β-methylmalyl-CoA (Figure. 2.9.D. and E.). This homolog produces and stores well, so others were not tested.

The lyase can perform three reversible reactions (Zarzycki, 2013) (Figure. 2.9.B. and C.). In addition to acetyl-CoA, propionyl-CoA can be condensed with glyoxylate to generate (2R,3S)-β-methylmalyl-CoA. Although propionyl-CoA is present in some versions of the cycle, this is a negligible issue because the cleavage of (2R,3S)-β-methylmalyl-CoA is mildly exergonic (-2.1 ± 5.9 kJ/mol), and the flux is driven forward by the favorable ATP-dependent carboxylation of propionyl-CoA (-5.0 ± 10.3 kJ/mol) and NADPH-

dependent reduction of glyoxylate (-41.1 ± 1.8 kJ/mol). It is also possible to condense acetyl-CoA with pyruvate, generating (S)-citramalyl-CoA. This isn't anticipated to be an issue because the cleavage of (S)-citramalyl-CoA is exergonic (-10.0 ± 3.1 kJ/mol), but in versions of the cycle employing pyruvate transaminases, reducing pyruvate back to L-alanine helps prevent this reaction.
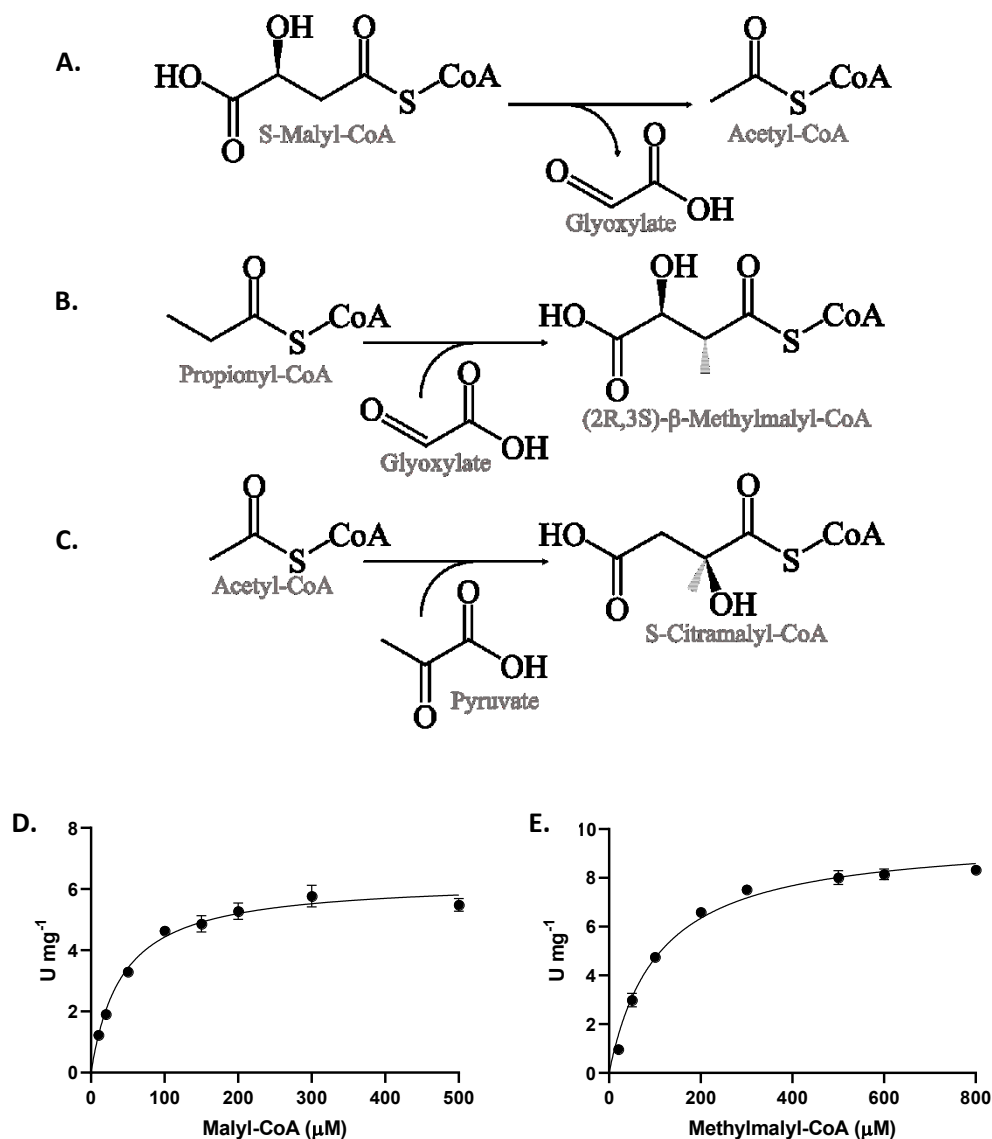
Figure. 2.9. **A.** Elimination of glyoxylate from (S)-malyl-CoA generating acetyl-CoA **B.** Condensation of glyoxylate with propionyl-CoA generating (2R,3S)-β-methylmalyl-CoA. **C.** Pyruvate with acetyl-CoA generating (S)-citramalyl-CoA. Michaelis–Menten kinetics of Mcl from *C. sphaeroides* on **D.** (S)-malyl-CoA. **E.** (2R,3S)-β-methylmalyl-CoA. Gxr was added and the oxidation of NADPH was monitored in real time at 360 nm. Assay described in Chapter 8.3.4.

2.4. Carboxylation of Acetyl-CoA to Malonyl-CoA

Acetyl-CoA carboxylases (Acc) (EC 6.4.1.2) are biotin-dependent enzymes that form a carbon-carbon bond between acetyl-CoA and bicarbonate (Figure. 2.10.A.). Although Acc are common among all domains of life, there are potential shortcomings for most homologs. Eukaryotic homologs are large, usually more than 200 kDa multi-domain proteins. Comparatively, bacterial Acc are often only half of the size but are comprised of multimeric complexes that are prone to dissociation (Tong, 2005).

The propionyl-CoA carboxylase (Pcc) (EC 6.4.1.3) of *M. extorquens* is a dimeric protein but of similar size to bacterial Acc, so we tested its promiscuity for carboxylation acceptors. Unfortunately, the rate of carboxylation was too low and prevented cycling. We investigated possible mutations to grant Pcc the ability to efficiently carboxylate acetyl-CoA. Intriguingly, the Acc of *S. coelicolor* is structurally very similar to Pcc sharing the larger subunit. It was previously determined (Diacovich, 2004) that mutating aspartate 422 to isoleucine changed substrate specificity to propionyl-CoA.

We mutated the analogous aspartate 407 in the active site of *M. extorquens* to isoleucine and found a similar swap of substrate activity (further referred to as Acc). This mutant has an activity of 16 Umg^{-1} and a Km of 0.56 mM on acetyl-CoA, an activity of 28 Umg^{-1} and Km of 0.14 mM on propionyl-CoA, with a Km of 50 μM on ATP (Figure. 2.10.B-D.).
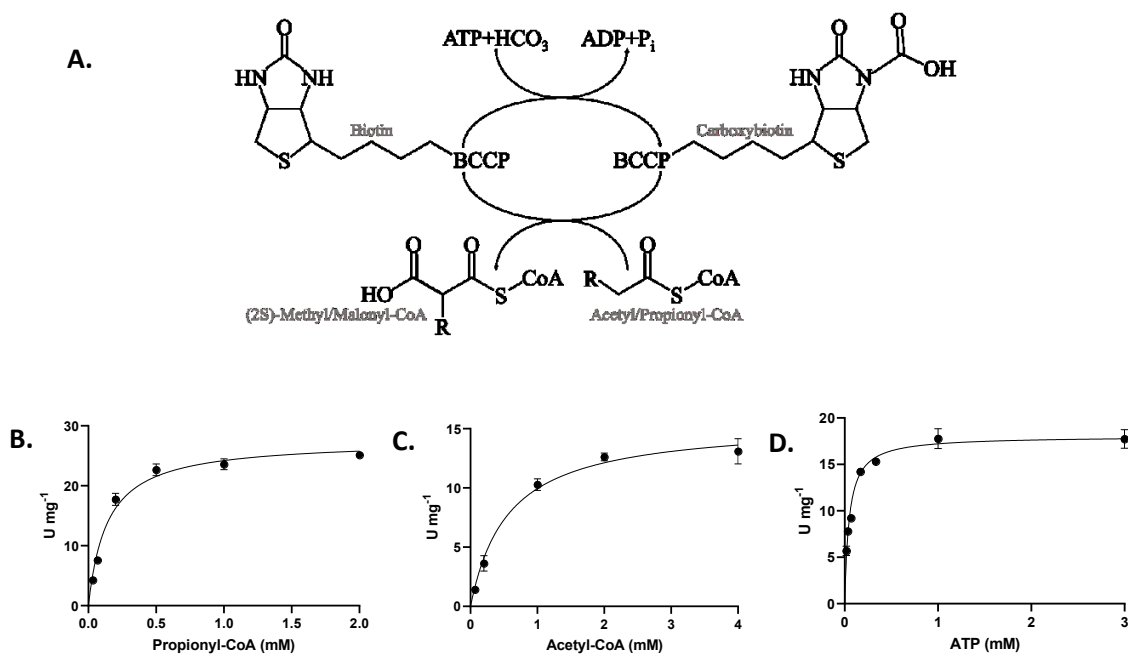
Figure. 2.10. **A.** Biotin-dependent, ATP-dependent carboxylation of acetyl-CoA (R=H) and propionyl-CoA (R=CH$_3$). Michaelis–Menten kinetics of Acc from *M. extorquens* on **B.** Acetyl-CoA. **C.** Propionyl-CoA. **D.**

Effect of ATP. The pyruvate kinase/lactate dehydrogenase from Sigma Aldrich was used, and the oxidation of NADH was monitored in real time at 360 nm. Assay described in Chapter 83.1.

2.5. Full Oxidative Pathway

With all of the requisite enzymes in hand and activities being established, we set out to demonstrate flux through the possible combinations. In all cases, (2S)-methylmalonyl-CoA is converted to succinyl-CoA by Mcm and Epi, and (S)-malyl-CoA is cleaved to acetyl-CoA by Mcl. For the intervening chemistry, there are four possibilities: succinyl-CoA is converted to (S)-malyl-CoA by **1.** Scs, Sdh, Fum, and Mcs, **2.** Sch, Sdh, Fum, and Mcs, **3.** Smt, Sdh, and Fum, and **4.** Mcd and Mch.
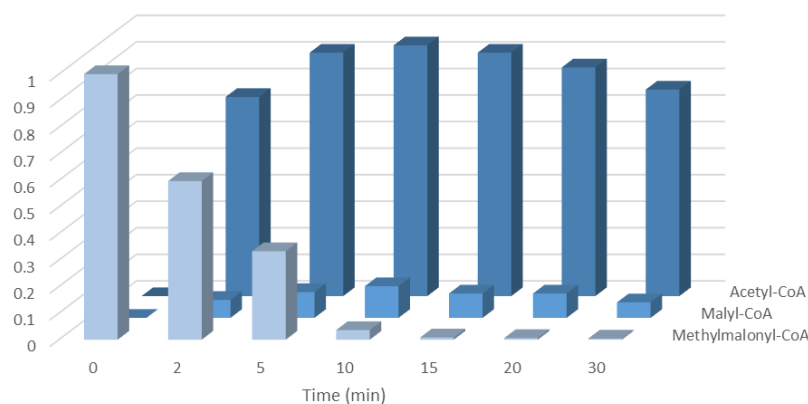
Figure. 2.11. Conversion of (2S)-methylmalony-CoA to acetyl-CoA by Mcm-Epi-Mcd-Mch-Mcl. Assay described in Chapter 8.5. Values are relative IC peak areas and are not meant to be quantitative. Ferrocenium was used as the terminal electron carrier for Mcd. Succinyl-CoA and fumaryl-CoA were consumed adequately quickly relative to their rate of production that they were not detectable in this assay.

For scenarios 1-3, we had difficulty producing significant quantities of acetyl-CoA. In the case of Smt, 20 µM of (S)-malate was provided for the transferase reaction to begin, and similar concentrations of acetyl-CoA were generated, suggesting little of the produced succinate managed to pass through the intervening enzymes. Given the high activity of Fum, it seems unlikely that this enzyme was the cause of the issue. As discussed previously however, there are problems for Scs, Sch, and Sdh. To rule out Scs and Sch as the primary bottleneck, we ran similar assays beginning with succinate and these also failed to produce appreciable concentrations of acetyl-CoA, even with an exorbitant concentration of Sdh as high as 250

μM. Due to the low activity of the SdhAB, it would require nearly two hours at peak activity to oxidise 250 μM of succinate, even at this concentration. This is likely to be a significant bottleneck for any version of the cycle making these scenarios impractical for the in vitro system.

For scenario 4, we found rapid, nearly complete conversion of (2S)-methylmalonyl-CoA to acetyl-CoA (Figure. 2.11.) making this not only the only functional version of the oxidative pathway, but a viable pathway for implementation in the full HOPAC cycle.

3. The Reductive Pathway

3.1. Reduction of Malonyl-CoA to Malonic Semialdehyde

Enzymes exist that independently reduce Malonyl-CoA to malonic semialdehyde such as malonyl-CoA reductase (EC 1.2.1.75), (Demmer, 2013) and malonic semialdehyde to 3-hydroxypropionate such as 3-hydroxypropionate dehydrogenase (EC 1.1.1.298), (Kockelkorn, 2009). However, these are sometimes promiscuous, reducing succinyl-CoA and succinic semialdehyde respectively. As succinyl-CoA is present in the cycle, we looked for a highly specific malonyl-CoA reductase (Mcr) and used one from *C. aurantiacus* (Hügler, 2002). In addition to being highly specific, it is also capable of performing both reactions reducing malonyl-CoA to 3-hydroxypropionate in one enzyme (Figure. 3.1.A.). It has an activity of 24 Umg^{-1} and 10 µM on malonyl-CoA with a Km of 10 µM on NADPH (Figure. 3.1.B. and D.).

Conveniently, this enzyme has previously been dissected (Liu, 2013) and each domain can be produced independently allowing for specific reduction of malonyl-CoA to 3-hydroxypropionate, malonyl-CoA to malonic semialdehyde (Figure. 3.1.D.), or malonic semialdehyde to 3-hydroxypropionate as is required. When 3-hydroxypropionate was to be produced, we utilised the full-length construct, when β-alanine was to be produced, we used a construct containing only the c-terminal domain (S557-V1219).
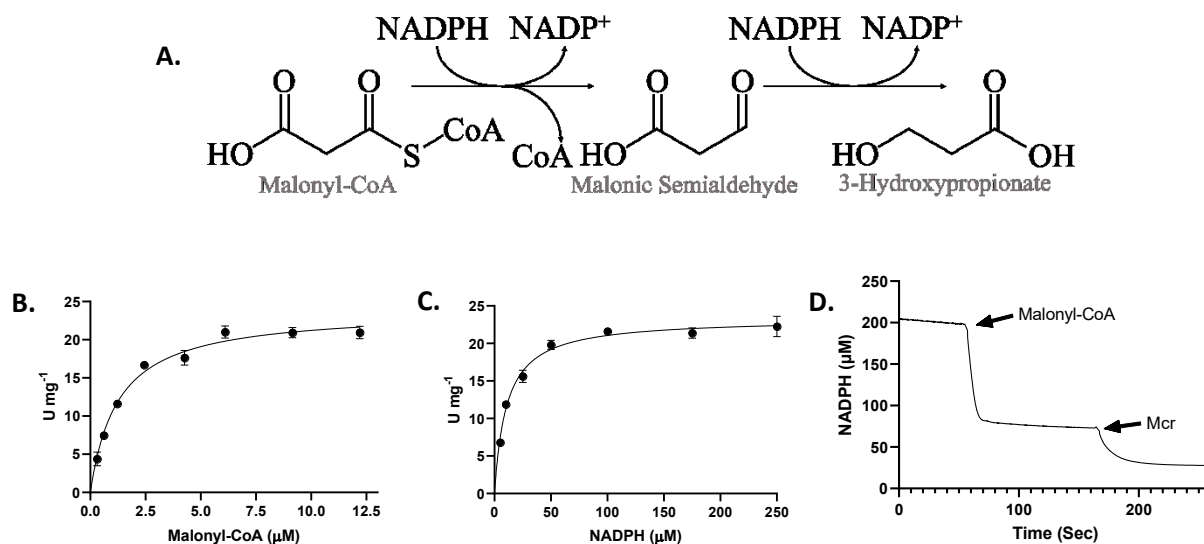
Figure. 3.1. **A.** Double reduction of malonyl-CoA first to malonic semialdehyde and then to 3-hydroxypropionyl-CoA. Michaelis–Menten kinetics of *C. aurantiacus* Mcr on **B.** Malonyl-CoA. **C.** Effect of NADPH. Mcr was added and the oxidation of NADPH was monitored in real time at 360 nm. It was assumed that every molecule of NADPH oxidised related to 0.5 molecules of malonyl-CoA. Assay described in

Chapter 8.3.2. **D.** Activity plot of Mcr from *C. aurantiacus*. Malonyl-CoA is reduced to malonic semialdehyde by the c-terminal domain of Mcr which accounts for the initial oxidation of NADPH. Full-length Mcr was added allowing for reduction of malonic semialdehyde to 3-hydroxypropionate accounting for the second oxidation of NADPH.

3.2. Conversion of Malonic Semialdehyde to Acrylyl-CoA

Two alternatives were investigated for the conversion of malonic semialdehyde to acrylyl-CoA. First, malonic semialdehyde is reduced to 3-hydroxypropionate and 3-hydroxypropionyl-CoA is dehydrated to acrylyl-CoA. Second, malonic semialdehyde is aminated to β-alanine and β-alanyl-CoA is deaminated to acrylyl-CoA. Both of these options are discussed in more detail below.

3.2.1. 3-Hydroxypropionate Route
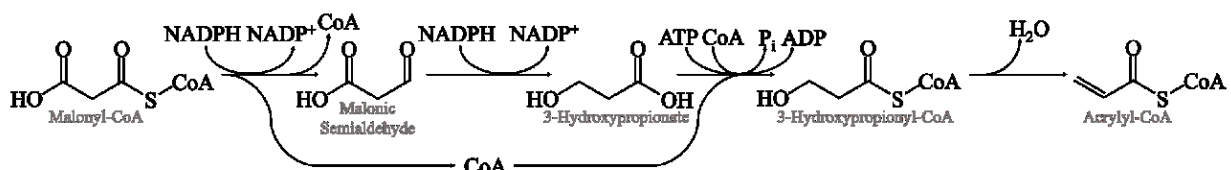
Figure. 3.2. In the primary design of the HOPAC cycle, the conversion of malonyl-CoA to acrylyl-CoA proceeded through 3-hydroxypropionate and 3-hydroxypropionyl-CoA. Malonyl-CoA and malonic semialdehyde are reduced by Mcr. The ligation of 3-hydroxypropionate to CoA is performed by hydroxypropionyl-CoA synthetase (Hps) or an acyl-CoA transferase. 3-hydroxypropionyl-CoA is dehydrated to acrylyl-CoA by enoyl-CoA hydratase (Ech).

3.2.1.1. Ligation of 3-Hydroxypropionate to CoA forming 3-Hydroxypropionyl-CoA

There are two methods to ligate 3-hydroxypropionate to CoA. First is the generation of a thioester bond utilising the energy from ATP by a synthetase (EC 6.2.1.36), the second transfers the thioester bond from a pre-existing acyl-CoA to an organic acid by an acyl-CoA transferase (EC 2.8.3.1) (Figure. 3.3.).

A.

B.
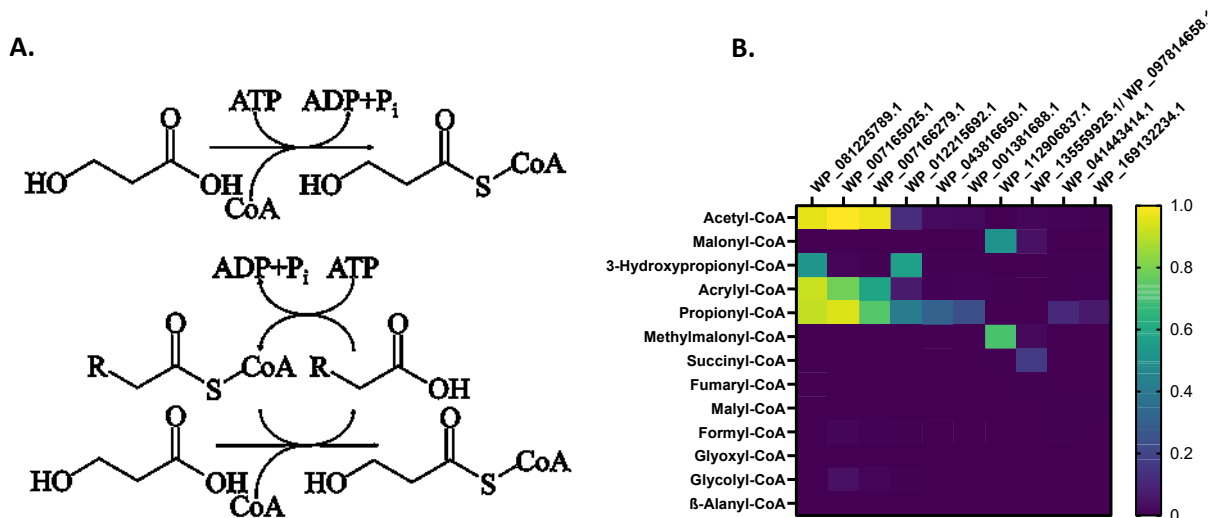
Figure. 3.3. **A.** Conversion of 3-hydroxypropionate and CoA to 3-hydroxypropionate by synthetase and transferase. **B.** Selection of acyl-CoA synthetase activity screen. WP_081225789.1 = propioyl-CoA synthetase from *C. necator*. WP_007165025.1 and WP_007166279.1 = acetyl-CoA synthetase from *Erythrobacter* sp, NAP1. WP_012215692.1 = 3-hydroxypropionyl-CoA from *Nitrosopumilus maritimus*. WP_043816650.1 = butyryl-CoA synthetase from *Deinococcus maricopensis*. WP_001381688.1 = propioyl-CoA synthetase from *Escherichia coli*. WP_112906837.1 = malonyl-CoA synthetase from *Rhizobium leguminosarum*. WP_135559925.1/WP_097814658.1 = succinyl-CoA synthetase from *E. coli*. WP_041443414.1 = phenylacetyl-CoA synthetase from *Thermus thermophilus*. WP_169132234.1 = phenylacetyl-CoA synthetase from *Aromatoleum evansii*. 1.0 = maximally detected activity, 0 = no activity detected. Assay described in Chapter 8.3.1.

We explored a variety of acyl-CoA-synthetases to find one that was capable of ligating 3-hydroxypropionate to CoA without having undesirable side activities. The first enzyme we used was the Hps from *N. maritimus* because it was specifically annotated as such. Although the enzyme does in fact have the desired activity, we found that it lost activity much faster than any other enzyme used in the cycle at the time. We feared that this instability might translate to a loss of activity while the cycle was running, so we looked for alternatives.

Two acetyl-CoA synthetases from *Erythrobacter* sp. Nap-1 and one from *Methylorubrum extorquens* (EC 6.2.1.1)*,* were explored but we found that the activity was too promiscuous for our purposes. We tried a number of ligases that had activity on larger acyl-CoAs (EC 6.2.1.2, EC 6.2.1.17, EC 6.2.1.30) in hopes that they would have less activity on small metabolites, but they did not have activity on 3-hydroxypropionate.

Finally, we settled on a propionyl-CoA ligase from *Cupriavidius necator* which was sufficiently active and specific (Figure. 3.3.).

As an alternative to Hps, we tested three acyl-CoA transferases for activity on 3-hydroxypropionate. If the CoA could be transferred from, for example, acetyl-CoA, the resulting acetate could then be religated to CoA by an acetyl-CoA synthetase. Although the desired activity was detected, Hps is a preferable route because the acyl-CoA donor must be present in order for the reaction to proceed. If all of the acetyl-CoA is carboxylated to malonyl-CoA before any 3-hydroxypropionate is generated, the cycle will stall.

3.2.1.2. Dehydration of 3-Hydroxypropionyl-CoA to Acrylyl-CoA

The dehydration of 3-hydroxypropionyl-CoA to acrylyl-CoA (Figure. 3.4.) is achieved with an (R)-specific enoyl-CoA hydratase (Ech) (EC 4.2.1.116/4.2.1.119). The Ech from *Pseudomonas aeruginosa* produced at high concentrations, stored well, and was highly active so we did not use alternatives.

Figure. 3.4. Dehydration of 3-hydroxypropionyl-CoA to acrylyl-CoA as performed by Ech.

3.2.2. β-Alanine Route
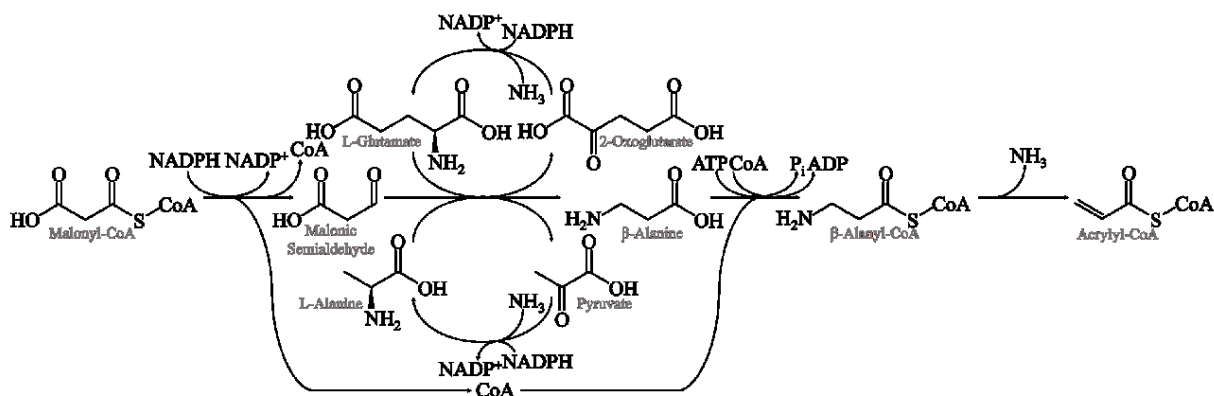
Figure. 3.5. As an alternative route, the conversion of malonyl-CoA to acrylyl-CoA proceeded through β-alanine and β-alanyl-CoA. Malonyl-CoA is reduced by a truncated C-terminal domain of Mcr. Malonic semialdehyde is aminated by an amino acid transaminase. The ligation of β-alanine to CoA is performed

by an acyl-CoA synthetase or an acyl-CoA transferase. β-alanyl-CoA is deaminated to acrylyl-CoA by β-alanyl-CoA ammonia-lyase.

3.2.2.1. Transamination of Malonic Semialdehyde to β-Alanine

To convert malonic semialdehyde to β-alanine, an amino-donor is required. β-alanine-pyruvate transaminase (βapt) (EC 2.6.1.18) makes use of the amino group from L-alanine generating pyruvate (Figure. 3.6). We found sufficient activity with the transaminase from *Rhizobium hidalgonense*. There are, however, drawbacks to using βapt.

First, there is often a side-activity with glyoxylate, the product of the HOPAC cycle. As malonic semialdehyde and L-alanine are converted to pyruvate and β-alanine, the amino group can be transferred to glyoxylate generating glycine. This can be partially mitigated by rapidly converting glyoxylate to another product such as glycolate as well as converting the β-alanine to β-alanyl-CoA to continue flux through the cycle. In principle, there is nothing wrong with converting glyoxylate to glycine so long as the pyruvate is recycled back into L-alanine. This is an exergonic reaction, but it does increase the overall amine demand of the cycle and may become limiting as the production of glyoxylate increases.

Second, due to the similarity between β-alanine and L-alanine, side-activities have been detected for β-alanyl-CoA transferases. As a result, β-alanyl-CoA generating enzymes must be highly specific or else L-alanyl-CoA will be generated. This isn't necessarily a dead-end product as long as the transferase can transfer the thioester bond between the L-alanyl moiety and β-alanine, however a significant portion of the L-alanine pool being lost to L-alanyl-CoA will prevent the transamination of malonic semialdehyde and stall the cycle.

Another enzyme, 4-aminobutyrate-2-oxoglutarate transaminase (Abot) (EC 2.6.1.19) performs a similar reaction transferring an amino group from L-glutamate to succinic semialdehyde, generating 2-oxoglutarate and 4-aminobutanoate. In some cases, a side-activity has been measured allowing for the transfer of the amino group to malonic semialdehyde instead, generating β-alanine (Buzenet, 1978; Schousboe, 1973). We selected the transaminase from *E. coli*, which has no activity on glyoxylate. Additionally, L-glutamate is significantly larger, which prevents the side activity with the acyl-CoA transferases we tested, however because this is a side-activity, the activity is lower.

A further possibility is taurine-2-oxoglutarate transaminase (T2ot) (EC 2.6.1.55) which transfers the amino group from L-glutamate to 2-sulfoacetaldehyde generating taurine and 2-oxoglutarate. A side-activity allows for the amino transfer from L-glutamate to malonic semialdehyde generating 2-oxoglutarate and

β-alanine (Yonaha, 1985). This is likely a viable approach, however it was not pursued due to success with Abot.
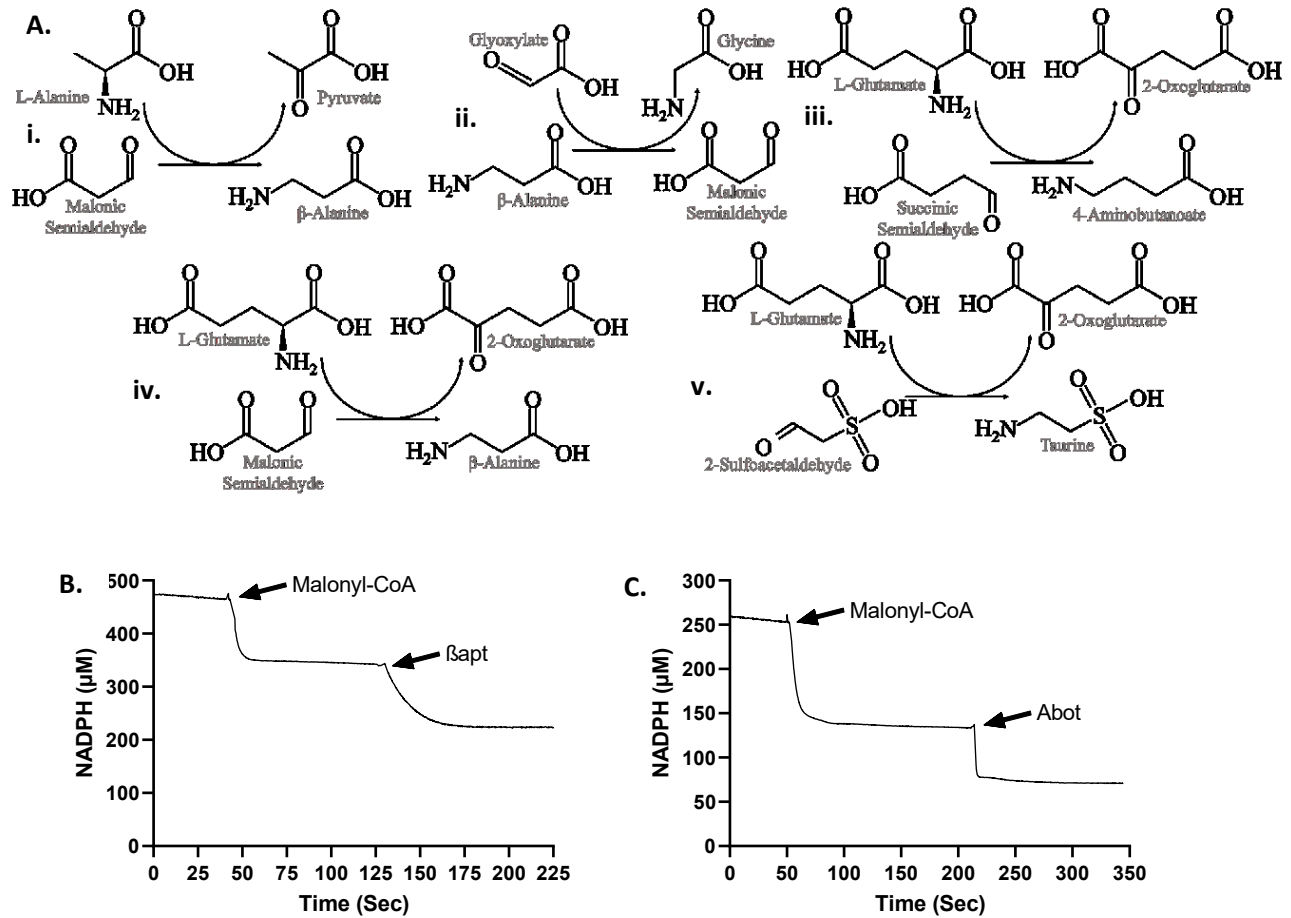
Figure. 3.6. **A.** Transaminations. **i.** Transfer from L-alanine to malonic semialdehyde generating pyruvate and β-alanine performed by βapt, Abot, and T2ot. **ii.** Transfer from β-alanine to glyoxylate generating malonic semialdehyde and glycine performed by βapt. **iii.** Transfer from L-glutamate to succinic semialdehyde generating 2-oxoglutarate and 4-aminobutanoate performed by Abot. **iv.** Transfer from L-glutamate to malonic semialdehyde generating 2-oxoglutarate and β-alanine performed by Abot and T2ot. **v.** L-glutamate to 2-sulfoacetaldehyde generating 2-oxoglutarate and taurine performed by T2ot. **B.** Activity plot of *E. coli* βapt. The C-terminal domain of Mcr was used to reduce malonyl-CoA to malonic semialdehyde which accounts for the initial oxidation of NADPH. βapt was added converting malonic semialdehyde to β-alanine producing pyruvate which is reduced by Adh accounting for the second oxidation of NADPH. **C.** Activity plot of Abot. The assay was the same as in B. except Abot was added in place of βapt generating 2-oxoglutarate which is reduced by Gdh.

3.2.2.2. Ligation of β-Alanine to CoA forming β-Alaninyl-CoA

As with 3-hydroxypropionyl-CoA, β-Alaninyl-CoA could, in principle, be generated with either an acyl-CoA synthetase or an acyl-CoA transferase (Figure. 3.7.). We tested for β-Alaninyl-CoA synthetase and transferase in the previous screen (Figure. 3.3.). Unfortunately we failed to find significant synthetase activity. We found sufficient transferase activity with the β-alanine CoA-transferase (βact) from *Anaerotignum propionicum* to test this portion of the cycle.
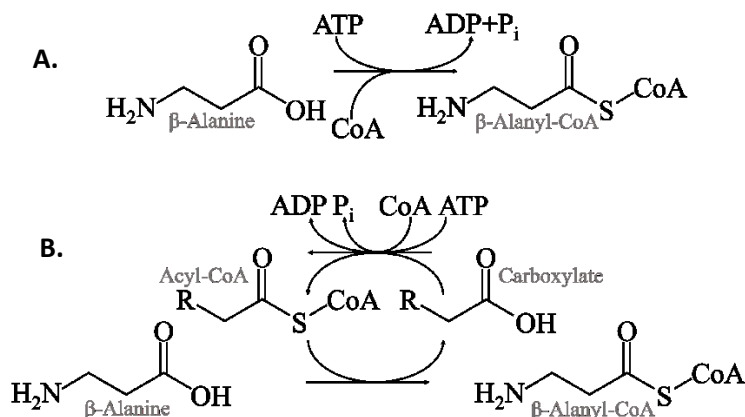
Figure. 3.7. A. ATP-dependent synthesis of β-Alanyl-CoA from β-Alanine. B. Synthesis of β-Alanyl-CoA from β-Alanine utilising the thioester bond from another acyl-CoA. The carboxylate can then be religated to CoA at the expense of ATP.

3.2.2.3. Deamination of β-Alaninyl-CoA to Acrylyl-CoA

Ammonia can be eliminated from β-Alanyl-CoA generating acrylyl-CoA by β-alanyl-CoA ammonia-lyase (βCal) (EC 4.3.1.6) (Figure. 3.8.A.). We selected the βCal from *Stigmatella aurantiaca* which had an activity of 12 Umg^{-1} with a Km of 70 µM on β-alanyl-CoA (Figure. 3.8.B.). This enzyme was prone to precipitating on ice but resolubilised at room temperature without loss of activity.
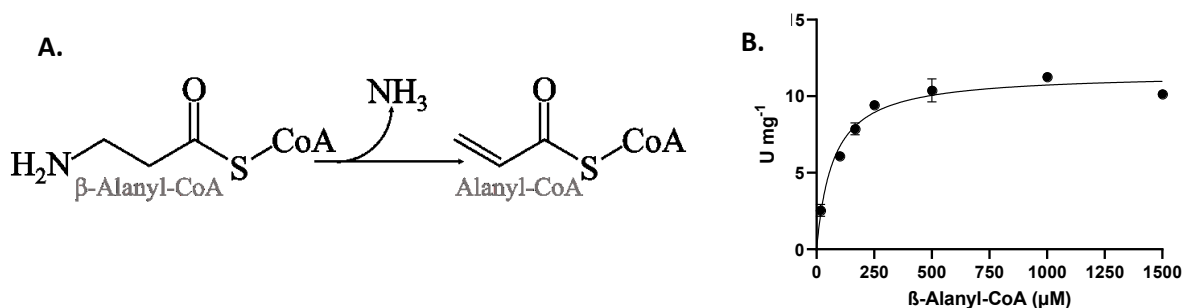
Figure. 3.8. **A.** Deamination of β-alanyl-CoA to acrylyl-CoA. **B.** Michaelis–Menten kinetics of *S. aurantiaca* βCal on β-alanyl-CoA. βCal and Ccr were added, and the oxidation of NADPH was monitored in real time at 360 nm. Assay described in Chapter 8.3.11.

3.3. Reductive Carboxylation of Acrylyl-CoA to (2S)-Methylmalonyl-CoA

Although it is possible to reduce acrylyl-CoA to propionyl-CoA at the expense of NADPH (Asao, 2013), and to then independently carboxylate propionyl-CoA to methylmalonyl-CoA in an ATP dependent manner, a useful alternative is reductive carboxylation. Acrylyl-CoA is carboxylated directly to methylmalonyl-CoA by exploiting a side activity (Peter, 2015) of crotonyl-CoA carboxylase/reductase (Ccr),(EC 1.3.1.85), (Erb, 2007),(Figure. 3.9.A.). Although the two-step carboxylation is more thermodynamically favorable (-62.5 ± 8.4 kJ/mol), the reductive carboxylation is still a highly feasible reaction (-23.7 ± 8.6 kJ/mol) and results in the consumption of one fewer ATP (Flamholz, 2012). We selected the Ccr from *M. extorquens* which has an activity of 274.4 Umg^{-1} with a Km of 0.78 mM on acrylyl-CoA and a Km of 0.21 mM on NADPH (Figure. 3.9.C. and D.).
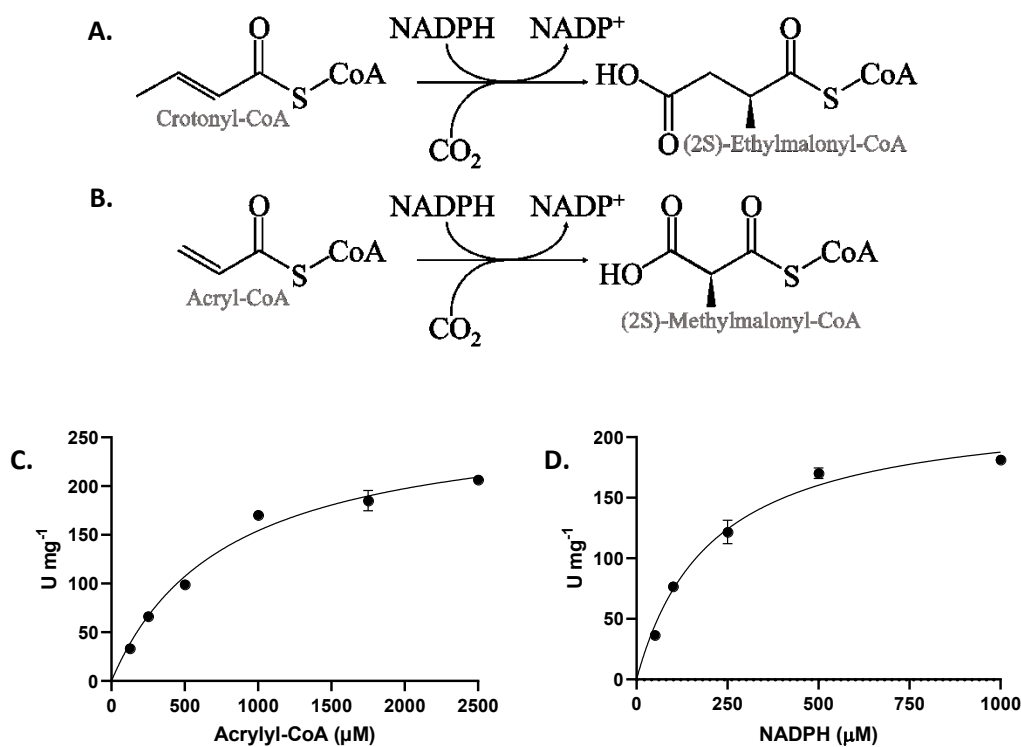
Figure. 3.9. Reductive carboxylation of **A.** crotonyl-CoA, the reaction for which the enzyme is named and **B.** acrylyl-CoA, the side-reactivity exploited in the HOPAC cycle. **C.** Michaelis–Menten kinetics of *M. extorquens* Ccr on acrylyl-CoA. **D.** Effect of NADPH. Assay described in Chapter 8.3.2.

3.4. Mutidomain Propionyl-CoA Synthetase

3.4.1. Propionyl-CoA Synthetase

Another interesting alternative for this sequence of reactions is the propionyl-CoA synthetase (Pcs) from *Erythrobacter sp.* NAP1. In addition to being specific for 3-hydroxyproionate, it is a multi-active site enzyme capable of replacing not only Hps, but also Ech and Ccr, reducing the total number of enzymes required (Figure. 3.10.A.). It contains a small reaction chamber in which acrylyl-CoA is generated and consumed without release (Bernhardsgrütter, 2018). This is an attractive feature as acrylyl-CoA is a strong electrophile capable of reacting with proteins and small organic molecules (Shimomura, 1994) and it has been shown to form covalent adducts with FAD (Shaw, 1985), four of which are included in the final version of HOPAC.

Unfortunately, this is not a perfect replacement because, although (2S)-methylmalonyl-CoA is produced by Pcs, the primary product is propionyl-CoA which is not otherwise found in the HOPAC cycle. Although this can easily be rectified by the addition of Pcc, it requires the expense of an additional ATP to complete carboxylation. A thorough dissection of this enzyme has previously been performed (Bernhardsgrütter, 2019) generating several mutants, some of which have a greater carboxylation efficiency (69 ± 3 %), which largely overcomes this issue albeit at the expense of catalytic efficiency. We tested the wildtype Pcs from *Erythrobacter* sp. NAP1 and found an activity of 140 mUmg^{-1} with a Km of 85 µM on 3-hydroxypropionate, 10 µM on ATP, 0.34 mM CoA, and 0.14 mM NADPH (Figure. 3.10.B-E.).
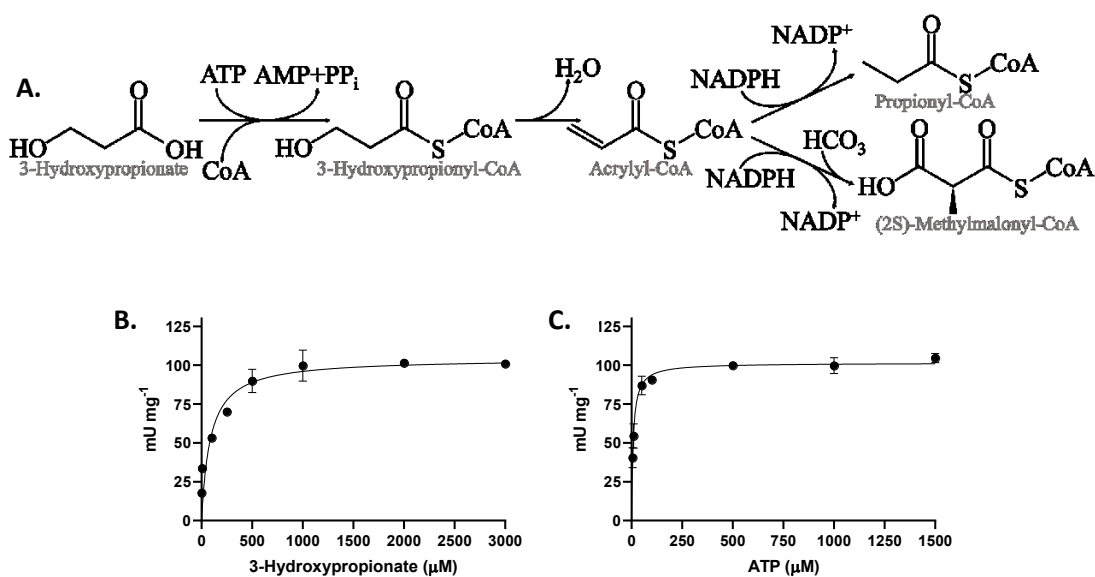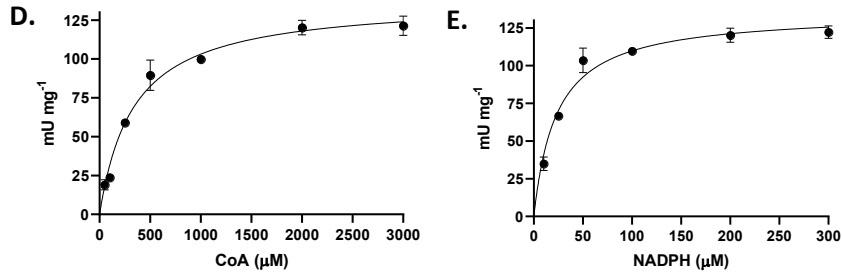
Figure. 3.10. **A.** Reaction scheme of WT Pcs from *Erythrobacter* sp. NAP1. This enzyme ligates 3-hydroxypropionate to CoA, dehydrates 3-hydroxypropionyl-CoA, and reduces acrylyl-CoA to propionyl-CoA, and to a much lesser extent (2S)-methylalonyl-CoA. Michaelis–Menten kinetics of *Erythrobacter* Pcs on **B.** 3-hydroxypropionate. **C.** Effect of ATP. **D.** Effect of CoA. **E.** Effect of NADPH. Pcs was added and the oxidation of NADPH was monitored in real time at 360 nm. Assay described in Chapter 8.3.2.

3.4.2. ATP-Dependent Carboxylation of Propionyl-CoA to (2S)-Methylmalonyl-CoA

When Pcs is used, the primary product is propionyl-CoA, an intermediate not otherwise found in the cycle. To convert propionyl-CoA to the next intermediate in the cycle, (2S)-methylmalonyl-CoA (Figure. 3.11.), we added the wild-type version of propionyl-CoA carboxylase from Chapter 2.4 as we knew it was active in this condition without unwanted side-reactions. The WT had an activity of 22 Umg^{-1} and a Km of 55 μM on propionyl-CoA, 0.27 mM on acetyl-CoA, and 0.33 mM on ATP.
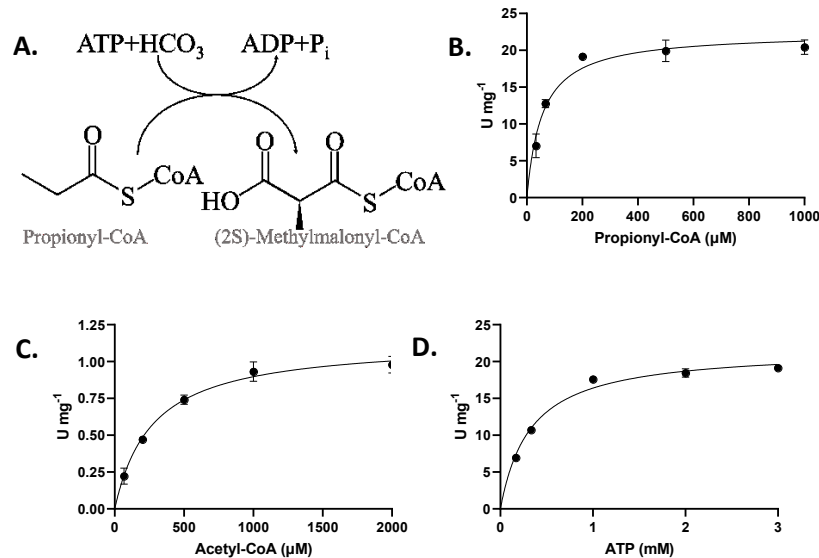
Figure. 3.11. **A.** ATP-dependent carboxylation of propionyl-CoA to (2S)-methylmalonyl-CoA. Michaelis–Menten kinetics of Pcc from *M. extorquens* on **B.** Propionyl-CoA. **C.** Acetyl-CoA. **D.** Effect of ATP. The

pyruvate kinase/lactate dehydrogenase from Sigma Aldrich was used, and the oxidation of NADH was monitored in real time at 360 nm. Assay described in Chapter 8.3.1.

3.5. Full Reductive Pathways

With all of the requisite enzymes in hand and activities being demonstrated, we set out to demonstrate flux through the possible combinations. Five scenarios were investigated: malonyl-CoA was converted to (2S)-methylmalonyl-CoA by **1.** C-terminal domain of Mcr, βapt, Act, βCal, and Ccr, **2.** C-terminal domain of Mcr, Abot, Act, βCal, and Ccr, **3.** Mcr, Act, Ech, and Ccr, **4.** Mcr, Hps, Ech, and Ccr, and **5.** Mcr, Pcs, and Pcc.

In the initial assays containing acyl-CoA transferases, we included the carboxylation of acetyl-CoA to malonyl-CoA by Acc, however we had minimal success producing (2S)-methylmalonyl-CoA. This is presumably due to the difficulty surrounding finding proper enzyme concentrations for transferases. If acetyl-CoA is carboxylated too slowly, the intermediates won't reach the end by the time the assay is quenched. If it is too fast however, there will be no acetyl-CoA left to transfer the CoA to 3-hydroxypropionate/β-alanine. To circumvent this problem, we simply began the assay with malonyl-CoA and a pool of acetyl-CoA which served as a CoA donor, and omitted Acc.

This led to a secondary problem for the scenario including βapt. L-alanine was added as an amino donor, but βapt has activity on L-alanine. This resulted in most of the acetyl-CoA and L-alanine being consumed in unwanted reactions and prevented the production of (2S)-methylmalonyl-CoA. As a work around, we ran the same assay without acetyl-CoA for five minutes allowing for the reduction of malonyl-CoA and transamination to β-alanine, then acetyl-CoA was added to allow for the transacylation. While the transferase scenarios were ultimately successful, they are not practical for full cycle assays due to these problems. These are worth revisiting if a β-alanyl-CoA synthetase can be developed.

For scenarios 4 and 5, we found rapid, nearly complete conversion to (2S)-methylmalonyl-CoA. This makes both of these pathways viable options for the construction of the full HOPAC cycle, however, as discussed previously, scenario 4 requires one fewer ATP.
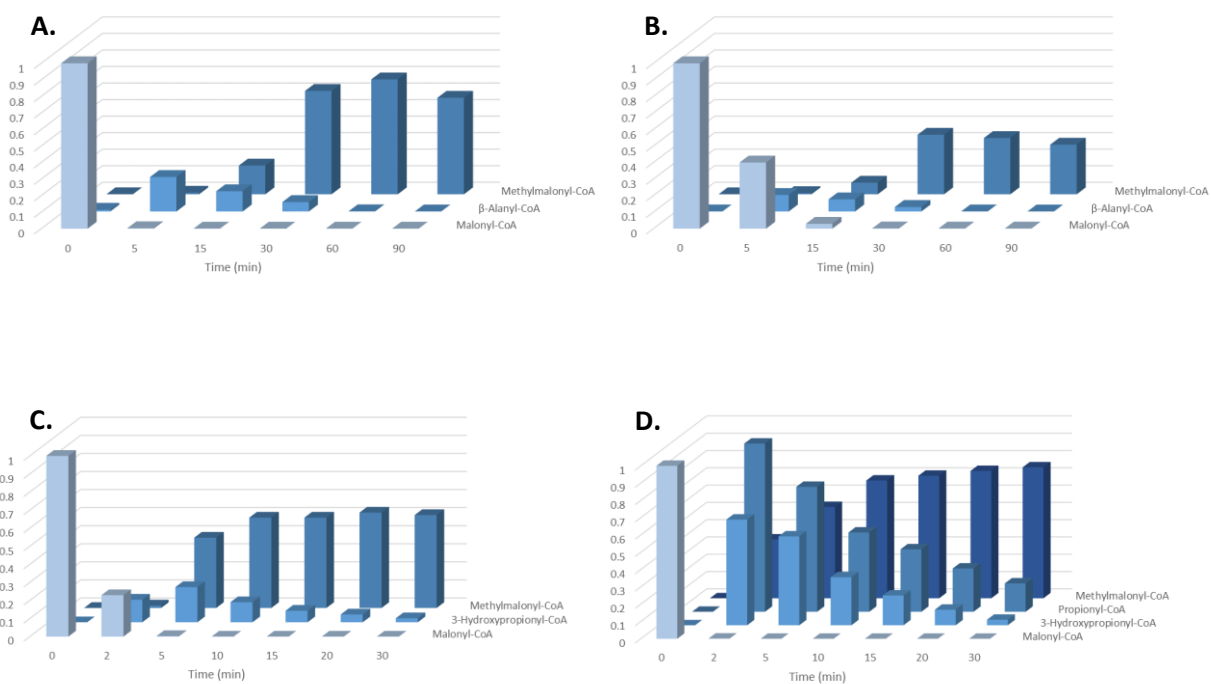
Figure. 3.12. Conversion of malonyl-CoA to (2S)-methylmalonyl-CoA by **A.** C-Mcr, βapt, Act, βCal, and Ccr, **B.** C-Mcr, Abot, Act, βCal, and Ccr, **C.** Mcr, Hps, Ech, and Ccr, **D.** Mcr, Pcs, and Pcc. Assay described in Chapter 8.5. Values are relative IC peak areas and are not meant to be quantitative. L-alanine and L-glutamate were added as amino donors for A and B respectively. Acetyl-CoA was added as CoA donor for A and B. Malonic semialdehyde, 3-hydroxypropionate, and β-alanine were not detected by this method, acrylyl-CoA was consumed as quickly as it was produced and was not detected. Similar results were found for scenario 3 as are seen in C.

4. Auxiliary Enzymes

The reactions described in the previous chapters relate to a core chemistry of the HOPAC cycle, converting one cycle intermediate into another until the original compound is regenerated and the cycle can continue. There are, however, several reactions that are employed on the periphery of the cycle to improve its performance. This chapter discusses these reactions and their intended effect on the cycle.

4.1. (2S)-Methylmalonyl-CoA Mutase-Associated GTPase MeaB

Mcm occasionally undergoes suicide inactivation during catalysis because it has a coenzyme B_{12} (AdoCbl) cofactor and utilises a radical intermediate (Padovani, 2006). This inactivation can be as frequent as one in ten turnovers (Thomä, 2000). It has also been seen that mutants lacking the accessory protein MeaB have a phenotype comparable to mutants lacking Mcm outright (Dobson, 2002; Korotkova, 2002). Because MeaB has been shown to have a protective effect on Mcm and is involved in the exchange of inactivated AdoCbl (Ruetz, 2019), it was clear that MeaB had the potential to extend the life of Mcm during cycling.

To investigate the extent to which Mcm inactivation affected the cycle, twin cycles were run either with additional Mcm added in the beginning or after a half hour. Consistent with inactivation, no change was seen with the former, but flux improved for the latter. To determine whether MeaB would have the desired protective effect, we developed a simple assay to intentionally inactivate Mcm. First, Mcm was incubated in the presence or absence of MeaB with (2S)-Methylmalonyl-CoA, next, samples were removed at regular intervals and added to succinyl-CoA dehydrogenase (SucD) and NADPH. SucD rapidly converts succinyl-CoA to succinic semialdehyde so if Mcm is active, the equilibrium will constantly be driven towards succinyl-CoA until everything is consumed. If, however, Mcm is inactivated, whatever portion of (2S)-methylmalonyl-CoA has been converted to succinyl-CoA will be consumed, but the remaining (2S)-methylmalonyl-CoA will be unaffected and can be viewed using LC-MS.

The result of this assay was clear (Figure. 4.1.), in the presence of methylmalonyl-CoA, Mcm was rapidly inactivated, but in the presence of MeaB, it remained active for at least 90 minutes. We attempted to determine whether the addition of ATP or GTP would further extend the life of the enzyme but were unsuccessful because it remained active for the full length of the assay without it. What was clear however was that the MeaB should protect Mcm for longer than we typically run the cycle, even in the absence of GTP.

A.

B.
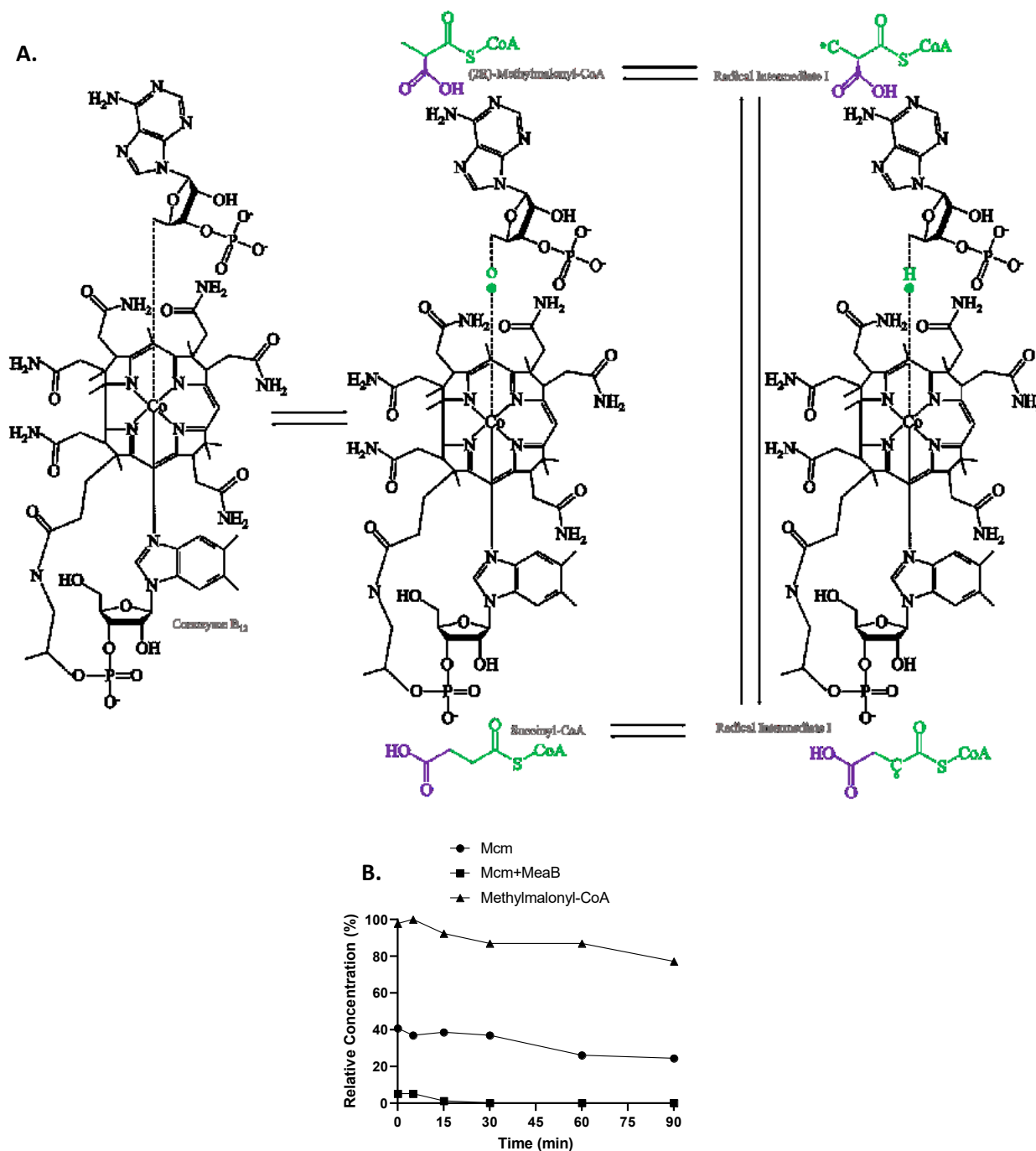
Figure. 4.1. **A.** Mechanism for (2S)-methylmalony-CoA to succinyl-CoA isomerisation utilising a radical intermediate. **B.** Mcm protection assay. After Mcm is added to (2S)-methylmalonyl-CoA, it is rapidly converted to succinyl-CoA until an equilibrium is reached. Mcm will continue to interconvert until it is inactivated. When Mcm is added alone, a little more than half of the (2S)-methylmalony-CoA is converted to succinyl-CoA, and it is inactivated. As such, ~40% remains after incubation with SucD. When Mcm is

added in concert with MeaB, the enzyme remains active. As succinyl-CoA is reduced by SucD, the equilibrium continues to regenerate succinyl-CoA until everything is converted to succinic semialdehyde. Assay described in Chapter 8.3.3.

4.2. Extension of the Electron Chain from Mcd

While oxidising succinyl-CoA, the FAD cofactor of Mcd is reduced to $FADH_2$. Mcd has minimal ability to oxidise its cofactor with O_2, and it is incapable of performing another succinyl-CoA oxidation until it does, so another electron acceptor must be provided. The inorganic electron acceptor ferrocenium is used for kinetic measurements, but it could not be added to full HOPAC cycle assays because it reacts directly with NADPH (Carlson, 1984). To circumvent this problem, we added electron transfer flavoprotein (Etf) which allowed Mcd to pass the electrons onto the FAD of Etf, and this allowed for modestly faster succinyl-CoA oxidation. Although both Mcd and Etf are capable of passing their electrons on to molecular oxygen, both are too slow for our purposes. In contrast, electron transfer flavoprotein quinone oxidoreductase (EtfQO), (Usselman, 2008), which allows Etf to pass its electrons on one step further, can pass its electrons onto molecular oxygen or soluble quinones. This dramatically increased the rate of oxidation of succinyl-CoA to levels nearly comparable to what is seen when ferrocenium is used as a direct electron acceptor (Figure. 4.2.).
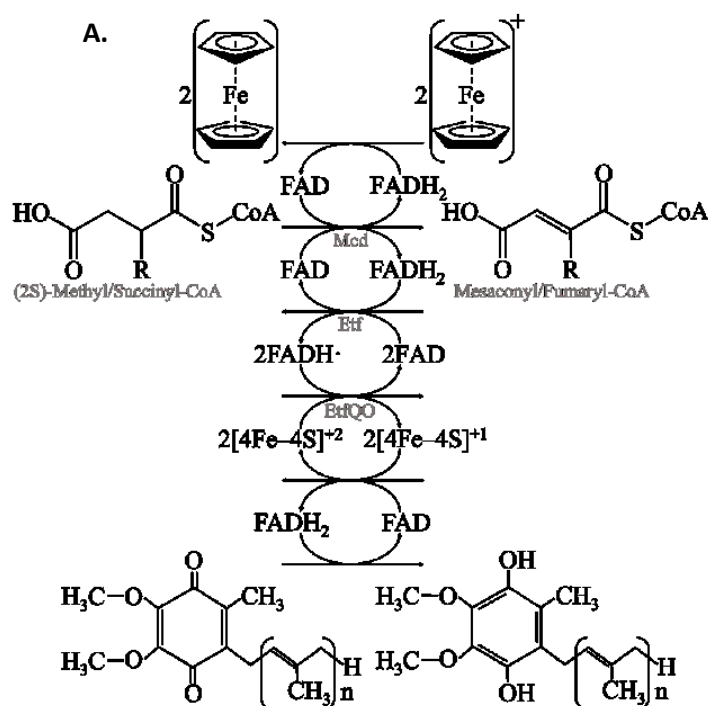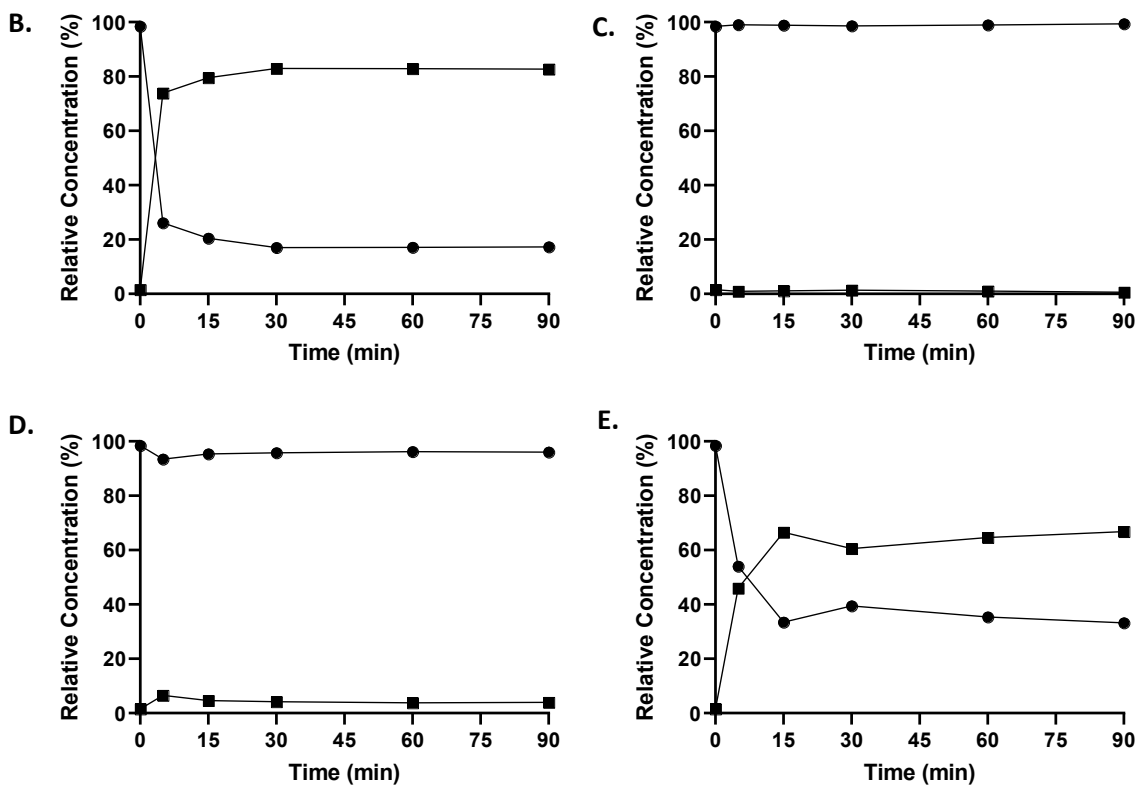
Figure. 4.2. **A.** Extension of the electron chain from Mcd. Electrons are passed from FAD in Mcd to FAD in Etf to 4Fe-4S and finally FAD in EtfQO. Circles are succinyl-CoA, squares are fumaryl-CoA. Oxidation of succinyl-CoA by Mcd in the presence of **B.** ferrocenium, **C.** O_2, **D.** Etf and O_2, **E.** Etf, Etf-QO, and O_2 as electron acceptors. E was also performed anaerobically, and no activity was detected. Assay described in Chapter 8.3.5.

4.3. Reactive Oxygen Species

4.3.1. Disproportionation of O_2^- and H_2O_2

The HOPAC cycle is always run aerobically because molecular oxygen is used as the terminal electron acceptor of the oxidation of succinate or succinyl-CoA. The result of this reaction is the production of reactive oxygen species. To consume superoxides, we used recombinant bovine superoxide dismutase (EC 1.15.1.1) from Sigma-Aldrich (CAS 9054-89-1), and the resulting peroxides were consumed by catalase (EC 1.11.1.6) from *Bos taurus* and an NADH-dependent peroxiredoxin (EC 1.11.1.26) from *E. coli* which was previously shown to be effective at decomposing peroxides at concentrations lower than catalase (Wan, 2019).

4.3.2. Coenzyme A Oxidation

A pool of coenzyme A is required for the HOPAC cycle due to its release during the reduction of malonyl-CoA in all versions, and succinyl-CoA in some versions. However, at least in part due to the generation of reactive oxygen species during the oxidation of succinate or succinyl-CoA, we suspected that the CoA might oxidise forming CoA dimers (CoAD). Indeed, when we monitored the concentration of CoA and CoAD under these conditions, the CoA pool was depleted as the CoAD concentration increased.

Our first solution to this issue was the addition of reducing agents DTT, BME, glutathione, or TCEP. Counterproductively, we found that BME and glutathione formed disulfide bonds with CoA, retaining it in an inaccessible form. In addition, it was found that reducing agents could accelerate the loss of cycle intermediates, presumably through the cleavage of the thioester bond (Simpson, 1981).

We selected instead a CoA-disulfide reductase (Cdr) (EC 1.8.1.14) from *Staphylococcus schweitzeri*. In exchange for one NADPH, Cdr cleaves one CoAD, releasing two CoA (Figure. 4.3.) specifically without sequestering CoA or cleaving CoA-thioesters (delCardayré, 1998). This addition allowed us to keep a lower concentration of free CoA throughout, without concern that the synthetase reactions would be prevented due to loss of one of their substrates.
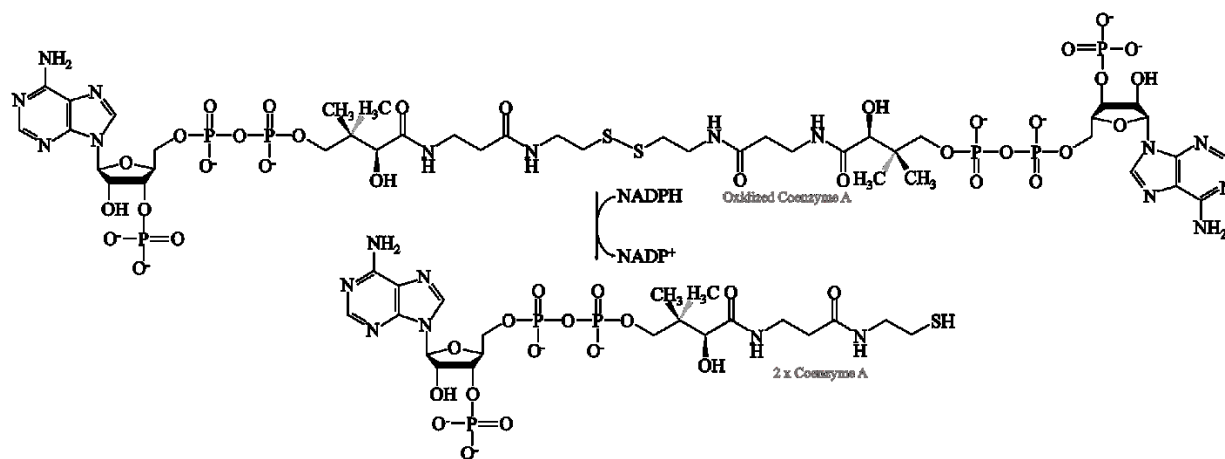
Figure. 4.3. Reduction of oxidised CoA dimers to two molecules of CoA at the expense of NAD(P)H as performed by Cdr.

4.4. Coenzyme A Dephosphorylation

One potential issue faced in the background of the HOPAC cycle is the dephosphorylation of CoA and acyl-CoAs. If the dephosphorylated compounds are not accepted by their respective enzymes, they will become dead-end products. Dephospho-CoA kinase (EC 2.7.1.24) was previously shown to have activity

not just on dephospho-CoA, but also dephospho-acetyl-CoA, dephospho-malonyl-CoA, and dephospho-succinyl-CoA (Wadler, 2007). We tested for activity on the remaining acyl-CoAs and found activity on all of them (Figure. 4.4.). The dephospho-CoA kinase (CoAE) from *E. coli* was chosen for this purpose.
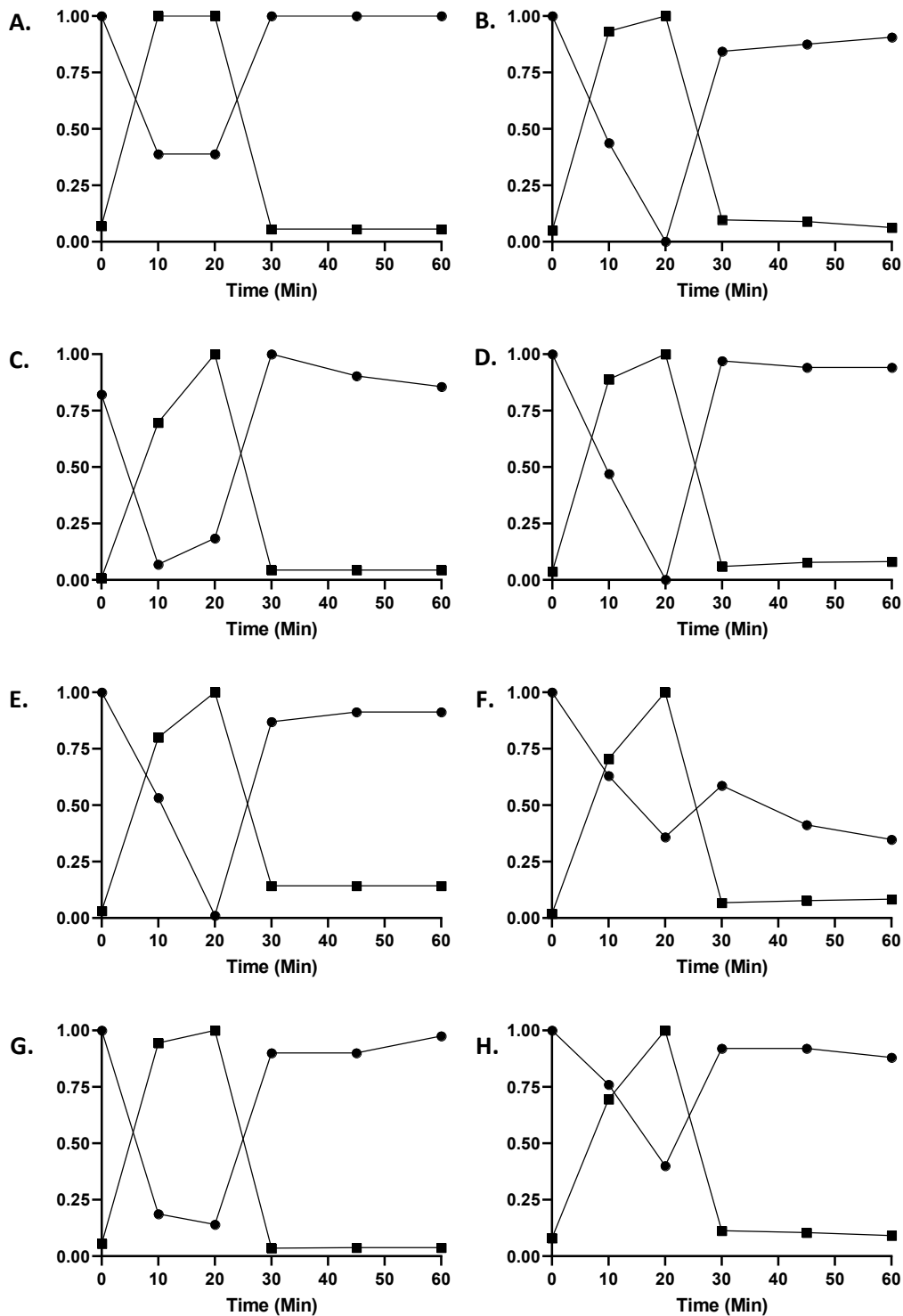
Figure. 4.4. Dephosphorylation and rephosphorylation of acyl-CoAs. **A.** acetyl-CoA. **B.** malonyl-CoA. **C.** 3-hydroxypropionyl-CoA. **D.** propionyl-CoA. **E.** methylmalonyl-CoA. **F.** fumaryl-CoA. **G.** (S)-malyl-CoA. **H.** β-alanyl-CoA. Circles are acyl-CoA, squares are dephosphoacyl-CoA. Samples were incubated with shrimp alkaline phosphatase for 20 minutes, passed through a 5 kDa cutoff filter to remove phosphatase, then added to CoAE. Assay described in Chapter 8.3.10.

4.5. ATP Regeneration

There are 2-4 ATP-dependent reactions present in different versions of the HOPAC cycle. Because high concentrations of ATP can be inhibiting for some reactions, and low concentrations will inevitably become limiting, we investigated multiple methods for regenerating ATP. Depending on the version of the cycle, ATP is converted to ADP and/or AMP. In principle, there are many enzymes that can serve this purpose, all of which exploit a high-energy bond to attach a phosphate group (Mordhorst, 2020). Common solutions include using adenylate kinase (EC 2.7.4.3) to convert an ATP and AMP to two ADP and using creatine kinase (EC 2.7.3.2), (Zhang, 2003) or pyruvate kinase (EC 2.7.1.40) to then convert the ADP to ATP at the expense of a pool of phosphocreatine or phosphoenolpyruvate respectively. We opted to use polyphosphate kinase (EC 2.7.4.1) to perform both reactions, one from *Acinetobacter johnsoni* for the conversion of AMP to ADP and one from *Sinorhizobium meliloti* for the conversion of ADP to ATP (Mordhorst, 2019).

4.6. NADPH Regeneration

4.6.1. NAD(P)H Oxidation

Much like ATP, the HOPAC cycle is dependent on multiple NAD(P)H-dependent reactions and there are several enzymes that could be used to recycle reducing equivalents. Common enzymes utilised for this purpose include isopropanol dehydrogenase (EC 1.1.1.80) and glucose dehydrogenase (E.C. 1.1.1.47), (Xu, 2007). We selected a formate dehydrogenase (EC 1.2.1.2) from *Mycobacterium vaccae* N10 which has been mutated to accept NADP$^+$ (D221A), (Hoelsch, 2013).

4.6.2. NAD(P)H Hydration

NAD(P)H can be hydrated to (R)-NADPHX and (S)-NADPHX (Figure. 4.5.) which can be inhibitory to NAD(P)H dependent enzymes. This process is usually enzyme mediated, but can also occur spontaneously. Typically, an epimerase (EC 5.1.99.6) is used to convert (R)-NADPHX to (S)-NADPHX which can then be dehydrated by an ADP-dependent dehydratase (EC 4.2.1.136) to NADPH. Conveniently, these enzymes are fused into one in *E. coli* (Marbaix, 2011) so the dual-activity enzyme was used for this purpose.
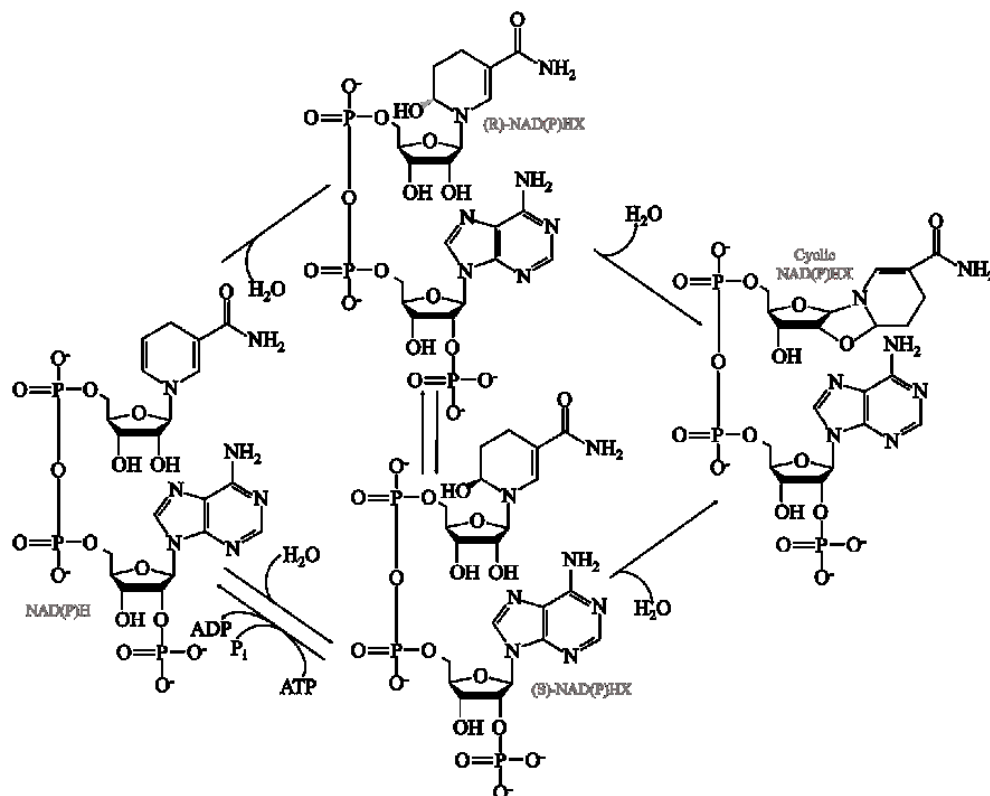
Figure. 4.5. Hydration of NAD(P)H is caused by glyceraldehyde 3-phosphate dehydrogenase but also occurs spontaneously. (R)-NAD(P)HX and (S)-NAD(P)HX can be interconverted by an epimerase, and (S)-NAD(P)HX can be dehydrated back to NAD(P)H by an ADP-dependent dehydratase. In the case of *E. coli*, these enzymes are united in one.

4.7. Soluble Carbon

Prior to the initiation of an assay, $NaHCO_3$ was added to the solution. This is useful both because HCO_3^- is the substrate of the biotin-dependent carboxylases (Ogita, 1988), but it also allowed for an easy method to introduce heavy carbon in the form of $^{13}C\text{-}HCO_3^-$ for labelling studies. The carbon source for the reductive carboxylase, however, is CO_2 (Erb, 2009). To accelerate the equilibrium between CO_2 and HCO_3^-, we used carbonic anhydrase (EC 4.2.1.1) from Sigma-Aldrich (CAS 9001-03-0).

4.8. L-Alanine and L-Glutamate Dehydrogenase

When transaminases are used to produce β-alanine, an amino acid needs to be provided as the amino donor. L-alanine is provided for βapt and L-glutamate is provided for Abot (Figure. 4.6.). If this pathway is successfully implemented into a full cycle, the amino acids will eventually become limiting. To overcome this, we added alanine dehydrogenase (Adh) (EC 1.4.1.1) or glutamate dehydrogenase (Gdh) (EC

1.4.1.2/1.4.1.3/1.4.1.4) with ammonium chloride. We selected the Adh from *C. sphaeroides* and the Gdh from *Paracoccus denitrificans* which has an activity of 47.58 Umg^{-1} with a Km of 35.87 µM on 2-oxoglutarate, 10.73 µM on NADPH, 85.87 mM on NH$_4$, 488.3 µM on L-glutamate, and 7.15 µM NADP$^+$.

L-amino acid dehydrogenases typically oxidise the L-amino acid to its corresponding 2-oxo-acid while releasing ammonia and generating a reducing equivalent. In spite of being endergonic (Dave, 2019), this reaction is driven towards oxo-acid production by maintaining a high Km for ammonia (Plaitakis, 2017). However, maintaining an excess of ammonia and a pool of reducing equivalents allows for the reduction of pyruvate or α-ketoglutarate to L-alanine and L-glutamate respectively.
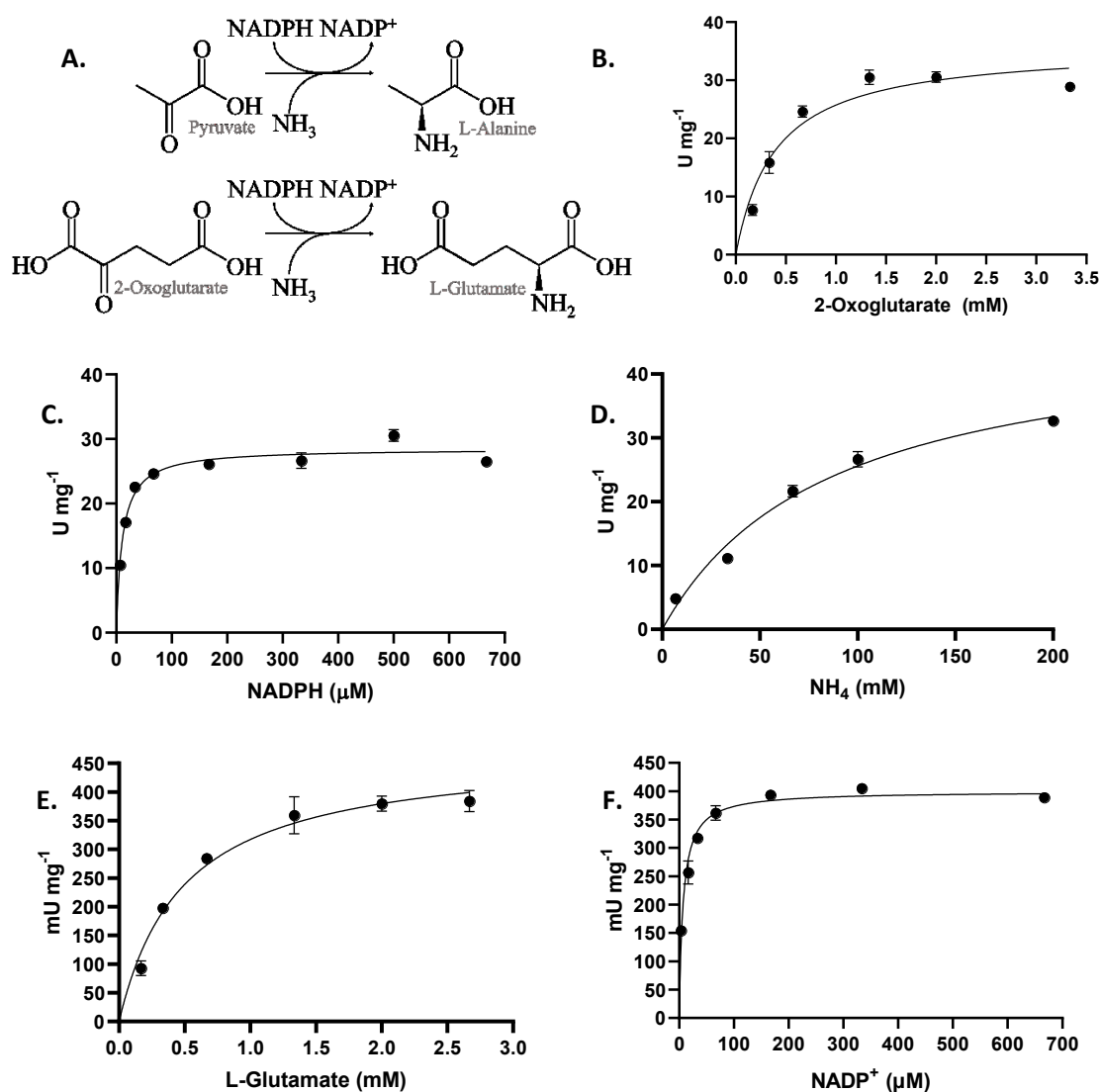
Figure. 4.6. **A.** Reductive amination of pyruvate to L-alanine and 2-oxoglutarate to L-glutamate. Michaelis–Menten kinetics of *P. denitrificans* Gdh **B.** 2-oxoglutarate. **C.** NADPH. **D.** NH$_4$. **E.** L-glutamate. **F.** NADP$^+$.

Oxidation of NADPH or reduction of $NADP^+$ was monitored in real time at 360 nm. Assay described in Chapter 8.3.2.

4.9. Read Out Modules

The primary product of the HOPAC cycle is glyoxylate which is generated during the cleavage of (S)-malyl-CoA to acetyl-CoA by Mcl. For in vitro assays, it is helpful to convert glyoxylate into another compound which prevents the reverse reaction. This is especially pertinent for versions of the cycle that contain propionyl-CoA because it can be condensed with glyoxylate by Mcl to generate (2R,3S)-β-methylmalyl-CoA. For in vivo applications, it is important to ensure that glyoxylate is efficiently integrated into central metabolism.

We explored natural reactions containing glyoxylate to determine which reactions are thermodynamically favourable and generate a central metabolite. Because the chemistry of the HOPAC cycle is similar to the 3-hydroxypropionate bicycle, versions that include propionyl-CoA can utilise mesaconyl-CoA C1-C4 CoA transferase (EC 5.4.1.3) and mesaconyl-C4-CoA hydratase (EC 4.2.1.153) from *Chloroflexus aurantiacus* to generate pyruvate (Figure 4.7.). Mch and Mcl are also required for this pathway, but conveniently, they are already present in the HOPAC cycle.

A slightly more complicated and more expensive output is the β-hydroxyaspartate cycle. Adding β-hydroxyaspartate aldolase (EC 4.1.3.14), β-hydroxyaspartate dehydratase (EC 4.2.1.38), iminosuccinate reductase (EC 1.4.3.16), and aspartate-glyoxylate aminotransferase (EC 2.6.1.1) allows the conversion of two glyoxylate to one oxaloacetate at the expense of one NADH. Although this method is complicated, it does have the interesting potential to act as an anapleurotic pathway. Oxaloacetate can be reduced to (S)-malate (EC 1.1.1.37/1.1.1.82/1.1.1.299), then ligated to CoA by adding Mcs and regenerating (S)-malyl-CoA.

A similar approach is to transaminate glyoxylate to glycine using L-glutamate (EC 2.6.1.4), L-aspartate (EC 2.6.1.35), L-alanine (EC 2.6.1.44), or L-serine (EC 2.6.1.45). The amino acid can then be regenerated by reductive transamination using their respective dehydrogenases: L-glutamate (EC 1.4.1.2/1.4.1.4), L-aspartate (EC 1.4.1.21), L-alanine (EC 1.4.1.1), and L-serine (EC 1.4.1.7). This is impractical in vivo due to the high Km of NH_3 but may be useful in vitro.

Another option is the addition of glyoxylate carboligase (EC 4.1.1.47) and tartronate semialdehyde reductase which converts two glyoxylate to one glycerate at the expense of one NADH (EC 1.1.1.60). Unfortunately, this method results in the release of one CO_2, partially undoing the work of the cycle.

We explored the above options but ultimately settled on the simplest option of using glyoxylate reductase (Gox) to reduce glyoxylate to glycolate in a single step at the expense of one NAD(P)H (EC 1.1.1.26). This is convenient for in vitro assays because it only requires a single enzyme and is highly exergonic (-41.1 ± 1.8 kJ/mol), especially when the NADPH pool is maintained by regeneration. It also has the potential to be useful in vivo when coupled to the TaCo pathway (Chapter 1.3.3).
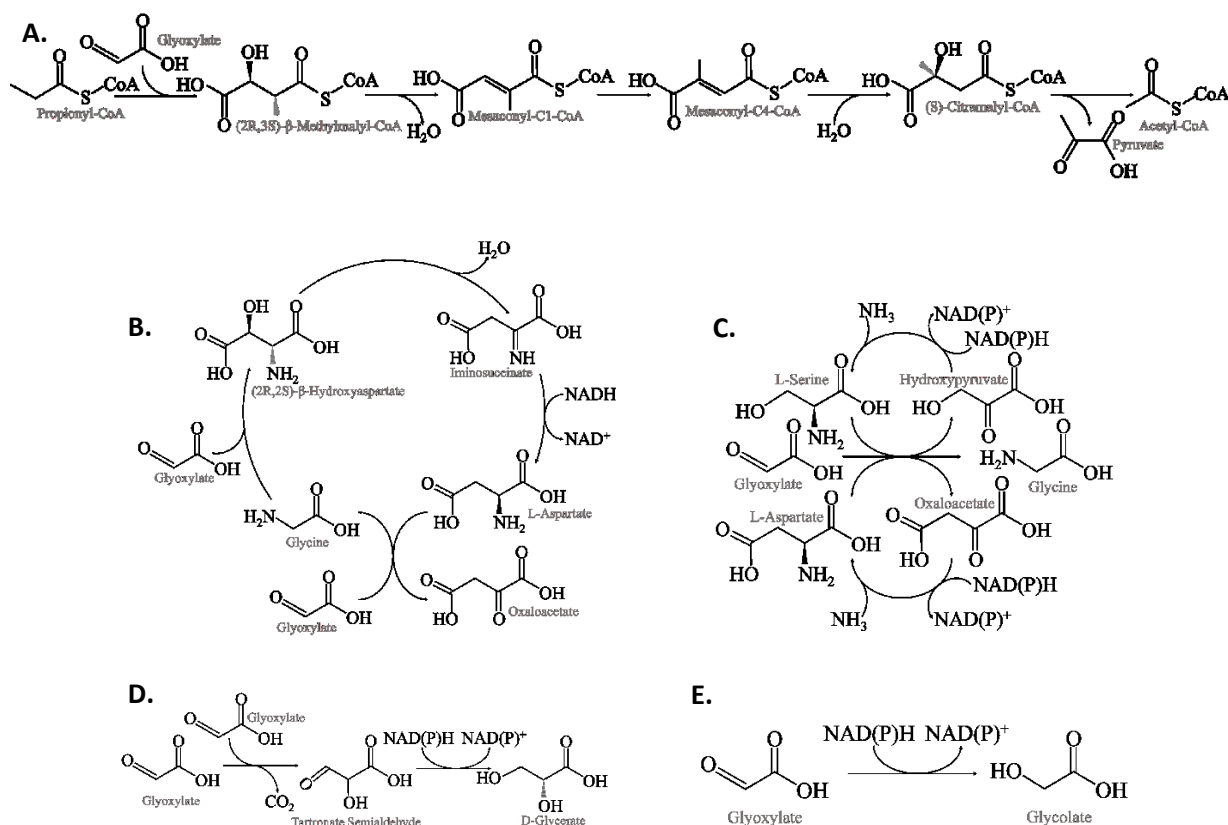
Figure. 4.7. Potential options for utilising glyoxylate, the C2 compound produced by the HOPAC cycle. **A.** Reactions borrowed from the 3HPB which converts glyoxylate to pyruvate. **B.** The β-hydroxyaspartate cycle which converts glyoxylate to oxaloacetate at the expense of NADH. **C.** Transamination of glyoxylate to glycine with amino acid regeneration at the expense of NAD(P)H. **D.** Carboligation of glyoxylate and reduction to D-glycerate at the expense of NAD(P)H and CO_2. **E.** Reduction of glyoxylate to glycolate at the expense of NAD(P)H, the method used in this project.

5. The HOPAC Cycle

5.1 Recapitulation

In previous chapters, the activity of individual enzymes was described, and the potential of different pathway alternatives was evaluated. For the oxidative pathway, converting (2S)-methylmalonyl-CoA to acetyl-CoA, four alternatives were explored. In all cases, (2S)-methylmalonyl-CoA was converted to succinyl-CoA, and acetyl-CoA was generated from (S)-malyl-CoA using the same enzymes. For the intervening chemistry, two broad approaches were used. First, succinyl-CoA was converted to succinate, succinate was oxidised to fumarate, and fumarate was hydrated to (S)-malate before synthesising (S)-malyl-CoA. Unfortunately, the oxidation of succinate proved to be an insurmountable bottleneck, and effectively ruled out these pathways in vitro. This left us with only one functional oxidative pathway, where succinyl-CoA is oxidised to fumaryl-CoA, and fumaryl-CoA is hydrated to (S)-malyl-CoA. Fortunately, this pathway functioned well, rapidly affecting a nearly complete conversion to acetyl-CoA (Chapter 2.5).

For the reductive pathway, converting acetyl-CoA back to (2S)-methylmalonyl-CoA, five alternatives were explored. In four of the five, acetyl-CoA is converted to malonic semialdehyde, and acrylyl-CoA is converted to (2S)-methylmalonyl-CoA using the same enzymes. In the intervening chemistry, again, two approaches were used. First, malonic semialdehyde was transaminated to β-alanine which is then ligated to CoA, and β-alanyl-CoA is deaminated to acrylyl-CoA. Two variants of this pathway were evaluated where a transaminase used either L-alanine or L-glutamate as an amino donor. Although it was possible to produce appreciable concentrations of (2S)-methylmalonyl-CoA utilising these pathways, they had to be held under artificial conditions to allow completion. An independent pool of acetyl-CoA, for example, needed to be maintained for the transacylation to move forward. Additionally, the transferase had activity on L-alanine, making this a problematic combination with the βapt transaminase. As such, while these may be interesting options to revisit for in vivo applications, they are impractical in vitro until a β-alanyl-CoA synthetase is developed.

For the next approach, malonic semialdehyde was reduced to 3-hydroxypropionate and ligated to CoA generating 3-hydroxypropionyl-CoA before being dehydrated to acrylyl-CoA. Two variants of this pathway were evaluated where either a transferase or a synthetase was used to generate 3-hydroxypropionyl-CoA. Much like the β-alanyl-CoA transferase, an independent pool of acetyl-CoA had to be maintained for this reaction to move forward and is likely impractical for in vitro applications. The synthetase, on the other hand, functioned well and saw a rapid and nearly complete conversion to (2S)-methylmalonyl-CoA.

The final alternative utilised the same enzymes to generate 3-hydroxypropionate, but then employed the multi-compartmental Pcs which is capable of ligating 3-hydroxypropionate to CoA, dehydrating 3-hydroxypropionyl-CoA to acrylyl-CoA, and reducing acrylyl-CoA to propionyl-CoA. Propionyl-CoA was then carboxylated to (2S)-methylmalonyl-CoA at the expense of ATP. This option also functioned well, although due to the additional ATP requirement, it is a less energetically efficient pathway.

To determine the feasibility of different versions of the HOPAC cycle, we created assays containing ^{13}C bicarbonate and carbonic anhydrase to ensure an excess of heavy bicarbonate and CO_2. We started the assay by adding acetyl-CoA, and quenched samples with formic acid. After centrifugation, supernatants were analysed by LCMS to determine which, if any, compounds were generated and to what extent ^{13}C was incorporated.

On its first trip around the cycle, an intermediate is carboxylated twice, and incorporates two ^{13}C. One of these ^{13}C is released in glyoxylate, the second is retained in the regenerated acetyl-CoA (Figure. 5.1). This allows us to determine how many times a particular molecule has passed through the cycle. Unlabelled acetyl-CoA is added to the assay, when it completes its first pass, it is labelled once, after its second pass, it is labelled twice. Fully labelled (S)-malyl-CoA are intermediates that are completing their third pass around the cycle. This is the extent that we can learn from this method because acetate is a C2 compound and there are no other carbons to label, so any additional revolutions of the cycle will also generate twice labelled acetyl-CoA.
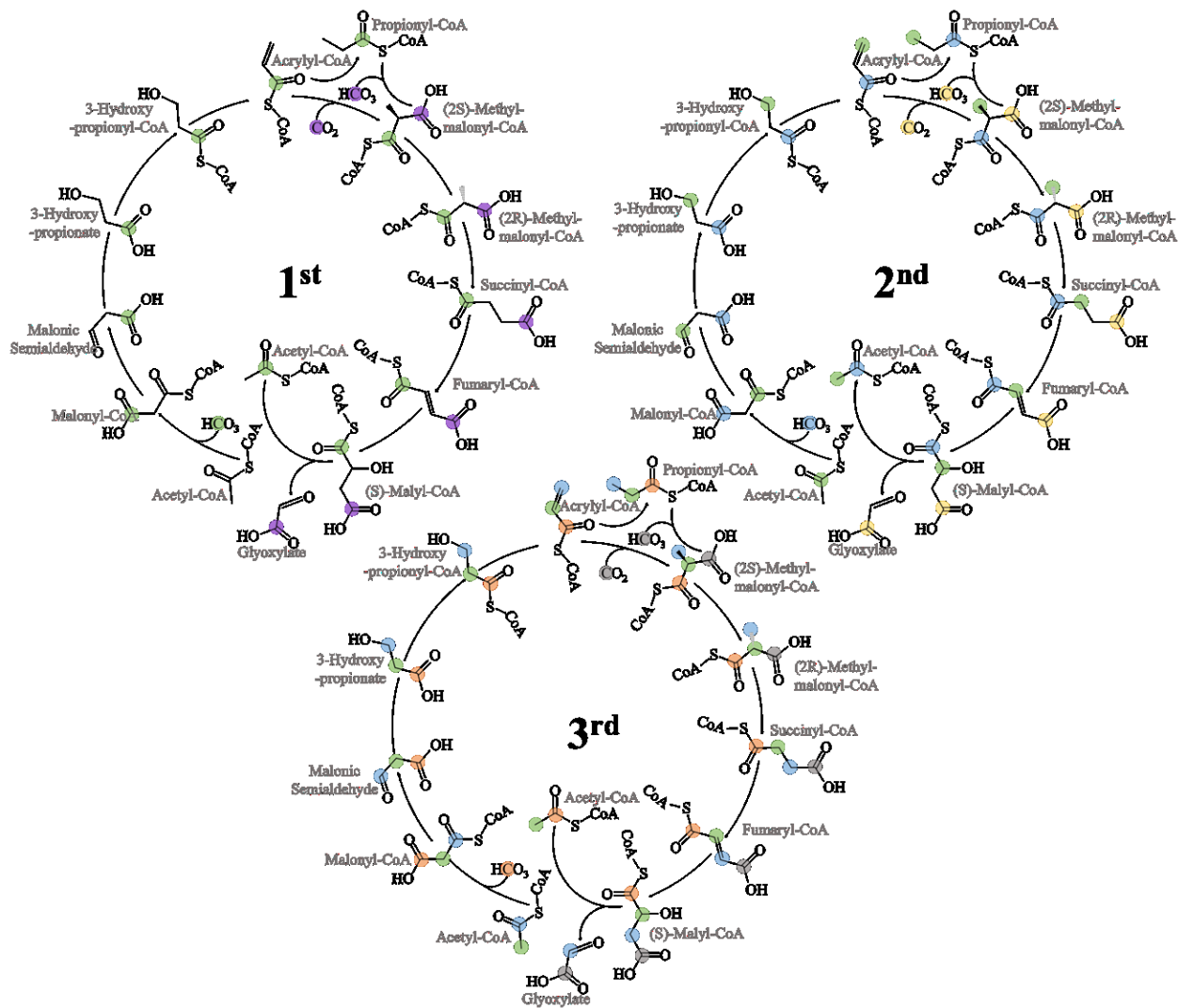
Figure. 5.1. ^{13}C labelling pattern in the HOPAC cycle. ^{13}C bicarbonate is added along with carbonic anhydrase to ensure heavy bicarbonate and CO_2 are available for their respective carboxylation reactions. In the first turn of the cycle, the green carbon is incorporated in the carboxylation of acetyl-CoA. The purple carbon is incorporated in the carboxylation of acrylyl-CoA or propionyl-CoA depending on which version of the HOPAC is used. At the cleavage of (S)-malyl-CoA, the initial carbon is retained as the C1 of a labelled acetyl-CoA which is free to travel around the cycle again, the second carbon is released in glyoxylate. At the end of the third turn of the cycle, (S)-malyl-CoA is completely labelled so the product will be twice labelled acetyl-CoA, the same product as the second turn of the cycle. As such, any additional revolution of the cycle should produce completely labelled intermediates and would be indiscriminable with this method.

5.2. Propionyl-CoA Synthetase Version

In early assays, we utilised an Hps from *N. maritimus* to ligate 3-hydroxypropionate to CoA, but quickly found that this enzyme was insufficient for our purposes because it rapidly lost activity. Although the version of HOPAC employing Pcs will be less energetically efficient, there are benefits to this enzyme. Even though Pcc must be used in tandem with Pcs to carboxylate propionyl-CoA to (2S)-methylsuccinyl-CoA, Pcs performs the ligation, dehydration, and reduction, resulting in a net one fewer enzyme required. An even more appealing aspect of Pcs is that it traps the acyl-CoA in an internal catalytic chamber until the reaction is complete. This is valuable because one of the intermediates, acrylyl-CoA is highly reactive, but unable to be involved in any number of unknown and unwanted non-enzymatic reactions while it is sequestered.

Unfortunately, the activity of Pcs is quite low, at just 140 mUmg^{-1}, so we had to use large volumes of Pcs to force the cycle to progress. Nevertheless, both Pcs and Pcc were active under the reaction conditions, and we were able to generate labelled acetyl-CoA (Figure. 5.2.) meaning that every reaction in the cycle was operational.

It is important to note that efforts have been made to mutate Pcs to a reductive carboxylase and these efforts have been rewarded (Bernhardsgrütter, 2019). The double mutant D1302S T1753M has a carboxylation efficiency of nearly 70%, an impressive improvement over the ~3% of the wild type. Utilising this mutant would greatly reduce the penalty of using Pcs, because only 1/3 of intermediates would need to be carboxylated by Pcc, the rest would be directly reductively carboxylated by Pcs saving ATP. Unfortunately, this mutant only has ~6% of the overall activity of the wild type Pcs. Given that Pcs concentration is already limiting for this version of the cycle, replacing it with a slower mutant is not practical.

This is, however, an interesting option if the cycle is implemented in vivo. Because this mutant is already a reasonably efficient carboxylase, and it is very slow, it may be possible to implement the cycle without Pcc, instead allowing the Acc to carboxylate any propionyl-CoA produced. In this case, there would be a strong selection for a faster enzyme, and as it became quicker, selection for greater carboxylation efficiency. This may facilitate a system to simultaneously optimise HOPAC and evolve a better carboxylating Pcs.
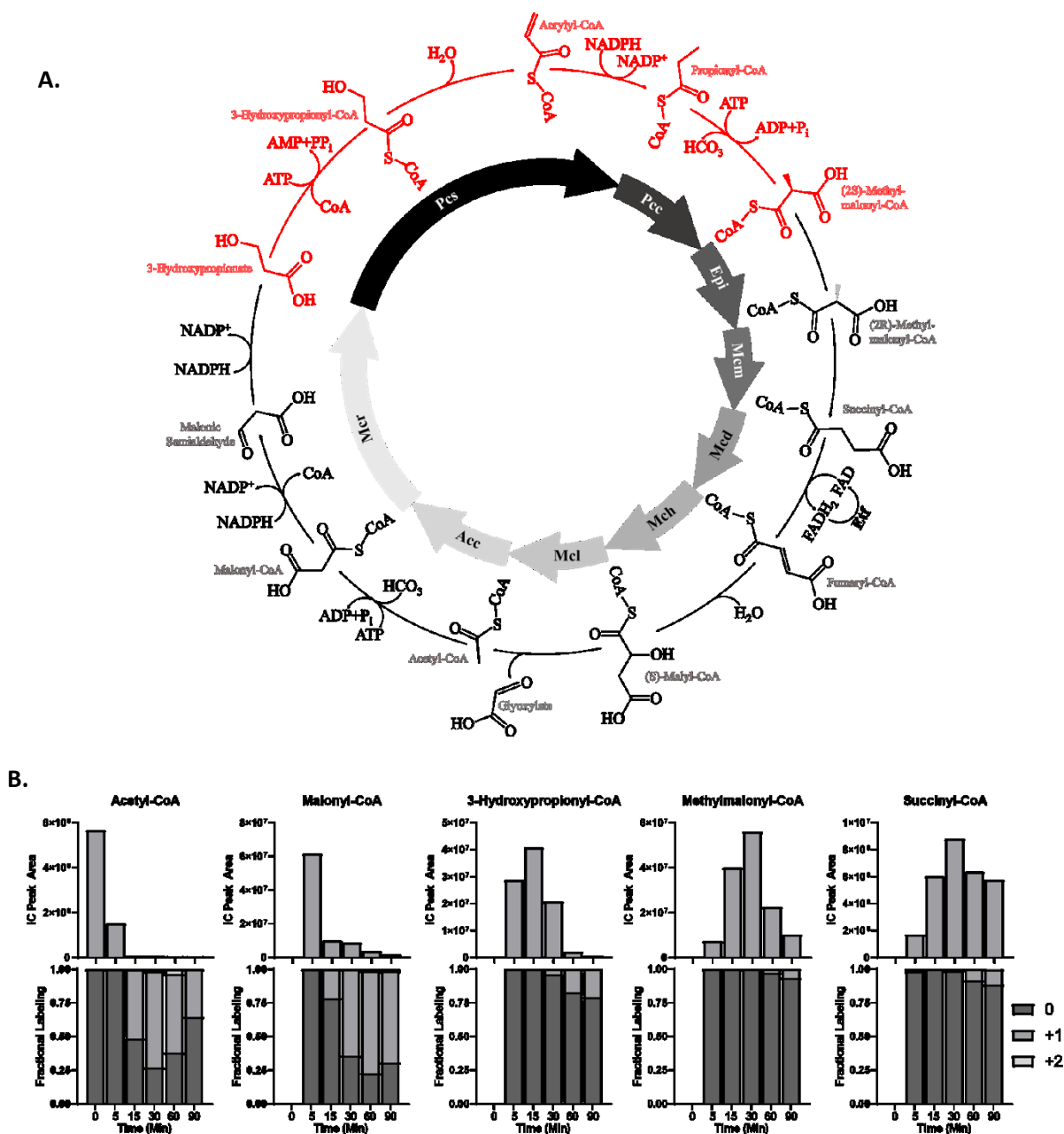
Figure. 5.2. The HOPAC cycle with Pcs and Pcc. **A.** Chemistry of the HOPAC cycle when Pcs is employed. Relevant reactions are highlighted in red. **B.** Intermediates as detected by LCMS. Above, total level (Ion Count), below, relative labelling. Some +1 compounds are produced indicating molecules are passing through every reaction in the cycle.

5.3. 3-Hydroxypropionyl-CoA Synthetase Version

Although the Pcs version of the cycle was functional, we continued to look for a 3-hydroxypropionyl-CoA synthetase. Ech, which dehydrates 3-hydroxypropionyl-CoA to acrylyl-CoA, and Ccr, which reductively

carboxylates acrylyl-CoA to (2S)-methylmalonyl-CoA are both highly active, easily produced, and store well at high concentrations. Additionally, Ccr has minimal reductase activity, achieving only 10% in the absence of CO_2 (Erb, 2009). Since HOPAC is provided bicarbonate and carbonic anhydrase, CO_2 concentration should be stable, and little propionyl-CoA produced. This results in a net savings of one ATP for every two carbons fixed.

We found a propionyl-CoA ligase from *C. necator* which generates propionyl-CoA from propionate and CoA, rather than the multifunctional Pcs that generates propionyl-CoA from 3-hydroxypropionate and CoA, discussed above. This enzyme has a significant activity generating 3-hydroxypropionyl-CoA from 3-hydroxypropionate and CoA, which allowed us to implement it with Ech and Ccr, and to determine if this more energetically favourable, but less thermodynamically favourable version of the cycle would function. Once again, the cycle was functional generating not only labelled acyl-CoA intermediates, but low concentrations of twice labelled intermediates (Figure. 5.3.) suggesting greater cycle processivity.

An important consideration when employing Ccr as a reductase is that the reaction is reversible. Most reactions are, but this is a potential problem for Ccr because, while the reductive carboxylation of acrylyl-CoA to (2S)-methylmalonyl-CoA is kinetically favoured, the reduction of acrylyl-CoA to propionyl-CoA is thermodynamically favoured (-57.5 ± 6.5 kJ/mol vs -23.7 ± 8.6 kJ/mol). This is not much of a problem when there is a steady flux through the cycle, but if a significant pool of methylmalonyl-CoA is maintained, it will be occasionally decarboxylated by Ccr. Since it is far more difficult to oxidise propionyl-CoA than it is to decarboxylate (2S)-methylmalonyl-CoA, an equilibrium will gradually convert the pool to propionyl-CoA, effectively negating the benefit of using Ccr instead of Pcs. Worse than this, Ccr doesn't have the capacity to carboxylate propionyl-CoA, so a Pcc will be required.

Conveniently, this problem can be mitigated relatively easily. By optimising enzyme concentrations, the methylmalonyl-CoA pool can be kept relatively small so that only an insignificant portion will be converted to propionyl-CoA. While this might otherwise be a dead-end product, our use of an engineered propionyl-CoA carboxylase to carboxylate acetyl-CoA results in a built-in recovery system for propionyl-CoA. This may become problematic at high concentrations of propionyl-CoA, not only because of the ATP expense, but also because of competitive inhibition of acetyl-CoA carboxylation, but if concentrations are kept low, this isn't anticipated to be a problem.
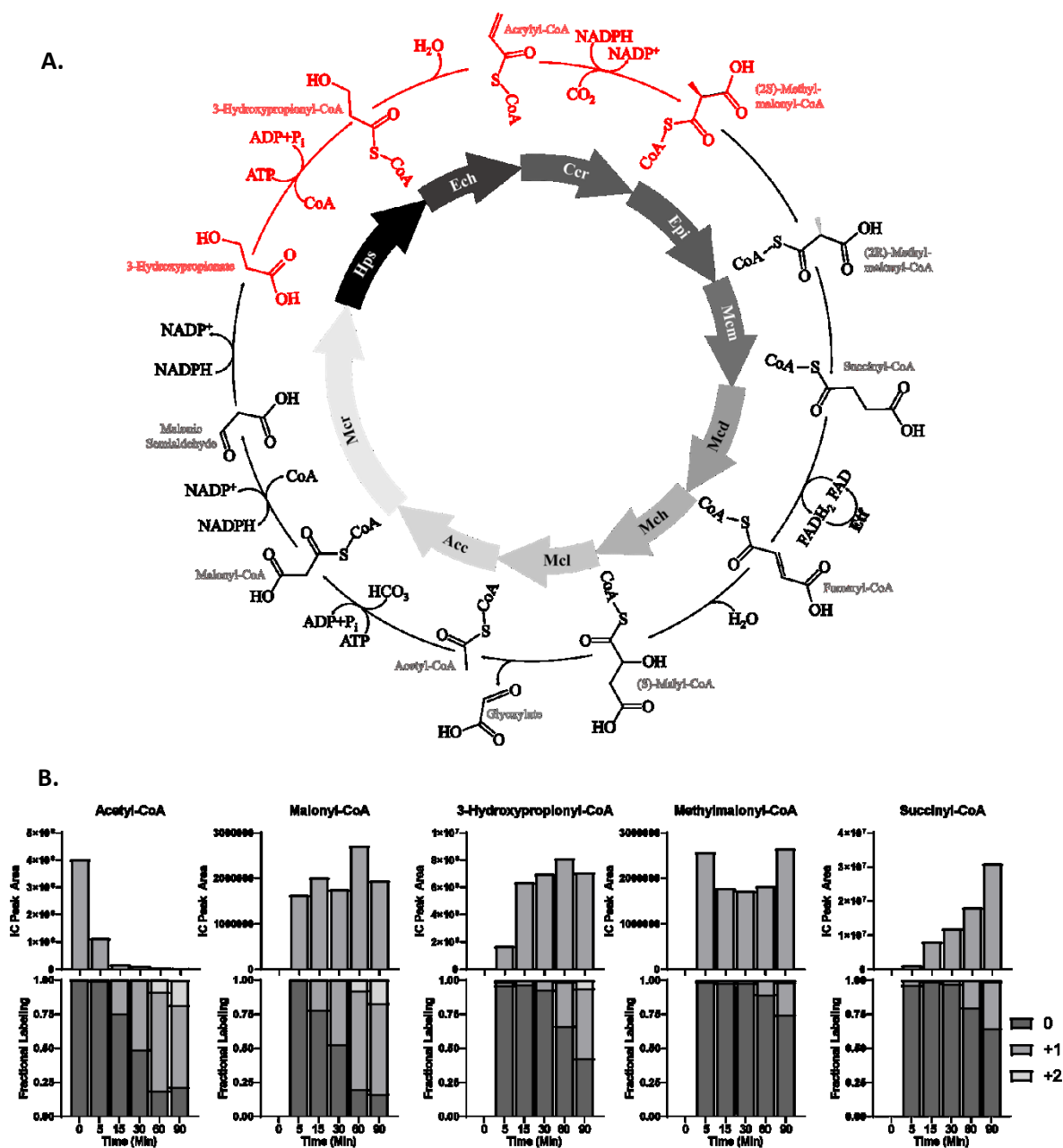
Figure. 5.3. The HOPAC cycle with Hps, Ech, and Ccr. **A.** Chemistry of the HOPAC cycle when Hps is employed. Relevant reactions are highlighted in red. **B.** Intermediates as detected by LCMS. Above, total level (Ion Count), below, relative labelling. There is an increase in +1 compounds, and the beginning of +2 compounds indicating molecules are passing through the cycle more than once.

5.4. Extension of Electron Chain

Although we were now seeing some fully labelled intermediates, the cycle consistently ran into a bottleneck at succinyl-CoA. This was not surprising for two reasons. First, Mcd, the enzyme that oxidises

succinyl-CoA to fumaryl-CoA has relatively low activity. Second, in kinetic assays and oxidative pathway assays, we used ferrocenium as an electron acceptor for this reaction, but this is impractical in the context of the full cycle because ferrocenium oxidises NAD(P)H nonenzymatically. As a more specific electron acceptor, we used an excess of Etf in full cycle assays.

To determine what was causing this bottleneck, we attempted to optimise around the concentration of Mcd. Even at excessive concentrations of Mcd, however, there was little change suggesting that Mcd was not the primary issue. Increasing Etf concentration, on the other hand, modestly alleviated the bottleneck. Unfortunately, this was not a practical approach, as more than half of the assay volume was occupied by Etf, so we looked to the native solution to this problem. In vivo, an additional enzyme EtfQO is utilised, which oxidises Etf and then reduces quinones.

We overexpressed the EtfQO from *P. migulae*, the same organism that the Mcd and Etf were acquired from, in *E. coli* and isolated it from membranes. We tested coenzyme Q1, coenzyme Q2, and decylplastoquinone to determine which quinone would be best accepted by EtfQO after solubilisation. Conveniently, none of the quinones increased the rate of Etf oxidation because O_2 was an effective electron acceptor for EtfQO, and it is capable of rapid oxidation of Etf without additional electron acceptors (Chapter 4.2). While the generation of reactive oxygen species is generally undesirable, they can be mitigated with SOD and catalase, whereas quinones may interact negatively with any other enzymes or cofactors.

With EtfQO implemented in the cycle, the succinyl-CoA bottleneck was reduced (Figure. 5.4.). There were no apparent unwanted reactions caused by the addition of EtfQO, and we saw greater ^{13}C labelling than in previous versions of the cycle.
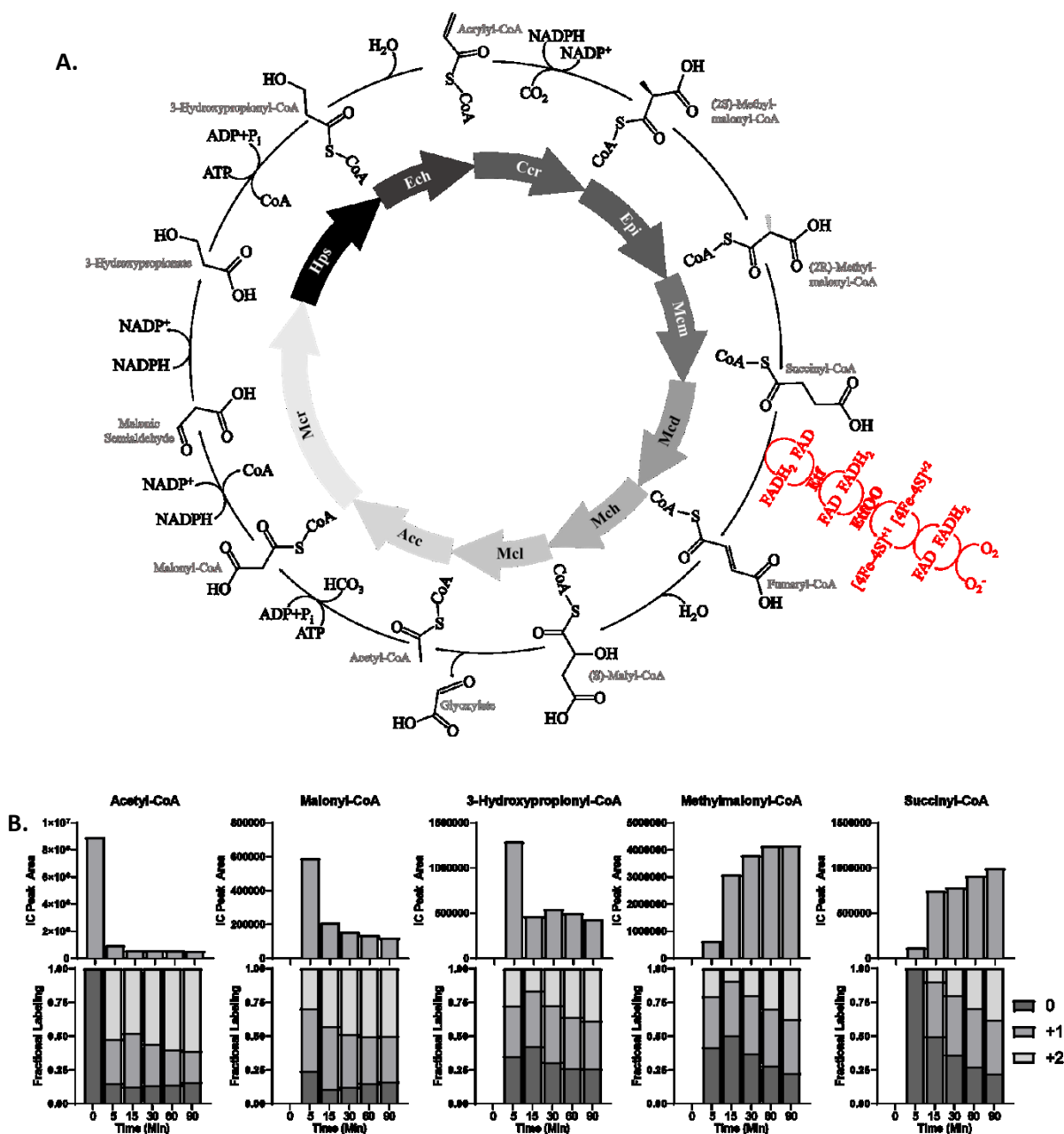
Figure. 5.4. The HOPAC cycle with EtfQO implemented to increase the rate of reoxidation of Mcd. **A.** Chemistry of the HOPAC cycle when EtfQO is employed. Relevant reactions are highlighted in red. **B.** Intermediates as detected by LCMS. Above, total level (Ion Count), below, relative labelling. There is an increase in +2 compounds, indicating a greater portion of compounds are passing through the cycle more than once. Since +3 looks identical to +2, it may be the case that some of the +2 has passed through the cycle multiple times.

5.5. Mcm Chaperone MeaB

With the succinyl-CoA bottleneck being relieved by EtfQO, we found a new bottleneck form at methylmalonyl-CoA. (2S)- and (2R)-methylmalonyl-CoA do not resolve well with our LCMS method, so it was initially unclear whether this was a problem with Epi, Mcm, or both. We began by running assays with varying concentrations of Epi and Mcm to see if this had any effect on the bottleneck but adding either enzyme in a large excess did not have a significant effect.

It has previously been reported that Mcm can undergo suicide-inactivation because its mechanism utilises a radical intermediate. During the reaction, the carbon-cobalt bond of AdoCbl is cleaved to generate a deoxyadenosyl radical and cob(II)alamin which is vulnerable to oxidation. Typically, AdoCbl is regenerated at the end of the reaction, but occasionally cob(II)alamin will be oxidised to aquacobalamin (OH$_2$Cbl) resulting in an inactive enzyme (Takahashi-Íñiguez, 2011).

Because AdoCbl appears purple, and Mcm typically purifies nearly colourless, we considered whether the binding of this cofactor might be more transient than previously reported. Since the enzyme itself is not damaged in the inactivation, if it spontaneously releases damaged cofactor, the addition of fresh cofactor might be sufficient to regenerate active enzyme. We ran an assay with higher concentrations of AdoCbl but again, there was no significant effect suggesting that the damaged cofactor is tightly bound.

To confirm that the bottleneck was in fact the result of Mcm inactivation, we ran side-by-side assays wherein one was given Mcm in the beginning, and the second was given the same amount of Mcm but spiked into the assay periodically. If Mcm is inactivated, the first assay will lose mutase activity and the bottleneck is expected to form, but the second will constantly be replenished with active enzyme and is expected to avoid this bottleneck. In this case, the bottleneck formed for the first assay, but was relieved in the second indicating the enzyme was indeed inactivated through use.

In hopes of finding a sustainable solution to this problem, we looked to the native system. In vivo, Mcm is coexpressed with the chaperone protein MeaB. This enzyme is thought to provide a protective effect to Mcm, and to accelerate the exchange of AdoCbl cofactors after inactivation. We performed assays with and without MeaB and tested the enhancing effect of ATP or GTP (Chapter 4.1). MeaB did significantly extend the lifespan of Mcm, in fact we were not able to quantify an effect from ATP or GTP because MeaB alone was sufficient to protect Mcm for the full length of the assay.

We then ran full cycle assays comparing Mcm alone, Mcm with MeaB, Mcm with MeaB and GTP, and an assay where Mcm is spiked in periodically to provide active enzyme throughout. Surprisingly, the presence

of MeaB in these assays had very little effect and this was not improved by the addition of GTP. It is not clear why MeaB has a limited protective effect in the more complex system, since it is natively functional in the far more complex environment of the cell, but it might suggest a specific interaction with something else present in the assay.

An interesting possibility not investigated in this study, is the reaction of the deoxyadenosyl radical of Mcm with cycle intermediates like acrylyl-CoA and fumaryl-CoA. It has previously been demonstrated that this radical will react with itaconyl-CoA and form a stable bi-radical, irreversibly inactivating the enzyme (Ruetz, 2019). The precise mechanism of this reaction was not determined, but it was hinted that a Michael addition might be involved. Since fumarate and acrylate are both Michael addition acceptors and the deoxyadenosyl radical is nucleophilic, it seems plausible that a similar reaction might occur here for either or both intermediates. This would also explain why MeaB did not resolve the issue, as it was incapable of preventing the itaconyl-CoA reaction as well.

Nevertheless, the regular addition of Mcm to the assay to continuously replenish active enzyme does succeed in reducing the methylmalonyl-CoA bottleneck. Surprisingly, the removal of this bottleneck did not have a significant effect on the ratio of incorporated ^{13}C (Figure. 5.5.). This is counter-intuitive but may be a limitation of the method. In longer assays, we have seen the labelling pattern reverse, incorporating more ^{12}C. It is unclear why this happens, since the ^{13}C bicarbonate should still be present in a large excess, but it does highlight the importance of using a secondary method for comparing the success of different versions of the cycle. The primary product of the HOPAC cycle is glyoxylate, which we reduced to glycolate, and quantified by LCMS, discussed in Chapter 5.6.
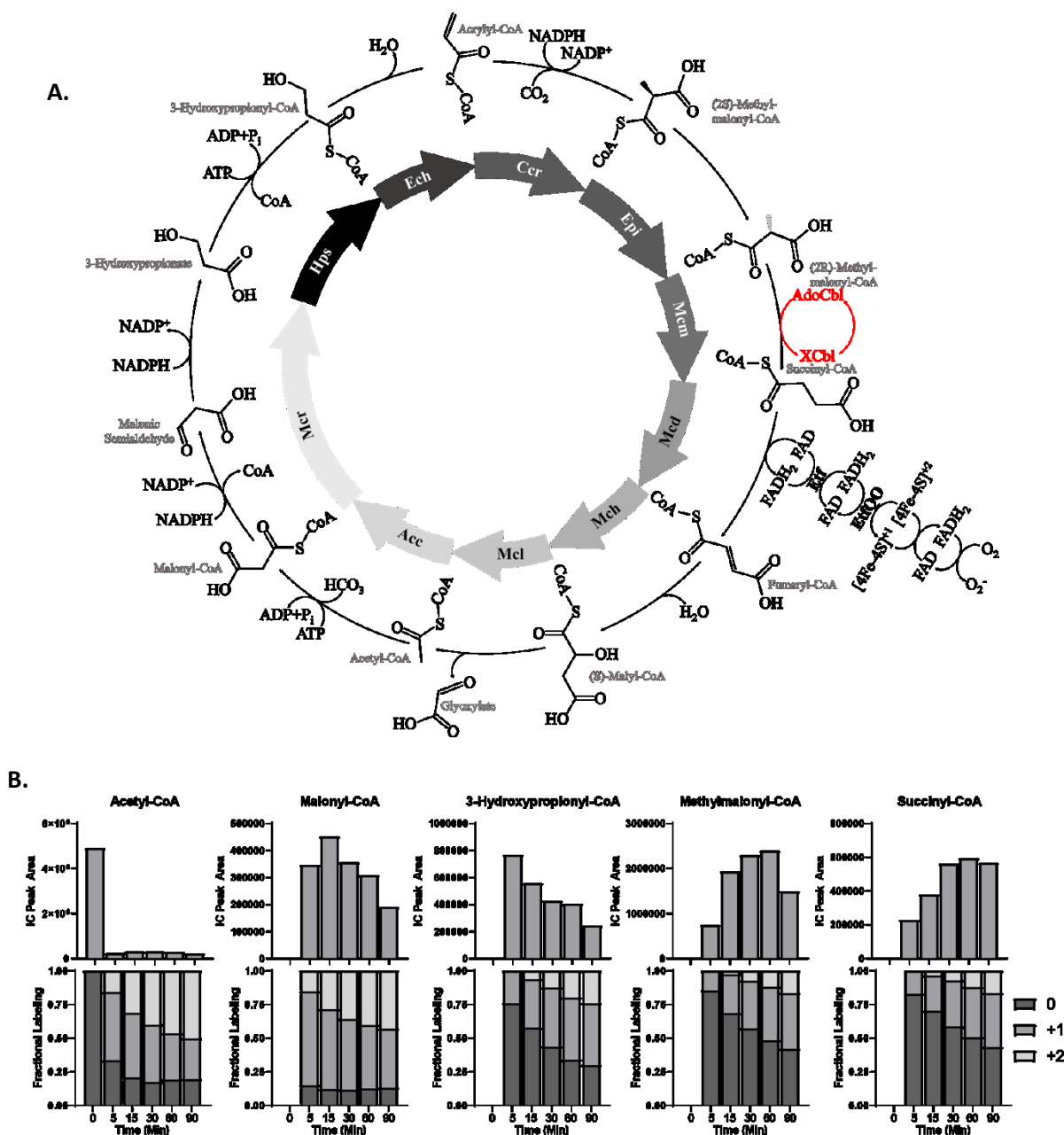
Figure. 5.5. The HOPAC cycle with periodic spiking of fresh Mcm. **A.** Chemistry of the HOPAC cycle when MeaB is employed. Relevant reactions are highlighted in red. **B.** Intermediates as detected by LCMS when fresh Mcm is spiked into the assay periodically. Above, total level (Ion Count), below, relative labelling.

5.6. Summary

Taken together, we have found enzymes capable of catalysing the reactions required for each version of the HOPAC. While some enzymes were so problematic that they prevented their pathways from functioning as a unit, others were functional in a segregated pathway but became problematic in the

greater context of the cycle. We primarily found two similar versions of the cycle that were capable of regenerating acetyl-CoA after being started with acetyl-CoA. Both utilised Mcm-Epi-Mcd-Mch-Mcl-Acc-Mcr to convert (2S)-methylmalonyl-CoA to 3-hydroxypropionate. In the first, Pcs was used to convert 3-hydroxypropionyl-CoA to propionyl-CoA at the expense of one ATP and one NADPH, and Pcc then carboxylated propionyl-CoA to (2S)-methylmalonyl-CoA at the expense of one ATP. In the second, Hps was used to convert 3-hydroxypropionate to 3-hydroxypropionyl-CoA at the expense of one ATP, Ech dehydrated 3-hydroxypropionyl-CoA to acrylyl-CoA, and Ccr carboxylated acrylyl-CoA to (2S)-methylmalonyl-CoA at the expense of one NADPH, for a net savings of one ATP.

In early assays, we had issues with Hps losing activity, and decided that Pcs was an acceptable replacement. It was still preferable, however, to find a stable Hps alternative in order to have a more energetically efficient cycle. When we found the synthetase from *C. necator*, it became clear that in addition to making the cycle more efficient, Hps had a much higher synthetase activity than Pcs. In Pcs incorporating cycles, nearly half of the total enzyme volume was occupied by Pcs. When we switched to Hps, we could run assays at lower concentrations leaving a greater volume available for increasing the concentration of other problematic enzymes. There is one potential benefit to utilising Pcs, it contains a small reaction chamber where 3-hydroxypropionyl-CoA is dehydrated to acrylyl-CoA and reduced to propionyl-CoA without acrylyl-CoA being released in between. This is desirable generally, because acrylyl-CoA is so reactive, but may be especially of interest if it is determined that acrylyl-CoA is responsible for inactivating Mcm, as discussed earlier.

While many bottlenecks were identified, most could be alleviated by optimising the concentration of enzymes already present in the assays. The first that could not be resolved in this matter was found at succinyl-CoA. After oxidising a molecule of succinyl-CoA, Mcd cannot perform a second reaction without being oxidised by an electron acceptor. Since we needed a solution that would not oxidise NADPH, we added Etf. The bottleneck can be modestly improved by adding excess Etf, but we quickly had another volume issue, where Etf occupied most of the enzyme volume in the assays. Presumably, the bottleneck would be cleared entirely if we were able to add sufficient Etf, but since this was impractical, we added EtfQO. It was determined that, in addition to utilising quinones as an electron acceptor, EtfQO can also be oxidised by O_2. Although the reactive oxygen species produced by this reaction are undesirable, it is convenient that we can dramatically reduce the volume of enzyme added because EtfQO can rapidly recycle its cofactor. After the addition of EtfQO, we saw an increase from ~100 μM glycolate to over 300 μM (Figure. 5.6.).

After this bottleneck was relieved, a new one formed at methylmalonyl-CoA. We identified Mcm inactivation as the cause of this problem. During reaction, the AdoCbl cofactor of Mcm can be oxidised to OH_2Cbl inactivating the enzyme. It was determined that the OH_2Cbl was sufficiently tightly bound to Mcm that simply adding excess AdoCbl for exchange did not recover activity. We attempted using MeaB, a chaperone protein for Mcm that protects it from inactivation and can replace OH_2Cbl in a GTP-dependent manner. This had a modest improvement of glycolate production, increasing to ~350 µM. Alternatively, we added fresh Mcm throughout the assay as old Mcm was inactivated, this had a more substantial improvement to nearly 500 µM glycolate (Figure. 5.6.). This suggests that MeaB does diminish Mcm inactivation, but that another unknown factor is able to inactivate Mcm anyway.

We implemented EtfQO and spiking Mcm to the Pcs version of the assay, however glycolate production was comparable to the Hps version without EtfQO and additional Mcm. This is not surprising because Pcs has low activity and was typically limiting in its assays. It may be possible to increase glycolate production with the Pcs version, but it would require either mutagenesis to increase catalysis, or adding prohibitive concentrations of enzyme.
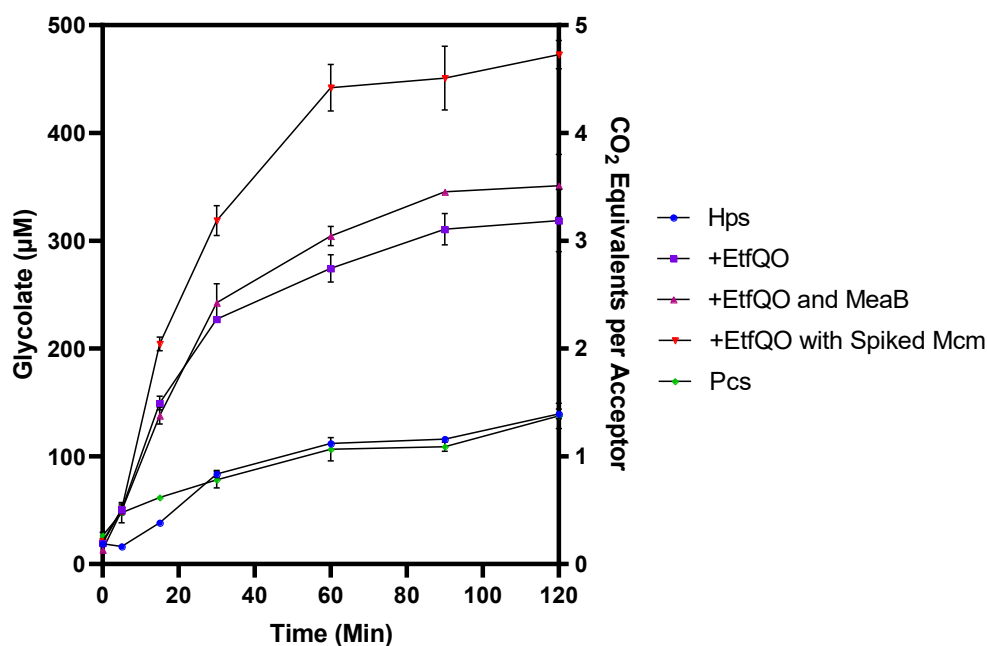
Figure. 5.6. Glycolate production by different versions of the HOPAC cycles. The primary product of the cycle is glyoxylate, but this was reduced to glycolate and quantified by LCMS. —●— The version utilising Hps, Ech, and Ccr to convert 3-hydroxypropionate to (2S)-methylmalonyl-CoA. —■— Hps version with EtfQO to transfer electrons to O_2. —▲— Hps version with EtfQO and MeaB. —▼— Hps version with EtfQO

and fresh Mcm spiked in periodically. ▬◆▬ The version utilising Pcs and Pcc to convert 3-hydroxypropionate to (2S)-methylmalonyl-CoA with EtfQO and fresh Mcm spiked in periodically.

6. (2S)-Methylsuccinyl-CoA Dehydrogenase

6.1. Background

The oxidation of succinyl-CoA to fumaryl-CoA is a reaction not currently annotated in any known metabolism (Borjian, 2017). In fact, fumaryl-CoA is currently absent in the Kyoto Encyclopedia of Genes and Genomes (KEGG) database (Kanehisa, 2000) and only found in side activities in the Braunschweig Enzyme Database (BRENDA) database (Chang, 2021). For example, succinyl-CoA:acetate CoA-transferase (EC 2.8.3.18) of *Acetobacter aceti* can accept fumarate and generate fumaryl-CoA in place of succinate and succinyl-CoA respectively albeit with an activity ~0.20% (Mullins, 2012) or the 2-methylfumaryl-CoA hydratase (EC 4.2.1.148) of *Haloarcula hispanica* which is capable of dehydrating (S)-malyl-CoA to fumaryl-CoA with an activity ~1.35% relative to (2R,3S)-β-methylmalyl-CoA (Borjian, 2017).

Despite its rarity, this reaction could be used in a variant of the TCA cycle (Figure. 6.1.). Succinyl-CoA could be oxidised to fumaryl-CoA which could then be hydrolysed to fumarate. Alternatively, the fumaryl-CoA could be hydrated to (S)-malyl-CoA which could then hydrolysed to (S)-malate. Likewise, in the 3-hydroxypropionate bicycle, succinyl-CoA is converted to (S)-malyl-CoA through succinate, fumarate, and (S)-malate and this could be bypassed with the direct oxidation of succinyl-CoA to fumaryl-CoA and subsequent hydration to (S)-malyl-CoA. It is not clear why no known organism has utilised one of these paths, but it has been proposed that the series of reactions in the TCA cycle were amongst the earliest metabolism, possibly even predating life itself (Muchowska, 2020). As such, it may be the case that a sort of metabolic entrenchment has occurred wherein the ubiquity of the TCA cycle has eliminated any significant selection to develop this bypass, preventing the enzymes from evolving.

Interestingly, methylsuccinyl-CoA dehydrogenase (Mcd) and mesaconyl-C1-CoA hydratase (Mch) are often found together in the proteome of bacteria lacking isocitrate lyase (EC 4.1.3.1) due to the presence of the ethylmalonyl-CoA pathway. At least some Mcd have a side activity on succinyl-CoA such as the *Cereibacter sphaeroides* homolog which was reported to have ~0.39% activity on succiny-CoA relative to (2S)-methylsuccinyl-CoA (Schwander, 2017). Likewise, as mentioned earlier, at least some Mch have a side activity on fumaryl-CoA. Although these activities are low, it seems likely, due to the prevalence of succinyl-CoA in central metabolism, that a small portion of succinyl-CoA must pass through these enzymes. The resulting (S)-malyl-CoA is presumably hydrolysed or is cleaved into acetyl-CoA and glyoxylate by (S)-malyl-CoA/ (2R,3S)-β-methylmalyl-CoA/(S)-citramalyl-CoA lyase (EC 4.1.3.24) which is also present in the ethylmalonyl-CoA pathway.
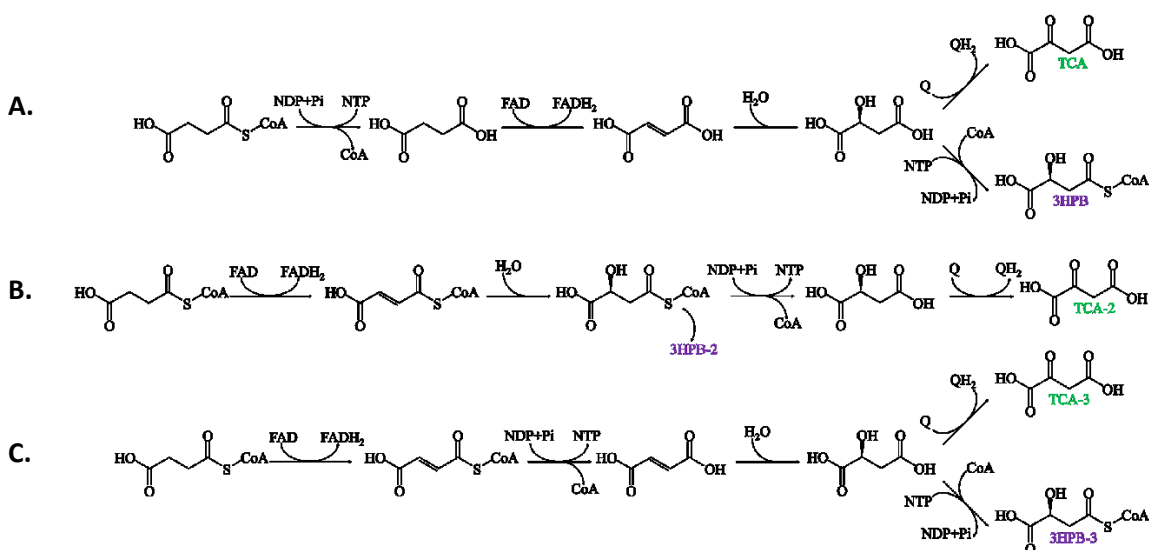
Figure. 6.1. Potentially useful alternative chemistries employing a succinyl-CoA dehydrogenase. **A.** Standard reaction scheme of the TCA cycle (-78.4 ± 21 kJ/mol) and 3-hydroxypropionate-bicycle (-36.2 ± 10 kJ/mol). **B.** Succinyl-CoA is oxidised to fumaryl-CoA and hydrated to (S)-malyl-CoA where it continues with the 3HPB (-64.2 ± 29 kJ/mol) or is cleaved to (S)-malate for the TCA cycle (-19.3 ± 20 kJ/mol). **C.** succinyl-CoA is oxidised to fumaryl-CoA which is cleaved to fumarate and then follows analogous chemistry to A (-76.2 ± 29 kJ/mol and -34 ± 22 kJ/mol).

This seems to indicate that there is some detriment to oxidising succinyl-CoA, or at least not a strong benefit, because the enzymes are present, and it should be trivial to develop the activity given enough time if there was a benefit. However, to date, there hasn't been an exhaustive screen of Mcds, so it may be the case that there are efficient succinyl-CoA dehydrogenases present in nature and they simply haven't been discovered. We set out to determine whether any Mcds have increased activity on succinyl-CoA, or if the trend of unsubstantial activity was consistent.

6.2. Selection of Mcd Homologs

To survey naturally occurring sequence diversity, we randomly selected 46 genes annotated as (2S)-methylsuccinyl-CoA dehydrogenases from NCBI and aligned them using ClustalO, (Sievers, 2011), (Figure. 6.2.). Eight sequences were selected to test a spectrum of the sequence diversity in hopes of finding one with enhanced succinyl-CoA dehydrogenase activity.
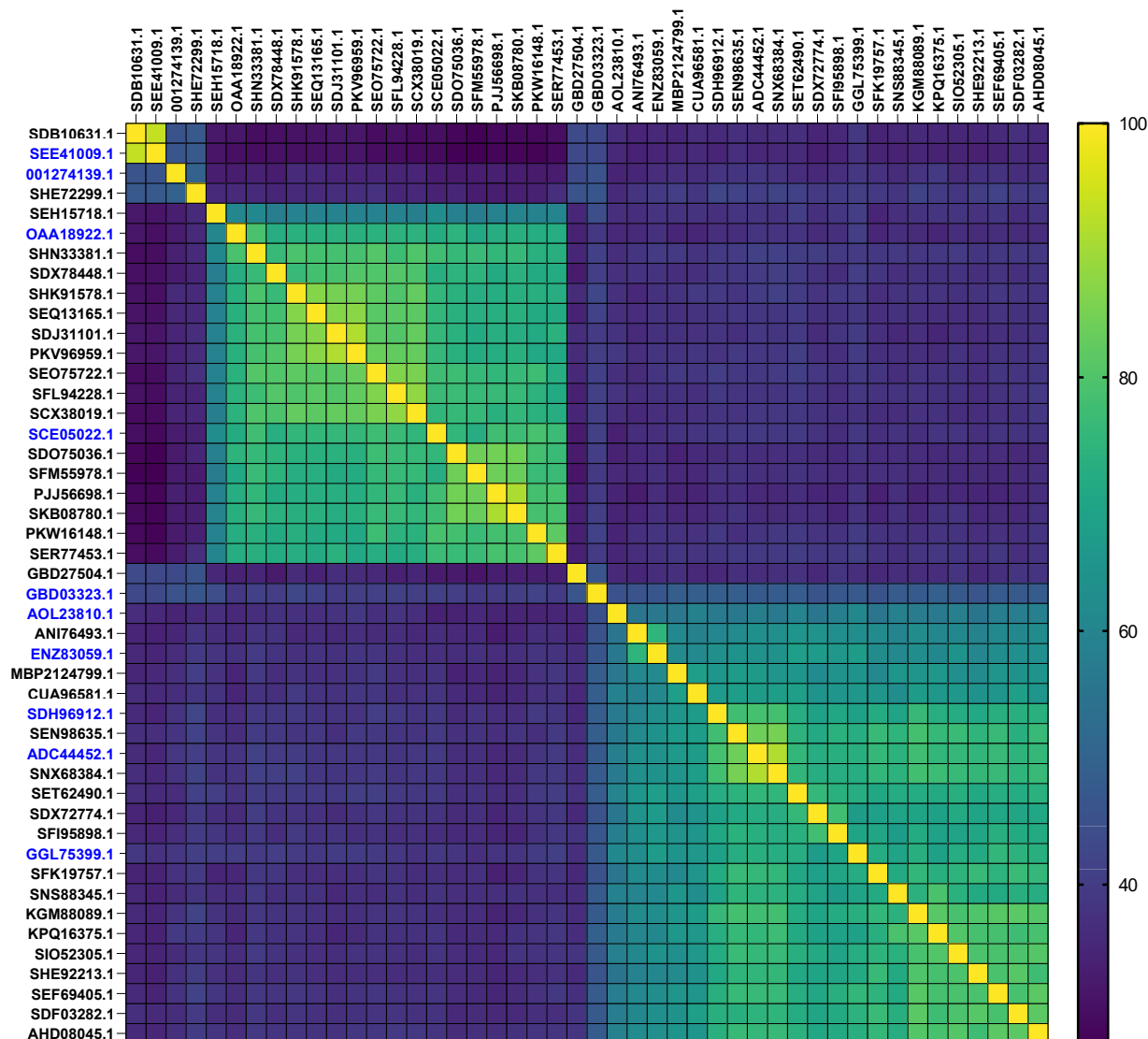
Figure. 6.2. Percent sequence identity of selected Mcd homologs. Labels highlighted in blue were selected for synthesis and further analysis.

Kinetics were measured for each of the selected homologs on both succinyl-CoA and (2S)-methylsuccinyl-CoA (Figure. 6.3. and 6.4.) and kinetic parameters are reported in Tables 6.2 and 6.3. The assay involved reducing the FAD of the Mcd to $FADH_2$ while oxidising the respective acyl-CoA, and the $FADH_2$ was then used to reduce ferrocenium to ferrocene. This reduction was monitored in real time at 300 nm with an extinction coefficient of $\varepsilon = 2.75$ mM^{-1}cm^{-1}.

Table. 6.1. Mcd homologs selected for further analysis in this study. Molecular weight and extinction coefficients were determined by ProtParam (Walker, 2005).

Organism	Abbreviation	Accession	MW (kDa)	ε_{280} (mM^{-1} cm^{-1})
Caulobacter vibrioides OR37	CvMcd	ENZ83059.1	60.47	57.87
Paracoccus denitrificans	PdMcd	SDH96912.1	59.92	68.41
Wenxinia marina	WmMcd	GGL75399.1	58.42	53.30
Cereibacter sphaeroides	CsMcd	ADC44452.1	59.77	57.41
Frankia sp. EI5c	FsMcd	OAA18922.1	43.72	33.35
Erythrobacter litoralis	ElMcd	AOL23810.1	59.59	69.90
Streptomyces sp. IgraMP-1	SsMcd	SCE05022.1	44.26	33.35
Bacterium HR19	HrMcd	GBD03323.1	44.74	66.81
Leptospira interrogans	LiMcd	WP_001274139.1	61.46	65.78
Pseudomonas migulae	PmMcd	SEE41009.1	59.71	41.37

To determine accurate Mcd concentrations, protein samples were measured at 280 nm and 450 nm. Because FAD absorbs at both wavelengths, the concentration of FAD was determined at 450 nm (ε_{450} = 11.3 mM^{-1} cm^{-1}), and the resulting 280 nm FAD absorbance was determined with a A_{450}:A_{280} of 0.57 (experimentally determined), which is a linear relationship between an absorbance of 0.04-0.3. The remaining A_{280} was used to determine the concentration of Mcd with specific extinction coefficients determined with the Expasy ProtParam tool (Walker, 2005) (Table. 6.1.).

Methylsuccinyl-CoA was synthesised using the CDI-method (Chapter 8.1.3). Because this method is expected to produce both 2- and 3-methyl isomers, it was assumed that only 50% of the resulting product was (2S)-methylsuccinyl-CoA. As an additional method, crotonyl-CoA was synthesised using the symmetric anhydride method (Chapter 8.1.1) from crotonic anhydride and purified. The crotonyl-CoA was then carboxylated to ethylmalonyl-CoA using Ccr and purified. Purified ethylmalonyl-CoA was then pre-incubated with ethylmalonyl-CoA mutase (Ecm) (EC 5.4.99.63) and Epi to generate (2S)-methylsuccinyl-CoA in situ. All reported kinetics were measured with purified racemic methylsuccinyl-CoA, however control conditions were confirmed with the latter method.

Both methods are problematic, in the case of the purified methylsuccinyl-CoA, it is a reasonable assumption that ~50% is (2S), however it is difficult to determine whether (2R) is inhibitory. On the other hand, generating methylsuccinyl-CoA from (2S)-ethylmalonyl-CoA with Ecm and Epi should result in effectively pure (2S)-methylsuccinyl-CoA, but some portion of the acyl-CoA added to the assay will

consistently be tied up in (2S)- and (2R)-ethylmalonyl-CoA making it complicated to accurately claim what concentration of (2S)-methylsuccinyl-CoA Mcd has access to at any given time. Nevertheless, reaction rates were similar between the two methods, suggesting that they should give a fair estimation of actual values.

A difficulty in using the ferrocenium method to measure kinetic parameters of Mcd, is that both succinyl-CoA and (2S)-methylsuccinyl-CoA are extremely labile, and ferrocenium can oxidise free CoA nonenzymatically. Because of the rotational flexibility of these compounds, the terminal carboxylate can perform a nucleophilic attack on the carbonyl of the thioester and cause hydrolysis in a process known as intramolecular general base catalysis (Wagner, 2017). As a result, succinyl-CoA has a reported half-life of ~70 minutes, and (2S)-methylsuccinyl-CoA has a reported half-life of just 24 minutes (Burgener, 2017). While this is sufficient for performing reactions, and for short-term storage of the acyl-CoAs, accurate determination of substrate concentration is always a concern. To mitigate this, we employed multiple methods. First, concentrations were measured at 260 nm with an extinction coefficient of 16.4 $cm^{-1} mM^{-1}$. Next, samples were incubated with 5,5'-dithio-bis-(2-nitrobenzoic acid) (DTNB) which reacts with free thiols and absorbs at 412 nm with an extinction coefficient of 13.6 $mM^{-1}cm^{-1}$. The measurement at 260 nm measures all CoA, whether in an acyl-CoA or free, whereas the 412 nm measurement only measures free CoA. The difference between determined concentrations is used as the actual acyl-CoA concentration. Free CoA, however, will reduce ferrocenium giving the false impression of acyl-CoA oxidation so the reaction mix should be set up, left to stabilise, and then the reaction can be started by the addition of the enzyme. Sufficiently high levels of free CoA, however, will prevent the accurate measurement of acyl-CoA oxidation, highlighting the importance of proper acyl-CoA storage.
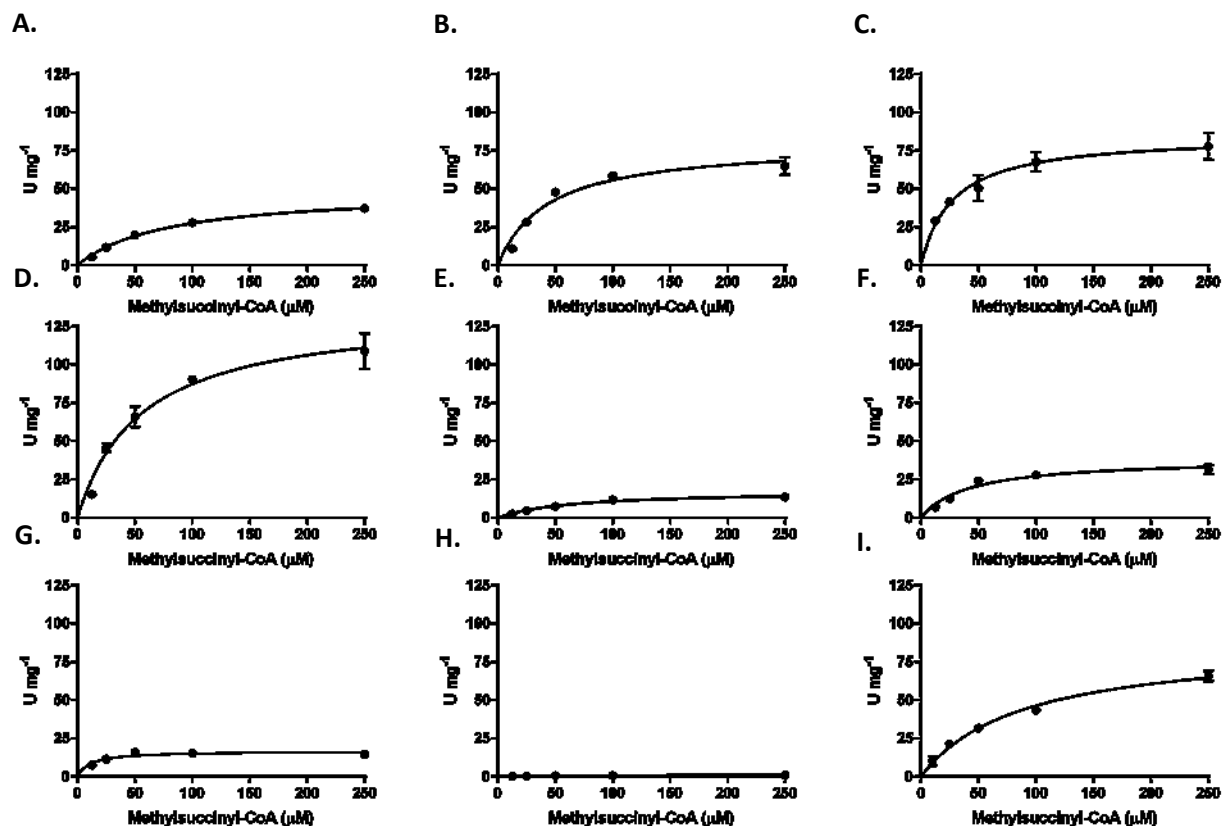
Figure. 6.3. Michaelis–Menten kinetics of Mcd on (2S)-methylsuccinyl-CoA by **A.** *P. migulae*. **B.** *C. sphaeroides*. **C.** *Streptomyces* sp. **D.** *W. marina*. **E.** *C. vibroides*. **F.** *E. litoralis*. **G.** *Frankia* sp. **H.** *P. denitrificans*. **I.** Bacterium HR19. Mcd was added and the reduction of ferrocenium to ferrocene was monitored in real time at 300 nm.

Table. 6.2. Kinetics parameters for Mcd homologs on (2S)-methylsuccinyl-CoA.

(2S)-Methylsuccinyl-CoA	U/mg	Km (µM)	kcat/Km ($s^{-1}mM^{-1}$)
Cereibacter sphaeroides	70 ± 6	40 ± 9	$1.8 \times 10^3 \pm 400$
Pseudomonas migulae	49 ± 2	80 ± 6	620 ± 52
Streptomyces sp.	17 ± 1	12 ± 4	$1.1 \times 10^3 \pm 300$
Wenxinia marina	85 ± 5	28 ± 5	$3.0 \times 10^3 \pm 600$
Caulobacter vibrioides	130 ± 9	55 ± 10	$2.5 \times 10^3 \pm 500$
Erythrobacter litoralis	18 ± 1	67 ± 10	263 ± 420
Frankia sp.	39 ± 3	42 ± 9	664 ± 150
Paracoccus denitrificans	87 ± 5	88 ± 12	$1.0 \times 10^3 \pm 150$
Bacterium HR19	1.1 ± 0.07	723 ± 11	11 ± 2
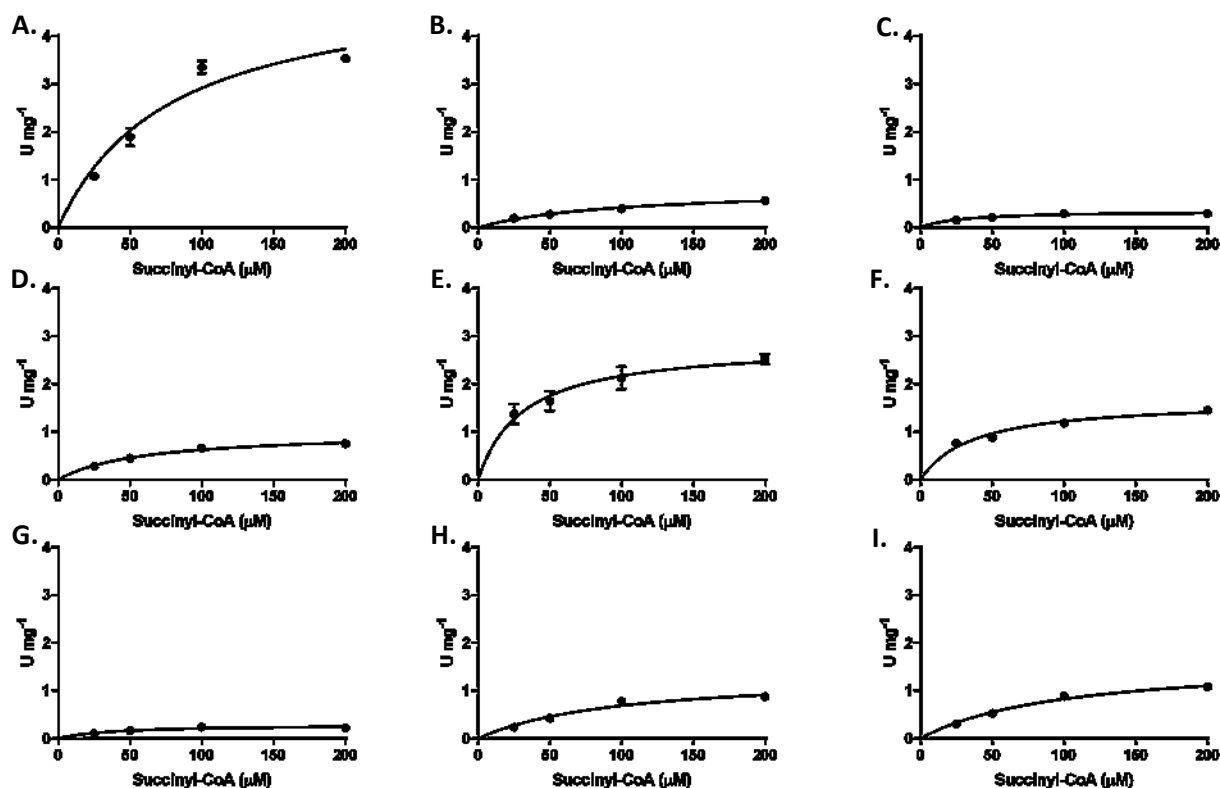
Figure. 6.4. Michaelis–Menten kinetics of Mcd on succinyl-CoA by **A.** *P. migulae*. **B.** *C. sphaeroides*.**C.** *Streptomyces* sp. **D.** *W. marina*. **E.** *C. vibroides*. **F.** *E. litoralis*. **G.** *Frankia* sp. **H.** *P. denitrificans*. **I.** Bacterium HR19. Mcd was added and the reduction of ferrocenium to ferrocene was monitored in real time at 300 nm.

Table. 6.3. Kinetics parameters for Mcd homologs on succinyl-CoA.

Succinyl-CoA	U/mg	Km (µM)	kcat/Km $(s^{-1}mM^{-1})$
Cereibacter sphaeroides	0.82 ± 0.071	94 ± 18	8.6 ± 1.8
Pseudomonas migulae	5.2 ± 0.66	78 ± 23	66 ± 21
Streptomyces sp.	0.29 ± 0.031	39 ± 13	5.6 ± 1.9
Wenxinia marina	0.35 ± 0.018	29 ± 5.2	12 ± 2.3
Caulobacter vibrioides	1.0 ± 0.053	60 ± 8.3	17 ± 2.5
Erythrobacter litoralis	2.8 ± 0.21	31 ± 7.7	91 ± 24
Frankia sp.	1.7 ± 0.092	37 ± 6.4	33 ± 6.1
Paracoccus denitrificans	1.7 ± 0.15	100 ± 9	30 ± 6.1
Bacterium HR19	1.4 ± 0.17	99 ± 27	10 ± 3.1

The greatest relative activity was found with the HrMcd which preferred succinyl-CoA, ~125%, but the total activity was extremely low (Figure. 6.4.). It is possible that this is a misannotated enzyme that happens to have a minor side activity on succinyl- and (2S)-methylsuccinyl-CoA, but the gene was found in a thermophilic metagenomics experiment so it may also be the case that this enzyme is more active at temperatures far higher than are relevant for our purposes. The next greatest relative activity was ElMcd, which had an activity on succinyl-CoA ~16% of that with (2S)-methylsuccinyl-CoA. PmMcd has a relative specificity on succinyl-CoA, ~10.5% of that with (2S)-methylsuccinyl-CoA, and an overall activity with succinyl-CoA nearly double that of ElMcd. We decided to focus our efforts on PmMcd.
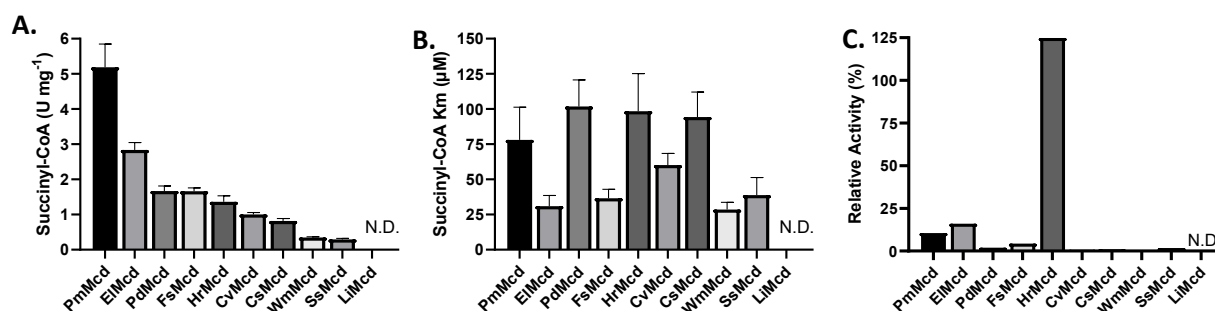
Figure. 6.4. Comparison of kinetic parameters of Mcd homologs on succinyl-CoA. **A.** Specific activity. **B.** Km. **C.** Activity on succinyl-CoA as a percentage of activity on (2S)-succinyl-CoA.

6.3. P. migulae Mcd Crystallisation

PdMcd was crystallised previously (Schwander, 2018b), however we were interested to learn what structural differences between PdMcd and PmMcd might lead to the difference in substrate preferences. PmMcd was crystallised with the sitting-drop vapor diffusion method at 16 $^{\circ}$C. Crystals grew in several conditions including 1 mM FAD and 1 mM methylsuccinyl-CoA with **a.)** 10% (w/v) PEG 6000, 50 mM tri-sodium citrate pH 4.0, 500 mM LiCl, **b.)** 22.5% (w/v) pentaerythritol propoxylate (5/4 PO/OH), 50 mM MES pH 6.5, 200 mM KCl, **c.)** 17.5% (w/v) pentaerythritol propoxylate (17/8 PO/OH), 50 mM sodium acetate, 100 mM $(NH_4)_2SO_4$, **d.)** 50 mM tri-Sodium citrate pH 5.5, 1M $(NH_4)_2SO_4$, **e.)** 10 % (v/v) 1,4-Butanediol, 50 mM Sodium acetate pH 4.5, **f.)** 1 M sodium phosphate pH 7.2, 50 mM Sodium acetate pH 4.5, **g.)** 50 mM Tris pH 7.0, 1 M $(NH_4)_2SO_4$, and **h.)** 10% (w/v) Polyethylene glycol 3,350, 100 mM Potassium thiocyanate.

A structure was determined at a resolution of 1.9 Å in complex with FAD and mesaconyl-C1-CoA (Table. 6.4.). The previously determined PdMcd structure was resolved in complex with FAD but without a

substrate/product complex. This allows for an interesting comparison to disambiguate the difference in preference, and possibly plan a route to enhance this difference.

Table. 6.4. X-ray diffraction data collection and model refinement statistics

Crystal	McdPm with bound FAD and mesaconyl-CoA
PDB ID	In Process
Data collection	
Beamline	DESY PETRA III P13
Wavelength (Å)	0.97625
Space Group	$C\,2\,2\,2_1$
Unit cell dimensions	
a, b, c (Å)	139.80, 169.56, 118.39
α, β, γ (°)	90.00, 90.00, 90.00
Resolution (Å)	25.01 – 1.93 (2.03 – 1.93)
Unique reflections	105292 (15053)
Multiplicity	13.2 (12.7)
Completeness (%)	99.7 (98.6)
$I\,/\,\sigma I$	14.6 (2.3)
R_{merge}	0.119 (1.165)
R_{pim}	0.034 (0.337)
$CC_{1/2}$	0.999 (0.892)
Refinement	
$R_{work}\,/\,R_{free}$	0.1737 / 0.2008
RMS bonds	0.011
RMS angles	0.782
Ramachandran	
favored (%)	98.46
allowed	1.54
(%)	0.00
outliers (%)	
Rotamer outliers (%)	0.93
Number of atoms	9057
Protein	8370
Ligands	249
Solvent	438
Average B-factor	41.89
Protein	41.80
Ligands	38.60
Solvent	44.70

Values in parentheses are for highest-resolution shell.

6.4. P. migulae Mcd Structure

The hydrogen-bond network binding FAD (Figure. 6.5) is largely conserved between PmMcd and PdMcd, including the fact that both subunits contribute to FAD binding, however there are a few exceptions. PmQ47/PdQ56, PmT278/PdT288, PmS284/PdS294, PmT310/PdT320, PmR437/PdR440,

PmQ504/PdQ508, PmG508/PdG512, PmE534/PdE539 are fully conserved, and PmI275/PdA285, PmI277/PdF287 maintain equivalent hydrogen-bonds. The β-carbon of PmT536 is involved in a hydrogen bond with the O2B hydroxyl group of FAD, however the equivalent residue, PdI540 is incapable of this interaction. Finally, in the PdMcd structure, the peptide carbonyl group of PdF534 is involved in a hydrogen bond with the O2' hydroxyl group of FAD, whereas this FAD hydroxyl group is hydrogen bonded to the CS1 carbonyl group of mesaconyl-C1-CoA in the PmMcd structure, suggesting that PmF530 is probably involved in FAD binding when the enzyme is not engaged with a substrate/product.
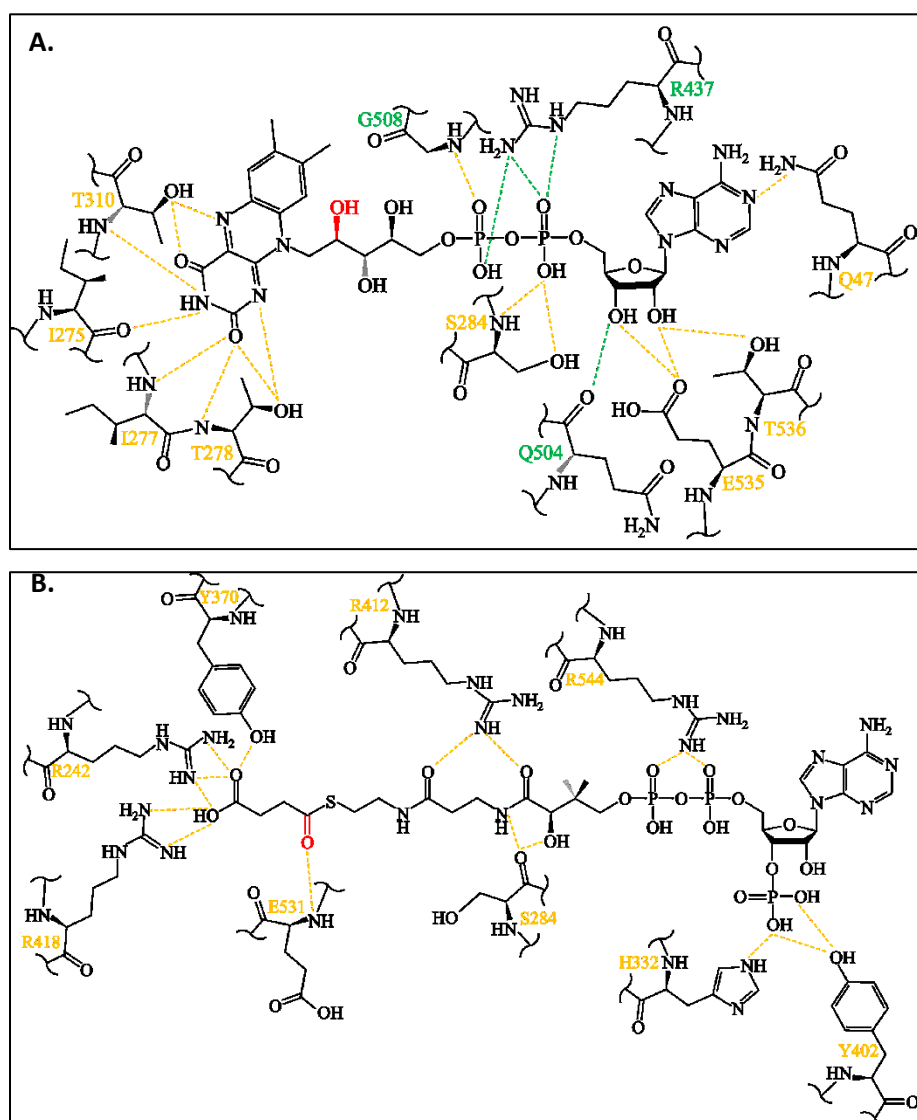
Figure. 6.5. Active site interactions of PmMcd. Hydrogen bond network of **A.** FAD and **B.** Succinyl-CoA. Residues labelled in yellow are found on one subunit, those highlighted in green are found on the other subunit highlighting the importance of the dimer for proper enzyme functioning. E531 is the catalytic

glutamate. An additional hydrogen bond is present between the red hydroxyl group of FAD and carbonyl of succinyl-CoA.

The hydrogen-bond network binding mesaconyl-C1-CoA is also largely conserved between PmMcd and PdMcd. PmR242/PdR252, PmS284/PdS294, PmR412/PdR415, PmR418/PdR421, PmE531/PdE535, PmR544/PdR547 are fully conserved, while PmY402/PdK405 maintains equivalent hydrogen-bonds. The τ secondary amine of PmH332 hydrogen bonds to the C3' phosphate of mesaconyl-C1-CoA, but this residue is replaced with PdW341 which is incapable of maintaining this bond.

Previously, it was proposed that PdR376 was involved in binding the CS4 carboxylate group in PdMcd. Interestingly, this residue is conserved in PmR371, but it is oriented in the opposite direction. In PmMcd, PmY370, which is also conserved in PdY375 is oriented into the active site and bonds with the carboxylate while it is oriented in the opposite direction in PdMcd. These residues are situated on a flexible loop, and it is unclear whether they have swapped roles between the two homologs or if this difference in positioning is the result of a conformational shift during substrate binding. Previously, isobutyryl-CoA Dehydrogenase (HsIbd) was crystallised in the presence and absence of methacrylyl-CoA (Battaile, 2004), and HsIbd W216, the homologous residue to PmY370/PdY375 is oriented into the active site, while HsIbd N217, analogous to PmR371/Pd375 is oriented out of the active site in both cases. Likewise, medium-chain acyl-CoA dehydrogenase (SsMcad) (Kim, 1993) was crystallised in the presence and absence of octanoyl-CoA and the analogous residues (SsMcadQ217 and R218)) were in the same position as PmMcd and were static, suggesting that this positioning is probably stable during substrate binding. If this is the case, a twist in the loop of PdMcd has been stabilised that has switched the residue in the active site.

The hydroxyl-group of PmY370 is within hydrogen bonding distance of the carboxylate of mesaconyl-C1-CoA, however PdR376 is in a retracted position and sits ~4.7 Å away. This distance could be bridged by a different rotamer of arginine, but this results in clashes with T320 and E380, suggesting at least some local movement upon substrate binding, if this residue is involved in substrate binding. If PdR376 can bridge this distance, a triplet of arginines, R251, R376, and R421 are involved in a salt-bridge network responsible for binding the carboxylate of succinyl-CoA. In PmMcd, salt-bridges from R242, R418, and the hydrogen bond from Y370 serve the same purpose (Figure 6.6.).
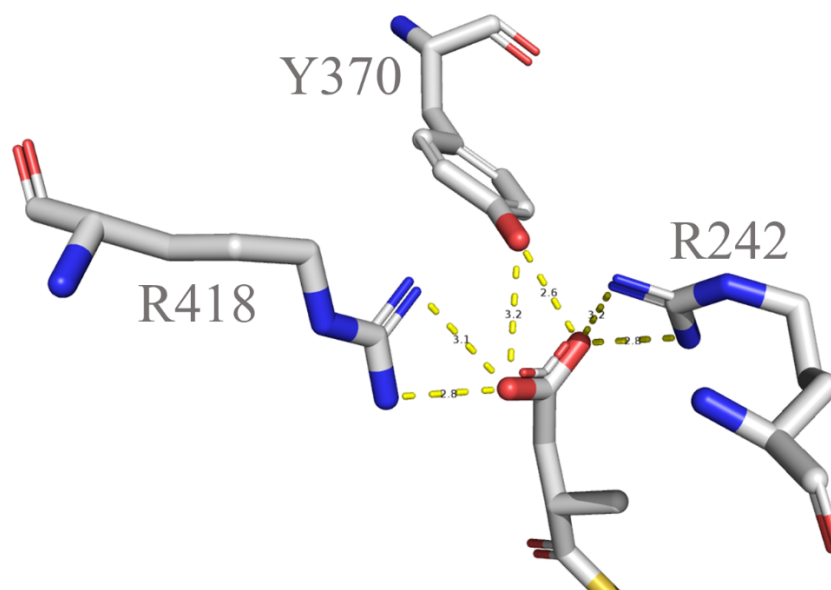
Figure. 6.6. Residues involved in coordinating the terminal carboxylate in PmMcd. Analogous residues between PdMcd and PmMcd are PmR242/PdR251, PmY370/PdR376, and PmR418/PdR421

6.5. Substrate Specificity

Given the extreme similarity in structure and properties of succinyl-CoA and methylsuccinyl-CoA, the strong preference for (2S)-methylsuccinyl-CoA is somewhat puzzling. If the preference was reversed, it would be predicted to be the result of the methyl group being physically occluded, but in this case, it is not as clear. Both the succinyl- and (2S)-methylsuccinyl- moieties have a great deal of rotational flexibility and it could plausibly be the case that careful coordination of the moieties is required for activity. Interestingly, HsIbd has a similar substrate specificity in that it has ~5% activity on propionyl-CoA relative to isobutyryl-CoA (Battaile, 2004). It was proposed that the additional methyl group of isobutyryl-CoA acts as a wedge, preventing rotation around this bond.

The OS1 carbonyl group of succinyl-CoA is involved in two hydrogen bonds, first to the O2' hydroxyl group of FAD, and second to the amine of the catalytic glutamate PmE531/PdE535. With the triplet coordination of the carboxylate discussed above, and these carbonyl hydrogen bonds, the succinyl- and (2S)-methylsuccinyl- moieties should be relatively constrained. This is important because the catalytic glutamate must be close enough to perform proton abstraction and at the same time, the CS3 of succinyl- or (2S)-methylsuccinyl-CoA must be above the N5' of FAD to allow hydride transfer. It may be the case that the CS1 and CS4 carbons are constrained due to the hydrogen bonds of their substituents, but that CS2 and CS3 remain flexible. If so, the succinyl-moiety would only be in the correct position for oxidation

occasionally. The methyl group of (2S)-methylsuccinyl-CoA, on the other hand, would constrain rotation around these bonds and may hold the substrate in the proper position, accelerating catalysis.

6.6. P. migulae Mcd Mutagenesis

Based on these considerations, we planned two approaches to potentially improve activity on succinyl-CoA. First, the introduction of an additional hydrogen-bond with the CS4 carboxylate. If the triplet of arginines all bind the carboxylate in PdMcd, it would be a stronger interaction than in PmMcd. Nevertheless, it is unclear whether all members of the triplet are involved, and it was hoped that increasing the strength of binding and/or altering the specific positioning of the carboxylate might stabilise the succinyl moiety. Second, the occlusion of the methyl group of the methylsuccinyl moiety. This is the approach taken previously (Schwander, 2018b), where A282V was inserted and activity on (2S)-methylsuccinyl-CoA was decreased by ~60% but activity on succinyl-CoA was modestly improved. It might be expected that a larger residue might enhance this effect, however mutation to leucine, isoleucine, and phenylalanine all knocked out activity. Interestingly, this residue is an isoleucine in PmMcd, possibly partially explaining the higher relative activity.

While occluding the methyl group of (2S)-methylsuccinyl-CoA might superficially reduce activity on methylsuccinyl-CoA and bring the relative activity closer to that of a succinyl-CoA dehydrogenase, it was hoped that the presence of a residue in the same physical space that the methyl group occupies might constrain the succinyl-moiety and have a similar stabilising effect. We identified three residues placed at the surface of the active site that might be modified to obstruct the methyl group of (2S)-methylsuccinyl-CoA and potentially stabilise succinyl-CoA. T241 (Figure. 6.7.), I245 (Figure. 6.8.), and I275 (Figure. 6.9.) were selected (Table. 6.4.) based on their potential to occlude this space without blocking the rest of the succinyl-moiety, FAD, and to minimise clashes with other residues. F530K was selected to introduce an additional hydrogen bond to the CS4 carboxylate. Some mutants such as T241E, T241N, and T241Q have the potential to simultaneously block the methyl group and introduce a new hydrogen bond with the carboxylate (Figure. 6.10.).

Table. 6.4. Mutations introduced to PmMcd in this study. T241, I245, and I275 are located in the active site near the methyl group of methylsuccinyl-CoA. F530 is positioned near the carboxylate.

Mutation	MW (kDa)	ε_{280} (mM^{-1} cm^{-1})
WT	59.71	41.37
T241E	59.73	41.37
T241N	59.72	41.37
T241Q	59.73	41.37
T241W	59.79	46.87
I245E	59.72	41.37
I245K	59.72	41.37
I245L	59.71	41.37
I245M	59.71	41.37
I245Q	59.72	41.37
I245R	59.75	41.37
I275H	59.73	41.37
I275K	59.72	41.37
I275L	59.71	41.37
I275Q	59.72	41.37
I275R	59.75	41.37
I275S	59.70	41.37
I275T	59.69	41.37
F530K	59.69	41.37
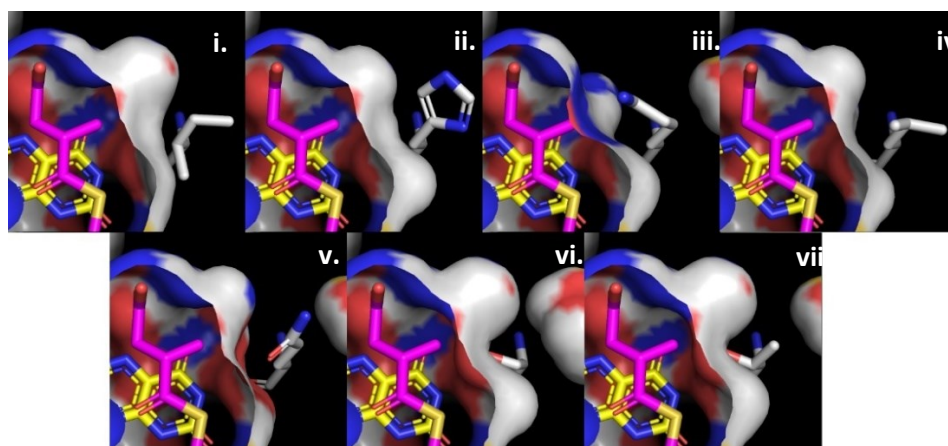
Figure. 6.7. Mutagenesis of PmMcd isoleucine 245 in an attempt to occlude the methyl group of (2S)-methylsuccinyl-CoA and improve activity on succinyl-CoA. **i.** Wild type I245, **ii.** I245E, **iii.** I245K, **iv.** I245L, **v.** I245M, **vi.** I245Q, and **vii.** I245R
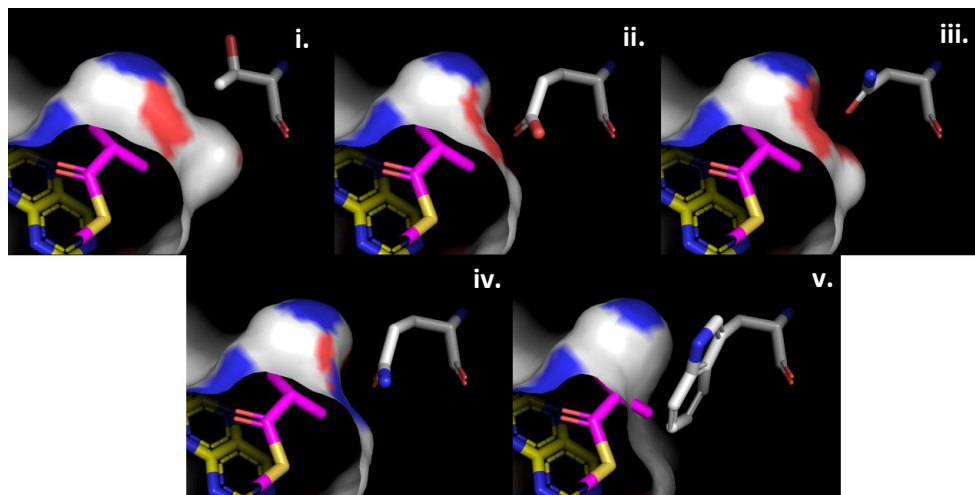
Figure. 6.8. Mutagenesis of PmMcd threonine 241 in an attempt to occlude the methyl group of (2S)-methylsuccinyl-CoA and improve activity on succinyl-CoA. **i.** Wild type T241, **ii.** T241E, **iii.** T241N, **iv.** T241Q, and **v.** T241W.
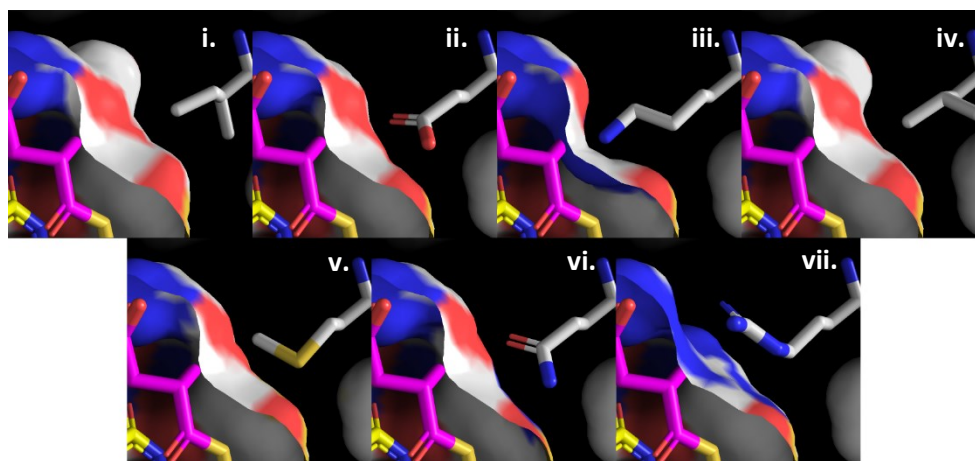
Figure. 6.9. Mutagenesis of PmMcd threonine 241 in an attempt to occlude the methyl group of (2S)-methylsuccinyl-CoA and improve activity on succinyl-CoA. **i.** Wild type I275, **ii.** I275H, **iii.** I275K, **iv.** I275L, **v.** I275Q, **vi.** I275S, and **vii.** I275T.
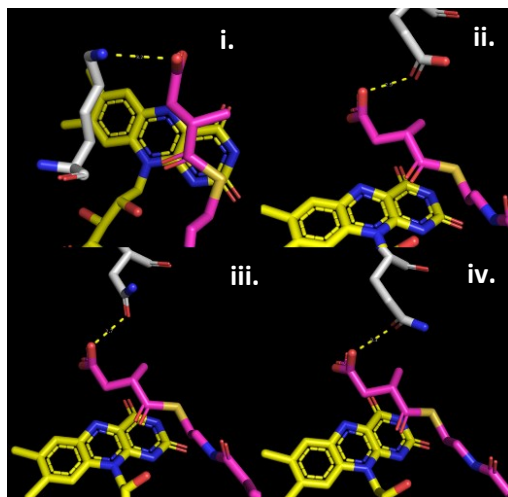
Figure. 6.10. Mutagenesis of PmMcd threonine 241 and phenylalanine 530 in an attempt to introduce an additional hydrogen bond with the succinyl-CoA carboxylate. **i.** F530K, **ii.** T241E, **iii.** T241N, and **iv.** T241Q.

6.7. Effects of Mutagenesis

Reactions were carried out on succinyl-CoA and (2S)-methylsuccinyl-CoA as described earlier, except rather than performing full kinetic characterisation, reactions were run at 500 µM of either substrate. This should be a sufficient condition to approximate maximal activity unless the Km of the mutant was dramatically increased. We used these specific activities to compare activity between mutants and between substrates (Figure. 6.11.).

Unfortunately, all mutants resulted in a dramatic loss of activity. The mutant with the next highest activity was F530K which lost ~75% activity on (2S)-methylsuccinyl-CoA and ~80% activity on succinyl-CoA, the next highest was I275L which lost ~90% activity on (2S)-methylsuccinyl-CoA and ~95% activity on succinyl-CoA.

Interestingly, some mutants did have an improvement in relative activity. I245L has ~32%, I245K has 34%, I275K has 84%, I275Q has 104%, and I245R has 153% activity on succinyl-CoA relative to (2S)-methylsuccinyl-CoA, however this is for a maximum of ~1% activity relative to the wild type on succinyl-CoA making these mutants impractical for use in a cycle.
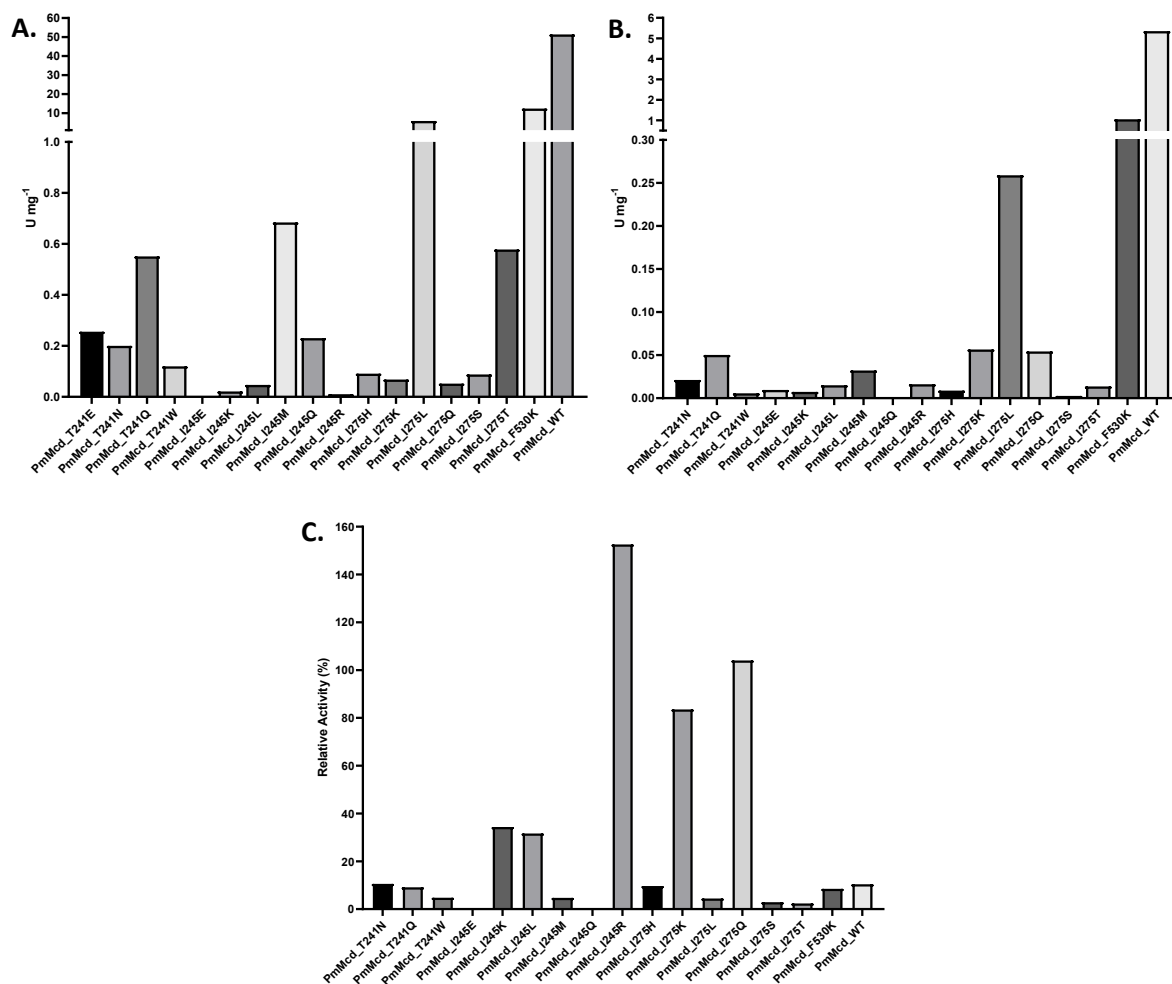
Figure. 6.11. Activity of PmMcd mutants on **A.** (2S)-methylsuccinyl-CoA and **B.** Succinyl-CoA. C. Activity on succinyl-CoA relative to (2S)-methylsuccinyl-CoA.

6.8. Conclusion

We set out to find or create a succinyl-CoA dehydrogenase. This activity is important for the most recent version of the HOPAC cycle, however the only reported activity is from *C. sphaeroides* and it is a minor activity relative to the primary activity of (2S)-methylsuccinyl-CoA. It is unclear why this activity would not evolve in nature, especially given the fact that Mcd is involved in the ethylmalonyl-CoA pathway, so it is typically found with an Mch, resulting in little risk of accumulating fumaryl-CoA. It seems plausible that some organisms might develop this activity, especially if mutations accumulate in Sdh and Fdr, but it is not obvious whether this would be advantageous.

We performed a screen of a diverse set of Mcd sequences in hopes of finding advanced succinyl-CoA dehydrogenase activity and were successful in finding PmMcd, which has an activity greater than 10%

relative to (2S)-methysuccinyl-CoA. This marks a significant improvement over the CsMcd which has only ~1% activity. We then successfully crystallised PmMcd in complex with FAD and mesaconyl-C1-CoA and used this structure to plan mutagenesis in an attempt to enhance activity with succinyl-CoA. Unfortunately, our attempts were unsuccessful, however multiple further approaches may still be fruitful.

It might be more productive to employ directed evolution to enhance activity. For example, Sdh and Fdr could be knocked out preventing succinate oxidation, and Mcd could be integrated with Mch and an (S)-malyl-CoA hydrolase (3.1.2.30). The cell could then be fed propionate as the primary carbon source which would be funneled into succinyl-CoA production. The heterologous enzymes would then oxidise succinyl-CoA to fumaryl-CoA which would then be hydrated to (S)-malyl-CoA and hydrolysed to malate, reconnecting the TCA cycle.

Additionally, a high-throughput microfluidics screen would likely prove valuable, where the reduction of ferrocenium could be used to measure activity. Random mutagenesis could be used, however there are multiple sites that should probably not be mutated. FAD binding residues as well as residues that mediate subunit interactions, and residues involved in Etf binding should probably be maintained as much as possible. As such, a semi-rational library design would likely be more successful. Finally, there are many acyl-CoA dehydrogenases. Glutaryl-CoA dehydrogenase, for example, performs the oxidation of the CS2-CS3 bond of a saturated, unbranched, dicarboxylated acyl-CoA without the stabilising effect of the methyl wedge. It may, therefore, be profitable to try gene shuffling to see if a similar stabilising effect could be conferred to Mcd.

7. Discussion

7.1. Synopsis

In this project, we built upon the foundational work of Schwander, 2018a to realise the Hydroxypropionyl-CoA/Acrylyl-CoA Cycle. Originally proposed in Schwander, 2016, the HOPAC cycle is similar to the 3-hydroxypropionate bicycle, except that it employs reductive carboxylation resulting in an equal amount of carbon fixation at a lower energetic cost. While establishing the cycle, we maintained flexibility regarding what chemistry would best achieve our goal of getting from one carboxylation reaction to another. As such, we explored several slightly different hypothetical versions of the HOPAC cycle to determine which was most effective.

In all versions of the cycle, (2S)-methylmalonyl-CoA was converted to (2R)-methylmalonyl-CoA, then to succinyl-CoA by two isomerisation reactions performed first by Epi, then Mcm. While Epi was well-suited to this task, it was determined that Mcm underwent inactivation during the assays. This is a well-known phenomenon, the AdoCbl cofactor is used to create a radical intermediate and can be oxidised to OH_2Cbl. We utilised MeaB, the native chaperone protein of Mcm which was demonstrated to dramatically extend the life of Mcm in the presence of its substrates, but this was found to be insufficient in the full HOPAC assay. This shortcoming can be overcome by adding fresh Mcm throughout the assay, suggesting that an additional reaction apart from oxidation is occurring. It may be that cycle intermediates such as fumaryl-CoA or acrylyl-CoA are reacting with the deoxyadenosyl radical by Michael addition, however this possibility has yet to be investigated.

For the conversion of succinyl-CoA to (S)-malyl-CoA, we first planned to use chemistry analogous to the TCA cycle because of the ubiquity of these enzymes which makes a multitude of homologous enzymes available for investigation. Unfortunately, this proved to be problematic in vitro. Although the hydration of fumarate to (S)-malate worked well, this was the only straightforward reaction. The oxidation of succinate to fumarate can be performed by succinate dehydrogenase and fumarate reductase. There are soluble fumarate reductases, however they reduce fumarate to succinate and are irreversible, so we were forced to use membrane-bound enzymes. To attempt to avoid working with membranes and detergents, we generated constructs of Sdh containing only the soluble domains. Although these constructs were active, they had low activity, and were an insurmountable bottleneck in coupled assays.

The cleavage of succinyl-CoA to succinate was no less problematic, three alternatives were tested and all three caused issues. First, Smt which is found in the 3HPB was employed. Paradoxically, in an in vitro

setting, one of the Smt substrates doesn't exist until it completes its first reaction, and this prevents the reaction from occurring. This can of course be rectified by the addition of extraneous (S)-malate, but this is not ideal because it complicates measuring the efficiency of the cycle. In all other cases, every molecule of acetyl-CoA added needs to pass through every reaction in the cycle to generate a single molecule of glycolate, but if (S)-malyl-CoA is added, it needs only to be ligated to CoA and cleaved to generate a molecule of glyoxylate, effectively bypassing most of the cycle.

^{13}C labelling is generally a less effective measure in versions of the cycle where succinyl-CoA is cleaved. During the first turn of the cycle, succinate is labelled at C1 and C4, so regardless of which carboxylate is ligated to CoA in the generation of (S)-malyl-CoA, one ^{13}C will be lost to glyoxylate and one will remain in singly labelled acetyl-CoA. This is consistent will all other versions of the cycle. During the second turn of the cycle, however, succinate is labelled at C1, C2, and C4. If the C1 carboxylate is ligated to CoA the result will be fully labelled acetyl-CoA, but if the C4 carboxylate is ligated the result will be singly labelled acetyl-CoA again, and this is a random process. This is especially problematic when Smt is employed because our ability to quantify glycolate is already compromised by the addition of malate.

The second method to cleave succinyl-CoA utilised Scs, which can cleave the thioester bond and regenerate an ATP in the process. This works in principle but has the drawback that the ADP/ATP ratio must be carefully maintained or the cycle will stall. Excess ATP will prevent other ATP-dependent reactions, while excess ATP may prevent succinyl-CoA cleavage. When succinyl-CoA cleavage is achieved, an excess of ATP will also result in succinate quickly being religated to CoA. The final method utilised Sch which hydrolyses the thioester bond without regenerating ATP. While this reaction conveniently doesn't require ADP, it is also less energetically efficient and promiscuity with (S)-malyl-CoA will generate a futile cycle in combination, and eventually deplete the total acyl-CoA pool.

It is important to note however, that Sdh and Scs work in tandem in the TCA cycle in vivo, and Sdh and Smt work in tandem in the 3HPB in vivo, so these are likely to be viable options when the HOPAC cycle is implemented in vivo. Sdh remains in membranes and the electrons harvested from the oxidation can be recycled. Likewise, the ADP/ATP balance is constantly in flux in complex metabolism, and (S)-malate will be available for the transferase. Although Sch is probably still not a desirable route, the other two are worth pursuing.

The version that worked best so far is the direct oxidation of succinyl-CoA to fumaryl-CoA by Mcd followed by hydration to fumaryl-CoA by Mch. These are not the primary activities for either enzyme, preferring

(2S)-methylsuccinyl-CoA and mesaconyl-C1-CoA respectively. Fortunately, Mch has a high activity with fumaryl-CoA. Mcd, on the other hand, is slow on succinyl-CoA. We investigated several Mcd homologs and found that the highest activity was achieved with PmMcd. We have made efforts to increase the activity on succinyl-CoA through mutagenesis, but to date, none have been successful. We found that oxidation by Mcd could be enhanced in full HOPAC assays, however, by employing an Etf in concert with an EtfQO which can be oxidised by O_2. This marked a significant improvement in the HOPAC design.

The conversion of (S)-malyl-CoA to malonic semialdehyde was consistent in all versions of the HOPAC cycle and was relatively unproblematic. Mcl was used to cleave (S)-malyl-CoA to glyoxylate and acetyl-CoA and without issue. There are many naturally occurring acetyl-CoA carboxylases in nature, but they are often large, multimeric, and prone to dissociation. We employed a mutated propionyl-CoA carboxylase which has significantly improved activity with acetyl-CoA. This enzyme is still a heterodimer, but it is smaller, less complex, and more stable than most natural Accs. The reduction of malonyl-CoA was performed by Mcr. This enzyme can perform two reductions generating 3-hydroxypropionate, but we also utilised a truncated C-terminal domain of Mcr to specifically generate malonic semialdehyde in versions of the cycle that didn't involve 3-hydroxypropionate.

For the conversion of 3-hydroxypropionate to methylmalonyl-CoA, three options were investigated. The first two use either a synthetase or a transferase to ligate 3-hydroxypropionate to CoA which is dehydrated to acrylyl-CoA, and finally reductively carboxylated to methylmalonyl-CoA. The required enzymes have been shown to be active in vitro and in series, however the transferase presents the potential problem of its acyl-CoA being consumed before 3-hydroxypropionate is produced. Acetyl-CoA is typically used as a CoA donor, but if it is completely carboxylated to malonyl-CoA before 3-hydroxypropionate is produced, the cycle will stall. The synthetase, on the other hand, functioned without issue. The only drawback to this method is that the acrylyl-CoA intermediate generated by the dehydration of 3-hydroxypropionyl-CoA is a strong electrophile and is potentially reactive towards various compounds present in the reaction mix such as FAD and AdoCbl.

The final option manages to get around the acrylyl-CoA problem by isolating it in the reaction chamber of Pcs from generation to consumption. Unfortunately, Pcs predominantly produces propionyl-CoA instead of (2S)-methylmalonyl-CoA. Propionyl-CoA can be carboxylated to methylmalonyl-CoA, but this is at the expense of an ATP. A double mutant of Pcs exists that has ~70% carboxylation efficiency, however it is at a sacrifice of catalytic efficiency (Bernhardsgrütter, 2019). In addition to being relatively wasteful, the wild type Pcs is slow, and is usually the limiting enzyme in this version of the cycle.

An alternative for generating acrylyl-CoA from malonic semialdehyde was explored which utilises an amino transferase to produce β-alanine. The β-alanine can then be ligated to CoA and subsequently deaminated to acrylyl-CoA. While this is an interesting approach, multiple issues arose. The primary concern was in finding a β-alanyl-CoA synthetase. While such an enzyme could presumably be engineered, we were unsuccessful in finding one with this activity naturally. As a result, we were forced to rely on an acyl-CoA transferase to generate β-alanyl-CoA. Conveniently, there are enzymes with this activity, but they have the same limitations imposed on the 3-hydroxypropionyl-CoA transferase.

To convert malonic semialdehyde to β-alanine, we investigated two aminotransferases. The first used L-glutamate as an amino donor, the second used L-alanine. In both cases, the amino acid was recycled using a glutamate dehydrogenase or alanine dehydrogenase respectively. These reactions worked reasonably well, however L-alanine was found to be a substrate for the acyl-CoA transferase making these activities incompatible.

The final step to regenerate (2S)-methylmalonyl-CoA is the reductive carboxylation of acrylyl-CoA by Ccr. This enzyme has high activity and unlike Pcs, nearly all carboxylation is achieved without the requirement of additional ATP. The only drawback to utilising Ccr is that a small subsection of reactions will be reduction rather than reductive carboxylation resulting in propionyl-CoA production. This is a minor issue and can be rectified by the Acc already present in the cycle.

In addition to the core reactions of the cycle, we implemented a variety of auxiliary enzymes to deal with various issues that arise as the cycle runs. As EtfQO is oxidised by O_2, O_2^- is formed. We employed a SOD to convert O_2^- to O_2 and H_2O_2 which is then converted to O_2 and H_2O by catalase. In this oxidising environment, CoA can be oxidised to a dimeric form, so we included a CoA disulfide reductase which reduces the dimer back to monomers at the expense of NAD(P)H. Since the HOPAC cycle is dependent on ATP and NADPH, we used polyphosphate kinases and formate dehydrogenase respectively to replenish these cofactors. Finally, cofactors can be chemically damaged, NADPH can be hydrated, and CoA can be dephosphorylated, and we employed an epimerase/dehydratase and kinase respectively to repair these cofactors. While these enzymes do not resolve all possible issues, they do extend the lifespan of the enzymes and cofactors in the reaction and allow them to perform as best they can under these conditions.

Taken together, we have moved the HOPAC cycle from its design through to in vitro realisation. Partial cycle assays have been carried out for all of the above-described alternate chemistries. While some are ruled out for in vitro study, most seem like plausible candidates for future in vivo applications. When we

converted glyoxylate, the product of the HOPAC cycle to glycolate for quantification we found that the initial HOPAC could produce ~100 µM. We implemented the EtfQO to extend the electron chain from Mcd to O_2 and saw an increase to ~300 µM. We then attempted to address the inactivation of Mcm during reaction by implementing MeaB, a protective chaperone of Mcm. This saw a modest improvement to glycolate production reaching ~350 µM. This served to highlight another background problem with Mcm however, because when fresh Mcm was added throughout the assay, glycolate levels reached ~500 µM.

This amounts to ~1 mM of carbon fixed, or five per molecule of acetyl-CoA. The previously published CETCH cycle produced ~550 µM malate, ~1.1 mM carbon fixed, or 5.5 per molecule of propionyl-CoA. There is work left to be done with the HOPAC cycle, but the initial bottlenecks appear to have been resolved and future improvements will likely be the result of optimising enzyme concentrations and/or implementing different homologs of the enzymes currently in use. An appealing aspect of the HOPAC cycle as currently presented, is that there are several different routes to bridge between the two carboxylation reactions. While some of these were problematic in vitro, they are plausibly realisable in vivo. Different pathways will interact with metabolism in different ways, and it will be valuable to have practical alternatives when conflicts inevitably arise.

7.2. Future Directions

7.2.1. Enzyme Engineering Efforts

Although we were successful in generating a functional HOPAC cycle, some variants may be improved by improving pre-existing activities, while others that are not currently practical at all may be made possible.

7.2.1.1. Succinyl-CoA Dehydrogenase/Oxidase

The oxidation of succinyl-CoA to fumaryl-CoA is important for the current best performing versions of the HOPAC cycle. While this side-activity is present in some Mcds, it is typically quite low. The previously reported activity of *C. sphaeroides* was only ~0.5% on succinyl-CoA relative to (2S)-methylsuccinyl-CoA (Schwander, 2018b). We evaluated several homologs of Mcd in hopes that one would have a higher activity and found the best was from *P. migulae* with an activity over 10% on succinyl-CoA relative to (2S)-methylsuccinyl-CoA for an absolute activity of 5.2 ± 0.66 Umg^{-1}. This is a significant improvement, and is sufficient for use in the HOPAC cycle, but it would be preferable to have greater activity for in vivo applications.

We implemented several mutations in the active site of PmMcd but none were successful in raising activity. Although some mutations increased the relative activity on succinyl-CoA, I245K, I275Q, and I245R

have activity ~25, 80, and 115% on succinyl-CoA relative to (2S)-methylsuccinyl-CoA, this was at the expense of 99% or more of the overall activity.

Given the difficulty introducing any mutations that don't reduce activity it may be worth revisiting other homologs as well. *E. litoralis* has an activity over 15% on succinyl-CoA relative to (2S)-methylsuccinyl-CoA and an overall activity ~55% that of PmMcd on succinyl-CoA and has one of the lowest Km on succinyl-CoA at 30 µM. The Bacterium HR19 has a preference for succinyl-CoA with activity over 125% on succinyl-CoA relative to (2S)-methylsuccinyl-CoA and an overall activity ~27% that of PmMcd on succinyl-CoA (Discussed in Chapter 6.2.).

Because it has proven difficult to modify the active site, it may be a more fruitful approach to use directed evolution. If Mcd, Mch, and an (S)-malyl-CoA hydrolase are integrated together, succinyl-CoA will be converted to (S)-malate. Knocking out Sdh and Frd will prevent the oxidation of succinate, and may help to drive the flux of the TCA cycle through these enzymes instead.

An option not explored in this work that may, nevertheless, be of value to the in vitro functioning of the HOPAC cycle is the modification of Mcd from a dehydrogenase to an oxygenase. Currently, a long sequence of redox reactions result in the production of reactive oxygen species, and Mcd could be modified accept O_2 as an electron acceptor, eliminating the need for Etf and EtfQO. Previously, the Mcd from *C. sphaeroides* was modified to perform as an oxidase (CsMco) with the introduction of three mutations (Burgener, 2017). In CsMcd, W315F, T317G, and E377N were introduced, these are analogous to PmMcd W308, T310, and S375. The set of mutations function to increase solvent accessibility to the active site. Mutating W308 and T310 may have a similar effect in PmMcd, although an S375N mutation would presumably limit, rather than increase solvent accessibility.

An interesting feature of PmMcd is the presence of a small tunnel, ~5.5 Å in circumference and ~12.5 Å in length, behind the C7M methyl group of FAD that leads to the surface of the protein. This tunnel is blocked in PdMcd by the repositioning of a loop from L373-R376 (I368-R371 in PmMcd). This tunnel is in a similar position to one found in cholesterol oxidase (Chen, 2008), which is essential for the exchange of O_2 and H_2O_2. It may be possible to expand this tunnel and increase oxygen exchange which may introduce an oxidase activity. Both T310 and S375 both flank the tunnel and mutation with smaller residues should expand its circumference. Interestingly, these mutations were already introduced in the CsMco. It might be the case that the previously mentioned loop blocking this tunnel in PdMcd is closer to the position of

the PmMcd and that this tunnel was unintentionally expanded in the previous work. PmD182 also flanks the tunnel, and a similar reduction in side-chain size might also improve O_2 movement.

7.2.1.2. Propionyl-CoA Synthetase

The multi-catalytic enzyme Pcs is appealing for multiple reasons not least of which is its ability to sequester acrylyl-CoA until it has been reduced. The unfortunate byproduct of using this enzyme though, is that its primary product is propionyl-CoA, rather than (2S)-methylmalonyl-CoA. As discussed earlier, previous studies have managed to increase carboxylation efficiency from ~3% to ~70%, but this resulted in a loss of nearly 95% of overall activity (Bernhardsgrütter, 2019). Ultimately, even the wild type was too slow for our purposes, so employing an even slower mutant was impractical.

This does open an opportunity for future engineering, however. It is unlikely that rational engineering would be very fruitful given the volume of previous work, but a directed evolution experiment may be useful. Since *E. coli* has a native Mcm, Epi, and Pcc, if Pcs or the mutant was integrated into its genome it should be capable of utilising 3-hydroxypropionate. In the case of a reductive carboxylation reaction, Mcm and Epi would convert the (2S)-methylmalonyl-CoA to succinyl-CoA. In the case of a reduction reaction, Pcc could carboxylate the propionyl-CoA and then Mcm and Epi would again convert it to succinyl-CoA.

If this isn't a sufficient selection pressure, a succinyl-CoA auxotroph can be created by knocking out the native Scs and 2-oxoglutarate dehydrogenase. This would leave *E. coli* dependent on Pcs to produce succinyl-CoA which is in turn required for lysine, methionine, and peptidoglycan synthesis.

7.2.1.3. β-Alanyl-CoA Synthetase

An interesting reductive pathway utilising β-alanine and β-alanyl-CoA was explored and ultimately was not successful. All required enzymes were sufficiently active on their own, but it was difficult to find a single condition where they would all function together. The primary shortcoming to this path was our ability to generate β-alanyl-CoA. We were successful in producing β-alanyl-CoA with an acyl-CoA transferase using acetyl-CoA as the CoA donor and this allowed for the validation of the complete β-alanyl-CoA reductive pathway but only under contrived conditions not relevant to a full cycle system.

A fruitful future effort may be to pursue the engineering of a β-alanyl-CoA synthetase. There are a number of enzymes that naturally utilise β-alanine and ATP as substrates including pantothenate synthetase (EC 6.3.2.1) (Webb, 2011), phosphopantothenate synthetase (EC 6.3.2.36) (Kishimoto, 2014), and homoglutathione synthase (EC 6.3.2.23) (Jez, 2004). Unfortunately (R)-pantoate, (R)-4-phosphopantoate,

and γ-glutamylcysteine respectively, are activated rather than β-alanine and are unlikely to be useful for this purpose.

Carnosine synthase (EC 6.3.2.11), which ligates β-alanine to L-histidine utilises a β-alanyl-phosphate intermediate (Drozak, 2010). β-alanyl-monoamine synthase (EC 6.2.1.3) such as the Drosophila melanogaster Ebony which ligates β-alanine to dopamine utilises a β-alanyl-adenylate intermediate (Richardt, 2003). Either of these may be a good jumping off point for β-alanyl-CoA synthesis or could be informative for mutagenesis of pre-existing acyl-CoA synthetases. Aminoacyl-CoA synthetases have been described that may be a good starting point such as the acyl-CoA synthetase of *Penicillium chrysogenum* which has highest activity on (R)-β-phenylalanine, generating (R)-β-phenylalanyl-CoA (Koetsier, 2011). Acyl-CoA synthetases have also been described that ligate 3-hydroxypropionate and butyrate which are similar to β-alanine and may be valuable as starting points.

7.2.1.4. Carboxylic Acid Reductase

In all versions of the HOPAC cycle, malonyl-CoA is reduced to malonic semialdehyde by Mcr at the expense of NADPH. Thermodynamically, the high energy thioester bond is important for this reaction. The reduction of malonate is endergonic (36.1 ± 8.8 kJ/mol) whereas the reduction of malonyl-CoA is exergonic (-4.3 ± 8.8 kJ/mol). Malonate reduction can be made exergonic by coupling it to the hydrolysis of ATP (-24.1 ± 8.8 kJ/mol). This is an activity that has been reported in at least one carboxylic acid reductase (Kramer, 2018), albeit with the extremely low activity 1.5 ± 0.2 min^{-1}. In principle, it seems possible to engineer a carboxylic acid reductase to reduce the carboxylic acid of malony-CoA generating 3-oxopropionyl-CoA. It would likely require extensive mutagenesis to establish this activity, especially to make it adequately specific that it doesn't also reduce succinyl-CoA, for example, but there are potential benefits if it could be established.

In the original HOPAC design, the thioester bond of an intermediate was cleaved in two reactions. First in the cleavage of succinyl-CoA, and again in the reduction of malonyl-CoA. Since succinyl-CoA is now directly oxidised to fumaryl-CoA and hydrated to (S)-malyl-CoA, if a carboxylic acid reductase was employed to reduce malonyl-CoA, the thioester bond would no longer be cleaved. This is appealing because free CoA can oxidise to form dimers which are unavailable for synthetase reactions, potentially stalling the cycle. Since succinyl-CoA undergoes spontaneous hydrolysis at a significant rate, it may even be possible to switch acetyl-CoA for dethiaacetyl-CoA in vitro which wouldn't cleave and might result in a longer lasting cycle.

If 3-oxopropionyl-CoA can be generated, there are two relevant reactions that are analogous to the chemistry investigated for malonic semialdehyde. First, an acyl-CoA β-transaminase could be used to generate β-alanyl-CoA, which can then be deaminated as described earlier. Similar activities have been reported, for example 3-aminobutanoyl-CoA transaminase (EC 2.6.1.111). L-alanine and L-glutamate can both be used as amino donors (Perret, 2011) allowing for the use of the same accessory proteins. Currently, a significant obstacle for using L-alanine as an amino donor is that the βact has activity on L-alanine. If the thioester bond is never cleaved, the acyl-CoA transferase will no longer be required making L-alanine a practical option again.

Alternatively, a reductase could be utilised to generate 3-hydroxypropionyl-CoA which can then be dehydrated as described earlier. This reaction may already have been reported in the literature (Ploux, 1988). This paper describes an acetoacetyl-CoA dehydrogenase (EC 1.1.1.36) and has been cited as reporting this activity. The paper does mention a side activity of 40% on 3-oxopropionyl-CoA relative to acetoacetyl-CoA, but it also refers to 3-oxopropionyl-CoA as a C5 compound. Later in the paper it appears that this activity is attributed to 3-oxopentanoyl-CoA, an actual C5 compound suggesting that this was probably just a typo. Nevertheless, acetoacetyl-CoA dehydrogenase would be a reasonable enzyme to screen for 3-oxopropionyl-CoA activity.

7.2.2. In vivo Prospects

It is important to note that several of the problems that arose in the in vitro implementation of the cycle could be mitigated in vivo. While in vivo systems come with a bevy of distinct issues that would need to be overcome, they can open a number of possibilities as well, discussed below.

7.2.2.1. Succinyl-CoA Cleavage and Succinate Oxidation

Due to the ubiquitous nature of the TCA cycle from psychrophiles to hyperthermophiles, homologs of succinyl-CoA synthetase, succinate dehydrogenase, and fumarase exist that function optimally under nearly any condition of interest to this project. Although the fumarase purified at high concentrations, was stable, and highly active, the other two proved to be problematic in vitro.

Scs is active in stand-alone assays, but in the context of the full cycle, where the ATP:ADP ratio is intentionally driven towards ATP, it is inhibited. This is a problem that could be circumvented by the careful fine-tuning of ATP-regeneration enzymes to maintain a pool of both ATP and ADP at any given time. While this optimisation is desirable for any version of the cycle, most versions will simply perform poorly if not carefully optimised, this one will fail outright if an ADP pool is not sustained. In native

metabolism, however, a constant flux through various pathways continuously replenishes both metabolites mitigating this issue.

We attempted multiple strategies with Sdh and managed to demonstrate activity in stand-alone assays. We were not, however, able to produce a functional oxidative pathway with Sdh even if the assay was started with succinate, which eliminates the possibility that it was a problem of succinyl-CoA cleavage. This is a problem that should be readily remedied in vivo given the native flux through these enzymes.

7.2.2.2. Transferases

We utilised multiple acyl-CoA transferases in this study for the generation of (S)-malyl-CoA, 3-hydroxypropionyl-CoA, and β-alanyl-CoA. While they perform their respective reactions well in an isolated assay, they have two shortcomings in a more complex system both relating to the fact that both substrates need to be present at the same time. First, one of the substrates will be absent in the first turn of the cycle. For example, in the case of Smt, the CoA is transferred from the succinyl moiety to (S)-malate generating (S)-malyl-CoA and succinate. The succinate is then oxidised to fumarate which is hydrated to (S)-malate. Of course, if (S)-malate is not present, the reaction cannot proceed, so succinate will not be generated, and there is no mechanism to produce more (S)-malate, so the cycle stalls.

This is less of an issue for the 3-hydroxypropionyl-CoA and β-alanyl-CoA transferases because acetyl-CoA is used as a CoA donor, but the resulting acetate isn't involved in the generation of 3-hydroxypropionate or β-alanine respectively. Instead, the acetate is religated to CoA using an acyl-CoA synthetase. This leads however, to the second problem which is essentially the opposite of the first. Namely, if 100% of the acetyl-CoA is carboxylated to malonyl-CoA prior to the generation of the first molecule of 3-hydroxypropionate or β-alanine, there is no CoA donor present and the cycle stalls.

The former problem can be resolved with the addition of extraneous (S)-malate to get the reaction started. While this should work, it complicates comparison with other versions of the cycle because it effectively starts some of the carbon after the oxidative step, arguably the most difficult reaction in any version of the cycle. The latter problem can be resolved by very carefully fine-tuning enzyme concentrations such that a pool of acetyl-CoA is maintained. Again, optimisation is desirable for all versions of the cycle, but this is another version that is simply incapable of proceeding without it.

It is worth noting that the combination of multiple transferases may help to alleviate some of these issues. For example, if 3-hydroxypropionyl-CoA or β-alanyl-CoA are generated from acetyl-CoA by their respective transferases, the other product is acetate. Later, after the acyl-CoA has been converted to succinyl-CoA,

a succinyl-CoA:acetate CoA-transferase (EC 2.8.3.18) could be applied which would cleave the succinyl-CoA to succinate and regenerate the acetyl-CoA from the previously produced acetate. Then, as (S)-malate is produced, it can be ligated to CoA by Mcs. We did not pursue this option because it still requires proper optimisation to get the first transfer to operate properly and would then require Sdh to operate properly, but this is an option that might be valuable in vivo.

7.2.2.3. Anaplerosis

Once we established flux through the HOPAC cycle, a significant problem was the gradual loss of cycle intermediates. It is still not clear why this occurs, we pursued a number of potential explanations, none of which could explain the effect and it may be that several different processes are at play simultaneously draining intermediates from the cycle. It is possible to regenerate these intermediates, for example, with the addition of acetate, propionate, etc. and with their respective acyl-CoA synthetase. The primary drawback to this method is the significant ATP demand.

As an alternative, acetyl-phosphate or propionyl-phosphate can be synthesised with an acetate kinase (EC 2.7.2.1) or propionate kinase (EC 2.7.2.15) respectively and purified. Acetyl-phosphate or propionyl-phosphate could then be added with a phosphate acetyltransferase (EC 2.3.1.8) or phosphate propanoyltransferase (EC 2.3.1.222) respectively. This has the same effect but utilised the high energy bond of the acyl-phosphate and doesn't require ATP. Alternatively, acetoacetyl-CoA could be added with an acetyl-CoA C-acetyltransferase (EC 2.3.1.9) or 2-Methylacetoacetyl-CoA or 3-Oxoadipyl-CoA could be added with an acetyl-CoA C-acyltransferase generating two molecules of acetyl-CoA, a molecule each of acetyl- and propionyl-CoA, or a molecule each of acetyl- and succinyl-CoA respectively.

Ultimately, we decided against employing these methods in vitro because it would invalidate the ^{13}C-labelling experiments without clarifying what was causing the loss of cycle intermediates in the first place. Nevertheless, anaplerosis is ever present in a functioning metabolism in a living cell. Due to the importance of various cycle intermediates like succinyl-CoA and acetyl-CoA, the cycle would be continuously replenished. An interesting option for in vivo applications is the addition of self-replenishing reactions. For example, utilising the second cycle of the 3-hydroxypropionate bicycle converts glyoxylate to pyruvate. Pyruvate dehydrogenase complex can then convert the pyruvate to acetyl-CoA at the expense of a molecule of CO2 but with an NADH return. Alternatively, the β-hydroxyaspartate cycle in concert with (S)-malate dehydrogenase can convert two molecules of glyoxylate to (S)-malate. Mcs can then be used to synthesise (S)-malyl-CoA. This isn't useful in vitro, because we completely lose the ability

to see if the cycle is functional, but if it is employed in vivo, the cell can utilise any of the cycle intermediates without stalling the cycle.

7.2.2.4. Practical in vivo Application

In order for the HOPAC cycle to be implemented in vivo, it must be adequately integrated with the native metabolism of the host. This is generally a complicated process because of the highly optimised nature of natural metabolism, but there are some inroads that can be made by exploiting native enzymes. Propionyl-CoA and acetyl-CoA carboxylases are common in Bacteria, Archaea, and Eukarya (Tong, 2013). Likewise, Mcm and Epi are found in most life apart from plants (Takahashi-Iñiguez, 2012). Naturally, Scs, Sdh, and Fum are ubiquitous as they are important enzymes in the TCA cycle. Taken together, a significant portion of the HOPAC cycle can be natively found in many organisms.

The HOPAC cycle could be implemented in extremely well characterised organisms such as *E. coli*, by integrating Mcr, Pcs, Mcs, and Mcl. All other reactions are found natively. This allows for a relatively straightforward integration with only four genes. Further work would almost certainly need to be done to allow the cycle to function as a unit, modifying gene expression for example, but the heterologous genes were overexpressed in *E. coli* in this work so it is anticipated that they should function as required in this system. Conveniently, a glyoxylate auxotroph already exists (Claassens, 2020) and would force the cell to utilise the cycle. This could function as a system to further engineer Pcs, as well as a platform for further HOPAC engineering. So long as growth was achieved, Mcd and Mch could be integrated, for example, or the Pcs could be replaced with Hps, Ech, and Ccr. Once this is established, Hps and Ech could be replaced with the acyl-CoA transferase and βCal since the Abot used in this study originates from *E. coli*. If this cycle is successful, it could function as a system to engineer a β-alanyl-CoA synthetase.

Various other organisms might also be worth investigating. *Erythrobacter* sp NAP1, for example, is the species that Pcs was isolated from, and it has a bifunctional Mcr, so the only genes that would need to be integrated are Mcs and Mcl. An alternate approach is to us an organism containing the ethylmalonyl-CoA pathway such as *Cereibacter sphaeroides*. This contains an Ech, Ccr, Mcd with Etf and EtfQO, Mch, and Mcl, so the only genes that would need to be integrated are Mcr and Hps. Although the native Mcd would likely need to be replaced, this might still be a valuable approach not only because it implements the best version of HOPAC, bypassing Pcs, but also because it is also a photosynthesising bacterium. Since RuBisCO can account for 50% of cellular protein (Ellis, 1979), replacing the RPPC with the HOPAC would allow for a significant protein budget.

7.3. Closing Remarks

With this project we sought to show that new combinations of preexisting enzyme activities can work together to form a functional carbon-fixing cycle. These data taken together will other recent successes such as the CETCH, TaCo, and rGPS/MCG highlight the value of pursuing synthetic metabolism. While we have a long way to go before we can implement cycles like these into engineered organisms on a mass scale, these studies serve to identify and rectify various problems that might arise, and can inform both future in vivo implementation as well as the design of new and better cycles.

As discussed in the introduction, reducing atmospheric carbon is imperative to the health of life on this planet. In spite our best intentions, anthropogenic CO_2 is still on the rise and likely will be for the forseeable future. While it is true that we should take steps to dramatically reduce the ammount of CO_2 that we release into the atmosphere, it is human nature to push back against the loss of creature-comforts that produce these emmissions. As such, our ability not only to reduce emmissions, but also to remove past emissions from the atmosphere will be crucial for future success. If we are successful in limiting global warming this century, the struggle will not be over, and it will be important to have technologies at our disposal to continually maintain CO_2 emmissions at managable levels.

8. Materials and Methods

8.1. Synthesis of Cycle Intermediates

8.1.1. Acetyl-, Propionyl-, and Succinyl-CoA

Acetyl-, propionyl-, crotonyl- and succinyl-CoA were synthesised using the symmetric anhydride method (Peter, 2016). 250 µmol of Coenzyme A was dissolved in 5 mL of 500 mM NaHCO$_3$. 410 µmol of either acetic, propionic, crotonic, or succinic anhydride were added, and the solution was stirred on ice for 1 hour. Completeness of reaction was monitored using Ellman's reagent as described previously (Ellman, 1959). Completed reactions were purified directly.

8.1.2. Fumaryl-CoA

Fumaryl-CoA was synthesised using the Ethylchloroformate method (Peter, 2016). 2.5 mmol of fumarate was dissolved in 10 mL of tetrahydrofuran (THF) and chilled on ice. 1.3 mmol of triethylamine and 1.3 mmol of ethylchloroformate were added and the solution was stirred on ice for 45 minutes. 250 µmol of Coenzyme A was dissolved in 10 mL of 500 mM NaHCO$_3$ and added to the solution. The solution was stirred for an additional 1 hour at room temperature. Completeness of reaction was monitored using Ellman's reagent as described previously (Ellman, 1959). Completed reactions were flash-frozen in liquid nitrogen, lyophilised, and resuspended in 20 mL of 25 mM HCOONa pH 4.2 prior to purification.

8.1.3. 3-Hydroxypropionyl-CoA

3-Hydroxypropionyl-CoA and methylsuccinyl-CoA were synthesised using the carbonyldiimidazole method (Peter, 2016). 2.5 mmol of CDI and 3 mmol each acid were dissolved in 10 mL THF and mixed on ice for 1 h. 600 µmol CoA was dissolved in 5 mL in 0.5 M NaHCO$_3$ and added to the THF. After an additional 45 minutes of mixing, the reaction was flash frozen in liquid nitrogen and lyophilised. The powder was resuspended in 20 mL 25 mM HCOONa pH 4.2 prior to purification.

8.1.4. Malonyl- and Methylmalonyl-CoA

Malonyl- and methylmalonyl-CoA were synthesised using the CoA ligase MatB from *Rhizobium leguminosarum* (Peter, 2016). 320 µmol of Coenzyme A, 1.6 mmol of either malonate or methylmalonate, and 1.6 mmol of ATP were dissolved in 50 mL of 50 mM MOPS pH 7.5, 15 mM MgCl$_2$. The reaction was initiated with the addition of 10 µM MatB and the solution was incubated at 30 °C with gentle agitation. Completeness of reaction was monitored using Ellman's reagent as described previously (Ellman, 1959).

Completed reactions were flash-frozen in liquid nitrogen, lyophillised, and resuspended in 20 mL of 25 mM HCOONa pH 4.2 prior to purification.

8.1.5. (S)-Malyl- and (2R,3S)-β-Methylmalyl-CoA

(S)-Malyl- and (2R,3S)-β-methylmalyl-CoA were synthesised using the Mcl method (Herter et al., 2002). 0.5 mM acetyl-CoA ((S)-malyl-) or propionyl-CoA ((2R,3S)-β-methylmalyl-), 10 mM glyoxylate, were dissolved in 50 mL of 50 mM MOPS pH 7.5. The reaction was initiated with the addition of 10 μM Mcl and the solution was incubated at 30 °C with gentle agitation. After one hour, the reactions were flash-frozen in liquid nitrogen, lyophillised, and resuspended in 20 mL of 25 mM HCOONa pH 4.2 prior to purification.

8.1.6. Acrylyl-CoA

Acrylyl-CoA was synthesised using a propionyl-CoA synthetase. 320 μmol of Coenzyme A, 2 mM acrylate, 3mM ATP, and 15 mM $MgCl_2$ were dissolved in 10 mL of of 50 mM MOPS pH 7.5. The reaction was initiated with the addition of 10 μM Pcs and the solution was incubated at 30 °C with gentle agitation. Completeness of reaction was monitored using Ellman's reagent as described previously (Ellman, 1959). Completed reactions were flash-frozen in liquid nitrogen, lyophillised, and resuspended in 4 mL of 25 mM HCOONa pH 4.2 prior to purification.

8.1.7. β-Alanyl-CoA

β-alanyl-CoA was synthesised using a β-alanyl-CoA transferase. 0.5 mM propionyl-CoA and 10 mM β-alanine, were dissolved in 20 mL of 50 mM MOPS pH 7.5. The reaction was initiated with the addition of 10 μM βat and the solution was incubated at 30 °C with gentle agitation. After one hour, the reactions were flash-frozen in liquid nitrogen, lyophillised, and resuspended in 20 mL of 25 mM HCOONa pH 4.2 prior to purification.

8.1.8. Purification

Samples were purified with a Gemini® 10μm NX-C18 110 Å Column (Phenomenex, Aschaffenburg, Germany) in a 1260 Infinity HPLC (Agilent Technologies GmbH) using a methanol/HCOONa pH 4.2 gradient. Purified fractions were flash-frozen in liquid nitrogen, lyophilised, and stored with desiccant at 20 °C for future use. CoA-thioester concentration was determined by spectrophotometric absorbance at 260 nm with ε = 22.4 mM-1 cm-1 for unsaturated (fumaryl-CoA) and ε = 16.4 mM-1 cm-1 for saturated CoA-thioesters (all others).

8.2. Protein Expression and Purification

8.2.1. General Expression Protocol

Plasmids were transformed into *E. coli* BL21 DE3 ArcticExpress (DE3)RIL competent cells (unless stated otherwise), plated on LB agar containing 34 µg/mL chloramphenicol and the appropriate antibiotic (100 µg/mL ampicillin, 50 µg/mL Kanamycin, 100 µg/mL streptomycin) and incubated at 37°C overnight. Colonies were picked and grown in 1 L of TB containing 34 µg/mL chloramphenicol and the appropriate antibiotic at 37 °C with moderate agitation until an OD_{600} of ~1.5 was reached. Cultures were then cooled to 20 °C and induced with 500 µM IPTG (unless stated otherwise). Cultures were incubated for an additional 16 hours prior to harvest.

Cells were harvested by centrifugation at 8000 g for 10 minutes. Cell pellets were resuspended in 20 mM MOPS pH 7.5, 500 mM NaCl, 5 mM $MgCl_2$, and 20 % (v/v) glycerol. Cell suspensions were then sonicated to homogeneity and centrifuged at 100 000 g for 1 hour. Lysates were then passed through a 0.45 µm cut-off filter before being loaded onto a 5 mL HisTrap FF column (GE Healthcare, Freiburg, Germany) (unless stated otherwise). The column was washed with the above resuspension buffer and eluted with a gradient of the same buffer apart from the addition of 500 mM imidazole.

Purified protein was concentrated to ~1 mL and passed through two HiTrap 5 ml Desalting Columns (GE Healthcare, Freiburg, Germany) for buffer exchange into 20 mM MOPS pH 7.5, 200 mM NaCl, 5 mM $MgCl_2$, and 20 % glycerol (v/v). Desalted proteins were then concentrated to a working stock concentration determined by spectrophotometric absorbance at 280 nm with extinction coefficients determined with ExPASy ProtParam (Walker, 2005), split into single-use aliquots, and flash-frozen in liquid nitrogen for storage at 80 °C.

8.2.2. Mcds, Etf, CoA-Disulfide Reductase

FAD containing proteins were purified as described except it was noticed that the ratio between FAD cofactor 450 nm absorbance and protein 280 nm absorbance was often low after purification. Since this is not thought to be a transient interaction, we suspected this might be an artifact of the purification protocol. To solve this issue, after Ni^+ affinity purification, protein solutions were incubated in 1 mM FAD for 30 minutes. The protocol was then continued as above, and the excess FAD was removed during the desalting step.

To determine enzyme concentration, absorbance was measured at 280 nm and 450 nm. The A_{450}/A_{280} ratio for FAD alone is 0.57 between A_{450} 0.04 - 0.3. Using this ratio, we determined the portion of A_{280}

absorption provided by FAD, subtracted that from the total A_{280}, then determined the resulting concentration of enzyme using extinction coefficients determined with ExPASy ProtParam (Walker, 2005).

8.2.3. Etf-QO

ETF-QO was purified as described previously (Usselman, 2008). Briefly, lysis was performed as above except after centrifugation at 100 000 g, the pellet was recovered instead of the supernatant. The pellet was resuspended in the same buffer with 5% (w/v) Dodecyl-β-D-maltoside (DDM) (CAS 69227-93-6) and briefly sonicated to homogeneity. Slurries were then incubated on ice for 1 hour and centrifuged at 100 000 g for one hour. Finally, the supernatant was applied to a 5 mL HisTrap FF column, and the purification was completed as above.

8.2.4. Acetyl-/Propionyl-CoA Carboxylase

Both Acc and Pcc require biotinylation of the active site for activity. If these enzymes are expressed in *E. coli*, biotinylation is possible to a limited extent by the native biotin ligase and activity is detected. If Pcc is co-expressed with its cognate biotin ligase (BirA), however, activity can be increased several fold. As such, both variants were always co-expressed with BirA, and 5 µmol biotin was added to the growth medium during induction.

8.2.5. 3-hydroxypropionyl-CoA synthetase

The 3-hydroxypropionyl-CoA synthetase from *N. maritimus* was purified as described above, however, it was determined that, even while frozen, Hps significantly lost activity in a matter of 1-2 days. As such, this enzyme was always purified as close to use as possible, a maximum of 24 hours prior to assays, and discarded afterwards.

8.2.6. ASKA Plasmids

The pCA24N vector used in the ASKA Collection (Kitagawa et al., 2005) cannot easily be screened if transformed into *E. coli* BL21 DE3 ArcticExpress cells due to commensurate resistances. As a result, these proteins were expressed in standard *E. coli* BL21 DE3 cells and were plated and grown with only 34 µg/mL chloramphenicol. All other purification steps were as described above.

8.3. Kinetics

8.3.1. ATP Dependent Reactions

The activity of Pcc, Acc, and acyl-CoA sythetases were determined by monitoring ATP hydrolysis with a coupled assay using pyruvate kinase and lactate dehydrogenase (Sigma-Aldrich). Various concentrations

of ATP were added to a final concentration of 1 mM triethanolamine, 1.6 mM phosphoenolpyruvate, 4.2 mM magnesium sulfate, 6.8 mM potassium chloride, 300 µM NADH, 40 units pyruvate kinase, and 100 units lactic dehydrogenase. The oxidation of NADH was monitored at 340 nm with the extinction coefficient $\varepsilon = 6.22$ $M^{-1}cm^{-1}$.

In the case of Pcc, 215 nM Pcc was added to (0.03-1 mM propionyl-CoA with 2 mM ATP and 65 mM NaHCO$_3$) or (0.015-3 mM ATP with 65 mM NaHCO$_3$ and 2 mM propionyl-CoA) or (0.06-2 mM acetyl-CoA with 2 mM ATP) and 65 mM NaHCO$_3$ in 50 mM MOPS pH 7.5.

In the case of Acc, 250 nM Acc was added to (0.03-2 mM propionyl-CoA with 2 mM ATP and 65 mM NaHCO$_3$) or (0.03-3 mM ATP with 65 mM NaHCO$_3$ and 2 mM propionyl-CoA) or (0.06-4 mM acetyl-CoA with 2 mM ATP) and 65 mM NaHCO$_3$ in 50 mM MOPS pH 7.5.

For the acyl-CoA synthetase screen, 2.5 µM of each acyl-CoA synthetase were added to 5 mM of each acid, 0.5 mM CoA, and 3 mM ATP in 50 mM MOPS pH 7.5. Endpoints were analysed by LCMS.

8.3.2. NADPH Dependent Reactions

The activity of Ccr, Gdh, Mcr, and Pcs were determined spectrophotometrically following the oxidation of NADPH. As NADPH is oxidised to NADP$^+$, the absorbance at 360 nm decreases with the extinction coefficient $\varepsilon_{360} = 3.4$ $mM^{-1}cm^{-1}$. 100 nM Ccr was added to 5 µM Ech with 0.125-2.5 mM 3-hydroxypropionyl-CoA, 50 mM NaHCO$_3$, 500 µM NADPH or 0.05-1 mM NADPH, 50 mM NaHCO$_3$, and 2 mM 3-hydroxypropionate in 50 mM MOPS pH 7.5.

9.7 µM Gdh was added to 0.3-3.5 mM 2-oxoglutarate, with 150 mM NH$_4$Cl and 0.5 mM NADPH or 5-650 µM NADPH with 150 mM NH$_4$Cl and 3 mM 2-oxoglutarate, or 5-200 mM NH$_4$Cl with 3 mM 2-oxoglutarate and 0.5 mM NADPH, or 0.15-2.5 mM L-glutamate with 2 mM NADP$^+$, or 3-650 µM NADP$^+$ with 2 mM L-glutamate.

Because Mcr is responsible for both the reduction of malonyl-CoA and malonic semialdehyde, the molarity of NADPH consumed was divided by two to determine the number of molecules of malonyl-CoA converted to 3-hydroxypropionate. 200 nM Mcr was added to 0.3-12 µM malonyl-CoA with 200 µM NADPH or 5-250 µM NADPH with 12 µM malonyl-CoA in 50 mM MOPS pH 7.5.

In the case of Pcs, the three-step reaction was monitored as a unit to determine the net kinetic rates rather than the individual ATP dependent CoA ligation and hydration reactions. 1 µM Pcs was added to (0.001-3 mM 3-hydroxypropionate with 200 µM NADPH, 5 mM ATP, 2 mM CoA), or (0.005-1.5 mM ATP

with 2 mM 3-hydroxypropionate, 200 μM NADPH, 2 mM CoA), or (0.05-3 mM CoA with 2 mM 3-hydroxypropionate, 200 μM NADPH, 5 mM ATP) or (10-300 μM NADPH with 2 mM 3-hydroxypropionate, 5 mM ATP, 2 mM CoA), in 50 mM MOPS pH 7.5.

8.3.3. Methylmalonyl-CoA Mutase and MeaB

Mcm activity was determined in a coupled assay with succinyl-CoA reductase (SucD). As Mcm converts methylmalonyl-CoA to succinyl-CoA, SucD reduces it to succinic semialdehyde. The oxidation of the NADPH required for this reaction can be monitored as described above. 6.5 nM Mcm was added to 5-550 μM (2R)-methylmalonyl-CoA with 5 μM SucD and 330 μM NADPH in 50 mM MOPS pH 7.5.

To determine if MeaB had a protective effect on Mcm, Mcm was incubated alone, or in the presence of MeaB methylmalonyl-CoA. At regular intervals, samples were removed and added to SucD and NADPH. The reactions were quenched with formic acid, centrifuged, and viewed with LCMS. Samples with methylmalonyl-CoA remaining were the result of Mcm inactivation. 3 μM Mcm was added to 600 μM (2R)-methylmalonyl-CoA or preincubated with 30 μM MeaB and then added to methylmalonyl-CoA. As a negative control, (2R)-methylmalonyl-CoA was incubated without enzyme in 50 mM MOPS pH 7.5.

8.3.4. (S)-Malyl-CoA Lyase

Mcl activity was determined with a coupled assay using Gox. Mcl was incubated with either (S)-malyl- or (2R,3S)-β-methylmalyl-CoA, Gox, and NADPH. As (S)-malyl- or (2R,3S)-β-methylmalyl-CoA were converted to glyoxylate and acetyl- or propionyl-CoA respectively, the glyoxylate was reduced by Gox and the NADPH oxidation was monitored as described above. 1 μM Mcl was added to either 10-500 μM (S)-malyl-CoA or 20-800 μM (2R,3S)-β-methylmalyl-CoA with 5 μM Gox and 100 μM NADH in 50 mM MOPS pH 7.5.

8.3.5. Methylsuccinyl-CoA Dehydrogenase and Succinate Dehydrogenase

The activity of MCD and Sdh were determined spectrophotometrically using ferrocenium hexafluorophosphate as an electron acceptor. When ferrocenium is reduced to ferrocene, the absorbance at 300 nm increases. Product formation is determined using the extinction coefficient $\varepsilon = 2.75$ mM^{-1}cm^{-1}. 30 μM SdhA or 10 μM SdhAB were added to 0.03-6.5 mM succinate with 0.25 mM ferrocenium in 50 mM MOPS pH 7.5.

To determine Mcd activities, enzymes at the concentrations in Table. 8.1. were added to 500 μM of (2S)-methylsuccinyl-CoA or succinyl-CoA with 0.25 mM ferrocenium in 50 mM MOPS pH 7.5.

When homolog kinetics were measured, enzymes at the concentrations in Table. 8.1. were added to 10-250 µM (2S)-methylsuccinyl-CoA or 25-200 µM succinyl-CoA with 0.25 mM ferrocenium in 50 mM MOPS pH 7.5.

Table. 8.1. Concentration in µM of mutants and homologs of Mcd used to determine relative activities and kinetic parameters.

	(2S)-Methylsuccinyl-CoA	Succinyl-CoA
PmMcd_T241E	5	10
PmMcd_T241N	10	10
PmMcd_T241Q	10	10
PmMcd_T241W	10	10
PmMcd_I245E	10	10
PmMcd_I245K	10	10
PmMcd_I245L	10	5
PmMcd_I245M	5	5
PmMcd_I245Q	10	20
PmMcd_I245R	10	10
PmMcd_I275H	10	10
PmMcd_I275K	10	50
PmMcd_I275L	1	10
PmMcd_I275Q	10	10
PmMcd_I275S	10	20
PmMcd_I275T	10	10
PmMcd_F530K	0.2	3.7
Pseudomonas migulae	0.02	0.5
Streptomyces sp.	0.1	3.0
Erythrobacter litoralis	0.1	1.1
Frankia sp.	0.03	0.5
Caulobacter vibrioides	0.02	4.0
Wenxinia marina	0.04	0.7
Bacterium HR19	4.1	4.1

To ensure the oxidation of ferrocenium to ferrocene was the result of oxidation of the acyl-CoA, representative samples were run on a 6550 iFunnel Q-TOF LC-MS system (Agilent Technologies) equipped with an electrospray ionisation source set to positive ionisation mode. Compounds were separated on an RP-18 column (50x 2.1 mm, particle size 1.7 µm; Kinetex XB-C18, Phenomenex, Aschaffenburg, Germany)

using a mobile phase system composed of 50 mM ammonium formate, pH 8.1, and methanol. LC-MS data were analysed using MassHunter qualitative analysis software (Agilent Technologies) and eMZed.

8.3.6. Etf and EtfQO

An endpoint assay was performed where 0.1 µM Mcd oxidised 100 µM methylsuccinyl-CoA alone, with 10 µM Etf, or with 10 µM Etf and 10 µM EtfQO. Reactions were quenched with formic acid, centrifuged, and viewed with LCMS. As a positive control, 0.1 µM Mcd oxidised 100 µM methylsuccinyl-CoA using 1 mM ferrocenium hexafluorophosphate as an electron acceptor. To determine whether O_2 was the terminal electron acceptor, the same assay was repeated under anaerobic conditions.

8.3.7. Mesaconyl-C1-CoA Hydratase

The activity of Mch was determined spectrophotometrically. As mesaconyl-C1- or fumaryl-CoA are converted to (2R,3S)-β-methylmalyl- or (S)-malyl-CoA respectively, the double bond is hydrated resulting in a loss of absorbance at 290 nm. Product formation was determined using the extinction coefficient $\varepsilon = 3.1$ $mM^{-1}cm^{-1}$ (Erb, 2010). 25 nM Mch was added to 20-850 µM fumaryl-CoA, 20-600 µM (S)-malyl-CoA, or 20-800 µM (2R,3S)-β-methylmalyl-CoA in 50 mM MOPS pH 7.5.

8.3.8. Fumarate Hydratase

The activity of fumarate hydratase was determined spectrophotometrically following the hydration of the double bond of fumarate at 240 nm using the extinction coefficient $\varepsilon = 2.4$ $mM^{-1}cm^{-1}$ (Kronen, 2015). The reverse reaction was monitored under the same conditions except the formation, rather than the depletion was measured. 65 nM Fum was added to 0.05-1.5 mM fumarate or 0.15-6.5 mM malate in 50 mM MOPS pH 7.5.

8.3.9. Succinyl-CoA Hydrolase

Promiscuity of Sch was determined by endpoint analysis. 500 nM Sch was added to 1 mM of each acyl-CoA in 50 mM MOPS pH 7.5. Samples were taken at 0, 5, and 15 minutes and viewed with LCMS.

8.3.10. Dephospho-CoA Kinase

Each acyl-CoA was incubated with shrimp alkaline phosphatase from Sigma-Aldrich (GEE70092Y) until they were dephosphorylated. Samples were then passed through a 5 kDa cutoff filter out phosphatase, and added to CoAE with ATP to rephosphorylate. Samples were quenched with formic acid and analysed with LCMS. 3 mM acyl-CoA was added to 5 units of SAP with 8 mM $MgCl_2$ in 50 mM MOPS pH 7.5. After removal of SAP, 10 µM CoAE with 5 mM ATP were added to the reaction mix.

8.3.11. β-Alanyl-CoA Lyase

βCal activity was determined with a coupled assay with Ccr. As β-alanyl-CoA was deamiated, acrylyl-CoA was carboxylated and the NADPH oxidation was monitored as described above. 1 nM βCal was added to 0.015-1.5 mM β-alanyl-CoA with 5 µM Ccr and 0.5 mM NADPH in 50 mM MOPS pH 7.5.

8.4. Thermodynamics

All thermodynamic approximations mentioned in the text were calculated by the eQuilibrator 3.0 database (Beber, 2022).

8.5. Partial Cycle Assays

To evaluate enzyme combinations, we investigated the cycle in two halves divided between carboxylation reactions. Converting acetyl-CoA to (2S)-methylmalonyl-CoA, the reductive pathway (Table. 8.2.), has five variants. Three variants utilise an acyl-CoA transferase. The L-Glutamate pathway and L-Alanine pathway use βapt and Abot respectively to generate β-alanine which is ligated to CoA by βact using acetyl-CoA as a CoA donor. The 3act pathway generates 3-hydroxypropionate with Mcr, and then ligates it to CoA by 3act, also using acetyl-CoA as a CoA donor.

While setting up the reactions, two solutions were created. One contained all enzymes, the other contained everything else, to prevent any unwanted reactions. The samples were warmed to 35 °C, combined, and started with the addition of malonyl-CoA. For transferase reactions, acetyl-CoA was added after five minutes to minimise unwanted transferase reactions. Samples were quenched with formic acid, centrifuged, and analysed with LCMS.

Converting (2S)-methylmalonyl-CoA to acetyl-CoA, the oxidative pathway (Table. 8.3.) has four variants. Reactions were treated similarly to the reductive pathway reactions, except assays were started with the addition of (2S)-methylmalonyl-CoA.

Table. 8.2. Concentration of enzymes and cofactors in reductive pathway assays. Cells highlighted in grey are in mM, all others are in µM.

	L-Glutamate	L-Alanine	Pcs	Hps	3act
MOPS pH 7.5	50	50	50	50	50
NaHCO$_3$	50	50	50	50	50
Formate	20	20	20	20	20
NH$_4$Cl	100	100	-	-	-
ATP	-	-	2	2	-
NADPH	2	2	2	2	2
L-Glutamate	250	-	-	-	-
L-Alanine	-	250	-	-	-
MgCl$_2$	-	-	5	5	-
CoA	-	-	1	1	-
PolyPO$_4$	-	-	25	25	-
Gdh	25	-	-	-	-
Adh	-	25	-	-	-
Fdh	30	30	30	30	30
Ppk$_{Sm}$	-	-	50	50	-
Ppk$_{Aj}$	-	-	50	-	-
Mcr$_{CT}$	20	20	-	-	-
Abot	60	-	-	-	-
βapt	-	60	-	-	-
βact	50	50	-	-	-
βCal	50	50	-	-	-
Ccr	25	25	-	-	-
Pcs	-	-	150	-	-
Hps	-	-	-	50	-
Ech	-	-	-	50	50
Ccr	-	-	-	50	50
Mcr	-	-	50	50	50
3act	-	-	-	-	50
Pcc	-	-	150	-	-
Malonyl-CoA	1	1	1	1	1
Acetyl-CoA	2	2	-	-	2

Table. 8.3. Concentration of enzymes and cofactors in oxidative pathway assays. Cells highlighted in grey are in mM, all others are in µM.

	Mcd	Scs	Sct	Sch
MOPS pH 7.5	50	50	50	50
ATP	-	2.5	-	2.5
ADP	-	2.5	-	2.5
MgCl$_2$	5	5	5	5
CoA	0	0.5	0	0.5
AdoCbl	65	65	65	65
FAD	30	30	30	30
Ascorbic Acid	3.375	3.375	3.375	3.375
Ferrocenium	-	1.5	1.5	1.5
Mcm	5	5	5	5
Epi	5	5	5	5
Mch	10	10	10	10
Mcl	40	40	40	40
Mcd	20	-	-	-
EtfAB	20	-	-	-
QO	60	-	-	-
SdhA/B	-	100	100	100
FumC	-	10	10	10
SucCD	-	100	-	-
Mcs	-	100	-	100
Smt	-	-	20	-
Malate	-	-	0.2	-
Sch	-	-	-	1
Methylmalonyl-CoA	1	1	1	1

8.6. Full Cycle Assays

Much like the partial cycle assays, full cycles (Table. 8.4.) were set up in two parts. One contained all enzymes, the other contained everything else. Samples were warmed to 35 °C, combined, and started with the addition of acetyl-CoA. When MeaB was used, it was mixed with Mcm and incubated on ice for 10 minutes prior to beginning the reaction in case time was required to initiate interactions. When Mcm was spiked throughout, instead of adding 5 µM in the beginning, the assay was started with 1.25 µM. The volume was adjusted as samples were removed so that 1.25 µM was added after 30 minutes, 60 minutes, and immediately prior to quenching the final sample.

Table. 8.4. Concentration of enzymes and cofactors in full HOPAC cycle assays. Cells highlighted in grey are in mM, all others are in μM.

	Hps	Hps+ EtfQO	Hps +EtfQO+MeaB	Hps+EtfQO +Mcm Spike	Pcs+EtfQO +Mcm Spike
MOPS pH 7.5	50	50	50	50	50
NaHCO3 ^{13}C	33	33	33	33	33
Formate ^{13}C	13	13	13	13	13
ATP	3	3	3	3	3
NADPH	3	3	3	3	3
NADH	2	2	2	2	2
MgCl$_2$	5	5	5	5	5
CoA	0.5	0.5	0.5	0.5	0.5
PolyPO$_4$	13	13	13	13	13
AdoCbl	65	65	65	65	65
FAD	30	30	30	30	30
Ascorbic Acid	3.375	3.375	3.375	3.375	3.375
CoADSB	15	15	15	15	15
Carbonic Anhydrase	5	5	5	5	5
SodB	5	5	5	5	5
KatE	35	35	35	35	35
Fdh	50	50	50	50	50
Ppk$_{Sm}$	50	50	50	50	50
Ppk$_{Aj}$	-	-	-	-	20
Pcs	-	-	-	-	50
Pcc	-	-	-	-	20
Hps	40	40	40	40	-
Ech	20	20	20	20	-
Ccr	50	50	50	50	-
Mcm	5	5	5	5	5
Epi	5	5	5	5	5
Mcd	20	20	20	20	20
Etf	20	20	20	20	20
EtfQO	-	60	60	60	60
Mch	10	10	10	10	10
Mcl	50	50	50	50	50
Gox	30	30	30	30	30
Acc	20	20	20	20	20
Mcr	5	5	5	5	5
MeaB	-	-	50	-	-
Acetyl-CoA	200	200	200	200	200

Samples were quenched with formic acid and analysed with LCMS. When ^{13}C labelling was monitored, assays were set up with ^{13}C bicarbonate and formate. When glycolate was monitored, ^{12}C bicarbonate and formate were used so that a ^{13}C glycolate internal standard could be used.

8.7. UPLC-high resolution MS

8.7.1. Acyl-CoA

Detection of acyl-CoAs was performed using isotope dilution mass spectrometry. The chromatographic separation was performed on an Agilent Infinity II 1290 HPLC system using a Kinetex EVO C18 column (150 × 1.7 mm, 3 μm particle size, 100 Å pore size, Phenomenex) connected to a guard column of similar specificity (20 × 2.1 mm, 5 μm particle size, Phenomoenex) a constant flow rate of 0.25 ml/min with mobile phase A being 50 mM Ammonium Acetate in water at a pH of 8.1 and phase B being 100 % methanol (Honeywell, Morristown, New Jersey, USA).

The injection volume was 5 μl. The mobile phase profile consisted of the following steps and linear gradients: 0 – 1 min constant at 2.5 % B; 1 – 6 min from 2.5 to 95 % B; 6 – 8 min constant at 95 % B; 8 – 8.1 min from 95 to 2.5 % B; 8.1 to 10 min constant at 2.5 % B. An Agilent 6550 ion funnel QTOF mass spectrometer was used in positive mode with an electrospray ionisation source and the following conditions: ESI spray voltage 3500 V, nozzle voltage 500 V, sheath gas 400° C at 12 l/min, nebuliser pressure 20 psig and drying gas 225° C at 13 l/min. Compounds were identified based on their accurate mass (mass error < 5 ppm) and retention time compared to standards. Chromatograms were integrated using MassHunter software (Agilent, Santa Clara, CA, USA).

8.7.2. Glycolate

Quantitative determination of Glycolate was performed using isotope dilution mass spectrometry. The chromatographic separation was performed on an Agilent Infinity II 1290 HPLC system using a Kinetex EVO C18 column (150 × 1.7 mm, 3 μm particle size, 100 Å pore size, Phenomenex) connected to a guard column of similar specificity (20 × 2.1 mm, 5 μm particle size, Phenomoenex) a constant flow rate of 0.1 ml/min with mobile phase A being 0.1 % formic acid in water and phase B being 0.1 % formic acid methanol (Honeywell, Morristown, New Jersey, USA) at 25° C .

The injection volume was 0.5 μl. The mobile phase profile consisted of the following steps and linear gradients: 0 – 4 min constant at 0 % B; 4 – 6 min from 0 to 100 % B; 6 – 7 min constant at 100 % B; 7 – 7.1 min from 100 to 0 % B; 7.1 to 12 min constant at 0 % B. An Agilent 6495B ion funnel mass spectrometer

was used in negative mode with an electrospray ionisation source and the following conditions: ESI spray voltage 2000 V, nozzle voltage 500 V, sheath gas 400° C at 11 l/min, nebuliser pressure 50 psig and drying gas 80° C at 16 l/min. Compounds were identified based on their mass transition and retention time compared to standards. Chromatograms were integrated using MassHunter software (Agilent, Santa Clara, CA, USA). Absolute concentrations were calculated based on an external calibration curve prepared in sample matrix, using uniformly 13C-labelled Glycolate as internal standard.

Mass transitions, collision energies, Cell accelerator voltages and Dwell times have been optimised using chemically pure standards. Parameter settings of all targets are given in Table 8.4.

Table. 8.4. Parameters used for the detection of glycolate by LCMS.

Compound	Quantifier	Collision Energy	Qualifier	Collision Energy	Dwell	Fragmenter voltage	Cell Accelerater Volatege
X1	75→75	0	75→47	9	150	380	5
X2	77→77	0	77→48	9	150	380	5

Abbreviations

3HP/4HBC - 3-hydroxypropionate/4-hydroxybutyrate cycle

3HPB - 3-hydroxypropionate bicycle

Abot - 4-aminobutyrate-2-oxoglutarate transaminase

Acc - acetyl-CoA carboxylases

Adh - alanine dehydrogenase

AdoCbl - coenzyme B_{12}

AMP/ADP/ATP - adenosine mono/di/triphosphate

βact - β-alanine CoA-transferase

βapt - β-alanine-pyruvate transaminase

βCal - β-alanyl-CoA ammonia-lyase

BirA - biotin ligase

BRENDA - Braunschweig Enzyme Database

Ccr - crotonyl-CoA carboxylase/reductase

CDI - carbonyldiimidazole

Cdr - CoA-disulfide reductase

CETCH - crotonyl-CoA/ethylmalonyl-CoA/hydroxybutyryl-CoA

CoA - coenzyme A

CoAD - CoA dimers

CoAE - dephospho-CoA kinase

DC4HBC - dicarboxylate/4-hydroxybutyrate cycle

DDM - dodecyl-β-D-maltoside

DTMB - 5,5'-dithio-bis-(2-nitrobenzoic acid)

ECF - ethylchloroformate

Ech - enoyl-CoA hydratase

Ecm - ethylmalonyl-CoA mutase

Epi - methylmalonyl-CoA epimerase

Etf - electron transfer flavoprotein

EtfQO - electron transfer flavoprotein quinone oxidoreductase

FAD - flavin adenine dinucleotide

Frd - fumarate reductase

Fum - fumarase

Gcd - glutaryl-CoA dehydrogenase

Gdh - glutamate dehydrogenase

Gox - glyoxylate reductase

Hps - hydroxypropionyl-CoA synthetase

HOPAC - hydroxypropionyl-CoA/acrylyl-CoA cycle

HsIbd - isobutyryl-CoA dehydrogenase

kDa - kilodalton

KEGG - Kyoto Encyclopedia of Genes and Genomes

Mcd - methylsuccinyl-CoA dehydrogenase

MCG - malyl-CoA-glycerate pathway

Mch - mesaconyl-C1-CoA hydratase

Mcl - (S)-malyl-CoA/ (2R,3S)-β-methylmalyl-CoA/(S)-citramalyl-CoA lyase

Mcm - methylmalonyl-CoA mutase

Mcr - malonyl-CoA reductase

Mcs - malyl-CoA synthetase

NAD(P)H - nicotinamide adenine dinucleotide (phosphate)

OH₂Cbl - aquacobalamin

Pcc - propionyl-CoA carboxylase

Pcs - propionyl-CoA synthetase

PEG - polyethylene glycol

RACP - reductive acetyl-CoA pathway/Wood-Ljungdahl pathway

rGPS - reductive glyoxylate and pyruvate synthesis cycle

RPPC - reductive pentose phosphate cycle/Calvin-Benson-Bassham cycle

RTCAC - reductive tricarboxylic acid cycle/Arnon-Buchanan cycle

RuBisCO - ribulose-1,5-bisphosphate carboxylase-oxygenase

Sch - succinyl-CoA hydrolase

Scs - succinyl-CoA synthetase

Sdh - succinate dehydrogenase

Smt - succinyl moiety of succinyl-CoA to (S)-malate

SsMcad - medium-chain acyl-CoA dehydrogenase

SucD - succinyl-CoA dehydrogenase

T2ot - taurine-2-oxoglutarate transaminase

TaCo - tartronyl-CoA pathway

THF - tetrahydro

References

Alexeev, Vladimir A., and Craig H. Jackson. "Polar amplification: is atmospheric heat transport important?" Climate dynamics 41.2 (2013): 533-547. https://doi.org/10.1007/s00382-012-1601-z

Asao, Marie, and Birgit E. Alber. "Acrylyl-coenzyme A reductase, an enzyme involved in the assimilation of 3-hydroxypropionate by *Rhodobacter sphaeroides*." Journal of bacteriology 195.20 (2013): 4716-4725. https://doi.org/10.1128/JB.00685-13

Auguet, Jean-Christophe, and Emilio O. Casamayor. "Partitioning of *Thaumarchaeota* populations along environmental gradients in high mountain lakes." FEMS microbiology ecology 84.1 (2013): 154-164. https://doi.org/10.1111/1574-6941.12047

Bassham, James Alan, and Melvin Calvin. "The path of carbon in photosynthesis." Die CO_2-Assimilation/The Assimilation of Carbon Dioxide. Springer, Berlin, Heidelberg, 1960. 884-922. https://doi.org/10.1007/978-3-642-94798-8_30

Bathellier, Camille, et al. "Rubisco is not really so bad." Plant, cell & environment 41.4 (2018): 705-716. https://doi.org/10.1111/pce.13149

Battaile, Kevin P., et al. "Structures of isobutyryl-CoA dehydrogenase and enzyme-product complex: comparison with isovaleryl-and short-chain acyl-CoA dehydrogenases." Journal of Biological Chemistry 279.16 (2004): 16526-16534. https://doi.org/10.1074/jbc.M400034200

Battin, Tom J., and Sebastiaan Luyssaert. "L. a. Kaplan, AK Aufdenkampe, A. Richter, and LJ Tranvik (2009), The boundless carbon cycle." Nature Geoscience 2.9: 598-600. https://doi.org/10.1038/ngeo618

Beber, Moritz E., et al. "eQuilibrator 3.0: a database solution for thermodynamic constant estimation." Nucleic acids research 50.D1 (2022): D603-D609. https://doi.org/10.1093/nar/gkab1106

Bello, Carolina, et al. "Defaunation affects carbon storage in tropical forests." Science advances 1.11 (2015): e1501105. doi: 10.1126/sciadv.1501105

Benson, Andrew A. "Identification Of Ribulose In $C^{14}O_2$ Photosynthesis Products." Journal of the American Chemical Society 73.6 (1951): 2971-2972.

Berg, Ivan A., et al. "A 3-hydroxypropionate/4-hydroxybutyrate autotrophic carbon dioxide assimilation pathway in Archaea." Science 318.5857 (2007): 1782-1786. https://doi.org/10.1126/science.1149976

Berner, Robert A. "The long-term carbon cycle, fossil fuels and atmospheric composition." Nature 426.6964 (2003): 323-326. https://doi.org/10.1038/nature02131

Bernhardsgrütter, Iria, et al. "The multicatalytic compartment of propionyl-CoA synthase sequesters a toxic metabolite." Nature chemical biology 14.12 (2018): 1127-1132. https://doi.org/10.1038/s41589-018-0153-x

Bernhardsgrütter, Iria, et al. "Awakening the sleeping carboxylase function of enzymes: engineering the natural CO_2-binding potential of reductases." Journal of the American Chemical Society 141.25 (2019): 9778-9782. https://doi.org/10.1021/jacs.9b03431

Borjian, Farshad, et al. "Succinyl-coa: mesaconate coa-transferase and Mesaconyl-Coa hydratase, enzymes of the methylaspartate cycle in haloarcula hispanica." Frontiers in microbiology 8 (2017): 1683. https://doi.org/10.3389/fmicb.2017.01683

Burgener, Simon, et al. "Molecular basis for converting (2 S)-methylsuccinyl-CoA dehydrogenase into an oxidase." Molecules 23.1 (2017): 68. https://doi.org/10.3390/molecules23010068

Buzenet, Anne M., et al. "Purification and properties of 4-aminobutyrate 2-ketoglutarate aminotransferase from pig liver." Biochimica et Biophysica Acta (BBA)-Enzymology 522.2 (1978): 400-411. https://doi.org/10.1016/0005-2744(78)90073-6

Canadell, J. G. C., M. R. Le Quéré, and C. B. Raupach. "Field, ET Buitenhuis, P. Ciais, TJ Conway, NP Gillett, RA Houghton, and G. Marland, 2007. Contributions to accelerating atmospheric CO_2 growth from economic activity, carbon intensity, and efficiency of natural sinks." Proc. Natl. Acad. Sci 104: 18866-18870. https://doi.org/10.1073/pnas.0702737104

Carlson, Brian W., et al. "Oxidation of NADH involving rate-limiting one-electron transfer." Journal of the American Chemical Society 106.23 (1984): 7233-7239. https://doi.org/10.1021/ja00335a062

Chang, Antje, et al. "BRENDA, the ELIXIR core data resource in 2021: new developments and updates." Nucleic Acids Research 49.D1 (2021): D498-D508. https://doi.org/10.1093/nar/gkaa1025

Chen, Lin, et al. "The binding and release of oxygen and hydrogen peroxide are directed by a hydrophobic tunnel in cholesterol oxidase." Biochemistry 47.19 (2008): 5368-5377. https://doi.org/10.1021/bi800228w

Claassens, Nico J., et al. "Replacing the Calvin cycle with the reductive glycine pathway in *Cupriavidus necator*." Metabolic Engineering 62 (2020): 30-41. https://doi.org/10.1016/j.ymben.2020.08.004

Dave, Ushmaben Chandrakantbhai, and Ravi-Kumar Kadeppagari. "Alanine dehydrogenase and its applications–A review." Critical Reviews in Biotechnology 39.5 (2019): 648-664. https://doi.org/10.1080/07388551.2019.1594153

delCardayré, S. B., et al. "Coenzyme A disulfide reductase: purification and characterization of the enzyme component of the primary thiol/disulfide redox system in Staphylococcus aureus." J. Biol. Chem 273 (1998): 5744-5751.

Demmer, Ulrike, et al. "Structural basis for a bispecific NADP+ and CoA binding site in an archaeal malonyl-coenzyme A reductase." Journal of Biological Chemistry 288.9 (2013): 6363-6370. https://doi.org/10.1074/jbc.M112.421263

Diacovich, Lautaro, et al. "Crystal structure of the β-subunit of acyl-CoA carboxylase: structure-based engineering of substrate specificity." Biochemistry 43.44 (2004): 14027-14036. https://doi.org/10.1021/bi049065v

Dobson, C. Melissa, et al. "Identification of the gene responsible for the cblA complementation group of vitamin B_{12}-responsive methylmalonic acidemia based on analysis of prokaryotic gene arrangements." Proceedings of the National Academy of Sciences 99.24 (2002): 15554-15559. https://doi.org/10.1073/pnas.242614799

Drozak, Jakub, et al. "Molecular identification of carnosine synthase as ATP-grasp domain-containing protein 1 (ATPGD1)." Journal of Biological Chemistry 285.13 (2010): 9346-9356. https://doi.org/10.1074/jbc.M109.095505

Ellman, G. L. "Tissue sulfhvdrvl sroups." Archives Biochem. & Biophvs 82 (1959): 72-7. https://doi.org/10.1016/0003-9861(59)90090-6

Ellis, R. John. "The most abundant protein in the world." Trends in biochemical sciences 4.11 (1979): 241-244. https://doi.org/10.1016/0968-0004(79)90212-3

Erb, Tobias J., et al. "Synthesis of C_5-dicarboxylic acids from C_2-units involving crotonyl-CoA carboxylase/reductase: the ethylmalonyl-CoA pathway." Proceedings of the National Academy of Sciences 104.25 (2007): 10631-10636. https://doi.org/10.1073/pnas.0702791104

Erb, Tobias J., et al. "Carboxylation mechanism and stereochemistry of crotonyl-CoA carboxylase/reductase, a carboxylating enoyl-thioester reductase." Proceedings of the National Academy of Sciences 106.22 (2009): 8871-8876. https://doi.org/10.1073/pnas.0903939106

Erb, Tobias J., et al. "The apparent malate synthase activity of *Rhodobacter sphaeroides* is due to two paralogous enzymes,(3 S)-malyl-coenzyme A (CoA)/β-methylmalyl-CoA lyase and (3 S)-malyl-CoA thioesterase." Journal of bacteriology 192.5 (2010): 1249-1258. https://doi.org/10.1128/JB.01267-09

Evans, M. C., Bob B. Buchanan, and Daniel I. Arnon. "A new ferredoxin-dependent carbon reduction cycle in a photosynthetic bacterium." Proceedings of the National Academy of Sciences of the United States of America 55.4 (1966): 928. https://doi.org/10.1073/pnas.55.4.928

Farquharson, Louise M., et al. "Climate change drives widespread and rapid thermokarst development in very cold permafrost in the Canadian High Arctic." Geophysical Research Letters 46.12 (2019): 6681-6689. https://doi.org/10.1029/2019GL082187

Flamholz, Avi, et al. "eQuilibrator—the biochemical thermodynamics calculator." Nucleic acids research 40.D1 (2012): D770-D775. https://doi.org/10.1093/nar/gkr874

Friedlingstein, Pierre, et al. "Global carbon budget 2021." Earth System Science Data 14.4 (2022): 1917-2005. https://doi.org/10.5194/essd-2021-386

Friedmann, Silke, et al. "Properties of succinyl-coenzyme A: L-malate coenzyme A transferase and its role in the autotrophic 3-hydroxypropionate cycle of *Chloroflexus aurantiacus*." Journal of bacteriology 188.7 (2006): 2646-2655. https://doi.org/10.1128/JB.188.7.2646-2655.2006

Gergely, J., P. Hele, and C. V. Ramakrishnan. "Succinyl and acetyl coenzyme a deacylases." Journal of Biological Chemistry 198.1 (1952): 323-334. https://www.ncbi.nlm.nih.gov/pubmed/12999747

Heinze, Christoph, et al. "The quiet crossing of ocean tipping points." Proceedings of the National Academy of Sciences 118.9 (2021). https://doi.org/10.1073/pnas.2008478118

Hoelsch, Kathrin, et al. "Engineering of formate dehydrogenase: synergistic effect of mutations affecting cofactor specificity and chemical stability." Applied microbiology and biotechnology 97.6 (2013): 2473-2481. https://doi.org/10.1007/s00253-012-4142-9

Horowitz, Cara A. "Paris agreement." International Legal Materials 55.4 (2016): 740-755. https://doi.org/10.1017/S0020782900004253

Huber, Harald, et al. "A dicarboxylate/4-hydroxybutyrate autotrophic carbon assimilation cycle in the hyperthermophilic Archaeum *Ignicoccus hospitalis*." Proceedings of the National Academy of Sciences 105.22 (2008): 7851-7856. https://doi.org/10.1073/pnas.0801043105

Hügler, Michael, et al. "Malonyl-coenzyme A reductase from *Chloroflexus aurantiacus*, a key enzyme of the 3-hydroxypropionate cycle for autotrophic CO2 fixation." Journal of bacteriology 184.9 (2002): 2404-2410. https://doi.org/10.1128/JB.184.9.2404-2410.2002

Hügler, Michael, et al. "Evidence for autotrophic CO_2 fixation via the reductive tricarboxylic acid cycle by members of the ε subdivision of *proteobacteria*." Journal of bacteriology 187.9 (2005): 3020-3027. https://doi.org/10.1128/JB.187.9.3020-3027.2005

Jez, Joseph M., and Rebecca E. Cahoon. "Kinetic mechanism of glutathione synthetase from *Arabidopsis thaliana*." Journal of Biological Chemistry 279.41 (2004): 42726-42731. https://doi.org/10.1074/jbc.M407961200

Kanehisa, Minoru, and Susumu Goto. "KEGG: kyoto encyclopedia of genes and genomes." Nucleic acids research 28.1 (2000): 27-30. https://doi.org/10.1093/nar/28.1.27

Kaushika, N. D., K. S. Reddy, and Kshitij Kaushik. "Earth's planetary temperature." Sustainable Energy and the Environment: A Clean Technology Approach. Springer, Cham, 2016. 31-42. https://doi.org/10.1007/978-3-319-29446-9_3

Kim, Hyeonjun, et al. "Characterization of ATPase activity of free and immobilized chromatophore membrane vesicles of *Rhodobacter sphaeroides*." Journal of microbiology and biotechnology 27.12 (2017): 2173-2179. https://doi.org/10.4014/jmb.1708.08068

Kim, J. J., Ming Wang, and Rosemary Paschke. "Crystal structures of medium-chain acyl-CoA dehydrogenase from pig liver mitochondria with and without substrate." Proceedings of the National Academy of Sciences 90.16 (1993): 7523-7527. https://doi.org/10.1073/pnas.90.16.7523

Kishimoto, Asako, et al. "Crystal structure of phosphopantothenate synthetase from *Thermococcus kodakarensis*." Proteins: Structure, Function, and Bioinformatics 82.9 (2014): 1924-1936. https://doi.org/10.1002/prot.24546

Kita, K., et al. "One-step purification from Escherichia coli of complex II (succinate: ubiquinone oxidoreductase) associated with succinate-reducible cytochrome b556." Journal of Biological Chemistry 264.5 (1989): 2672-2677. https://www.ncbi.nlm.nih.gov/pubmed/2644269

Kitagawa, Masanari, et al. "Complete set of ORF clones of *Escherichia coli* ASKA library (A Complete S et of E. coli K-12 ORF A rchive): Unique Resources for Biological Research." DNA research 12.5 (2005): 291-299. https://doi.org/10.1093/dnares/dsi012

Kockelkorn, Daniel, and Georg Fuchs. "Malonic semialdehyde reductase, succinic semialdehyde reductase, and succinyl-coenzyme A reductase from *Metallosphaera sedula*: enzymes of the autotrophic 3-hydroxypropionate/4-hydroxybutyrate cycle in Sulfolobales." Journal of bacteriology 191.20 (2009): 6352-6362. https://doi.org/10.1128/JB.00794-09

Koetsier, Martijn J., et al. "Aminoacyl-coenzyme A synthesis catalyzed by a CoA ligase from *Penicillium chrysogenum*." FEBS letters 585.6 (2011): 893-898. https://doi.org/10.1016/j.febslet.2011.02.018

Könneke, Martin, et al. "Ammonia-oxidizing archaea use the most energy-efficient aerobic pathway for CO_2 fixation." Proceedings of the National Academy of Sciences 111.22 (2014): 8239-8244. https://doi.org/10.1073/pnas.1402028111

Korotkova, Natalia, et al. "Glyoxylate regeneration pathway in the methylotroph *Methylobacterium extorquens* AM1." Journal of bacteriology 184.6 (2002): 1750-1758. https://doi.org/10.1128/JB.184.6.1750-1758.2002

Kramer, Levi, et al. "Characterization of carboxylic acid reductases for biocatalytic synthesis of industrial chemicals." ChemBioChem 19.13 (2018): 1452-1460. https://doi.org/10.1002/cbic.201800157

Kronen, Miriam, and Ivan A. Berg. "Mesaconase/fumarase FumD in *Escherichia coli* O157: H7 and promiscuity of *Escherichia coli* class I fumarases FumA and FumB." PLoS One 10.12 (2015): e0145098. https://doi.org/10.1371/journal.pone.0145098

Kypke, Kolja L., et al. "Topological climate change with permafrost feedback." Journal of Physics: Conference Series. Vol. 1730. No. 1. IOP Publishing, 2021. Doi:10.1088/1742-6596/1730/1/012090

Lancaster, C. Roy D., et al. "Structure of fumarate reductase from *Wolinella succinogenes* at 2.2 Å resolution." Nature 402.6760 (1999): 377-385. https://doi.org/10.1038/46483

Le Quéré, Corinne, et al. "Fossil CO_2 emissions in the post-COVID-19 era." Nature Climate Change 11.3 (2021): 197-199. https://doi.org/10.1038/s41558-021-01001-0

Leigh, Deborah M., et al. "Estimated six per cent loss of genetic variation in wild populations since the industrial revolution." Evolutionary Applications 12.8 (2019): 1505-1512. https://doi.org/10.1111/eva.12810

Leys, David, et al. "Structure and mechanism of the flavocytochrome c fumarate reductase of *Shewanella putrefaciens* MR-1." Nature structural biology 6.12 (1999): 1113-1117. https://doi.org/10.1038/70051

Li, Rongrong, and Shuyu Li. "Carbon emission post-coronavirus: continual decline or rebound?" Structural Change and Economic Dynamics 57 (2021): 57-67. https://doi.org/10.1016/j.strueco.2021.01.008

Liu, Changshui, et al. "Dissection of malonyl-coenzyme A reductase of *Chloroflexus aurantiacus* results in enzyme activity improvement." PloS one 8.9 (2013): e75554. https://doi.org/10.1371/journal.pone.0075554

Liu, Yinge, et al. "Climate change and its impacts on mountain glaciers during 1960–2017 in western China." Journal of Arid Land 11.4 (2019): 537-550. https://doi.org/10.1007/s40333-019-0025-6

Ljungdhal, L. G. "The autotrophic pathway of acetate synthesis in acetogenic bacteria." Annual Reviews in Microbiology 40.1 (1986): 415-450. https://doi.org/10.1146/annurev.mi.40.100186.002215

Lu, Xinda, Brent J. Seuradge, and Josh D. Neufeld. "Biogeography of soil *Thaumarchaeota* in relation to soil depth and land usage." FEMS microbiology ecology 93.2 (2017): fiw246. https://doi.org/10.1093/femsec/fiw246

Luo, Shanshan, et al. "A cell-free self-replenishing CO_2-fixing system." Nature Catalysis 5.2 (2022): 154-162. https://doi.org/10.1038/s41929-022-00746-x

Mahlstein, Irina, and Reto Knutti. "Ocean heat transport as a cause for model uncertainty in projected Arctic warming." Journal of Climate 24.5 (2011): 1451-1460. https://doi.org/10.1175/2010JCLI3713.1

Marbaix, Alexandre Y., et al. "Extremely conserved ATP-or ADP-dependent enzymatic system for nicotinamide nucleotide repair." Journal of Biological Chemistry 286.48 (2011): 41246-41252. https://doi.org/10.1074/jbc.C111.310847

Mauna Loa Global Monitoring Laboratory. Trends in Atmospheric Carbon Dioxide. April, 2022. https://gml.noaa.gov/ccgg/trends/mlo.html

Mordhorst, Silja, et al. "Several Polyphosphate Kinase 2 Enzymes Catalyse the Production of Adenosine 5'-Polyphosphates." ChemBioChem 20.8 (2019): 1019-1022. https://doi.org/10.1002/cbic.201800704

Mordhorst, Silja, and Jennifer N. Andexer. "Round, round we go–strategies for enzymatic cofactor regeneration." Natural Product Reports 37.10 (2020): 1316-1333. Doi: 10.1039/D0NP00004C

Muchowska, Kamila B., Sreejith J. Varma, and Joseph Moran. "Nonenzymatic metabolic reactions and life's origins." Chemical Reviews 120.15 (2020): 7708-7744. https://doi.org/10.1021/acs.chemrev.0c00191

Mullins, Elwood A., and T. Joseph Kappock. "Crystal structures of *Acetobacter aceti* succinyl-coenzyme A (CoA): acetate CoA-transferase reveal specificity determinants and illustrate the mechanism used by class I CoA-transferases." Biochemistry 51.42 (2012): 8422-8434. https://doi.org/10.1021/bi300957f

Nerem, R. S., and Beckley BD. "Fasullo JT, Hamlington BD, Masters D. and Mitchum GT." Climate-change–driven accelerated sea-level rise detected in the altimeter era. Proc. National Academy of Science USA 115 (2018): 2022-2025. https://doi.org/10.1073/pnas.1717312115

Padovani, Dominique, and Ruma Banerjee. "Assembly and protection of the radical enzyme, methylmalonyl-CoA mutase, by its chaperone." Biochemistry 45.30 (2006): 9300-9306. https://doi.org/10.1021/bi0604532

Pagani, Mark, et al. "High Earth-system climate sensitivity determined from Pliocene carbon dioxide concentrations." Nature Geoscience 3.1 (2010): 27-30. https://doi.org/10.1038/ngeo724

Perret, Alain, et al. "A novel acyl-CoA beta-transaminase characterized from a metagenome." PLoS One 6.8 (2011): e22918. https://doi.org/10.1371/journal.pone.0022918

Peter, Dominik M., et al. "Screening and engineering the synthetic potential of carboxylating reductases from central metabolism and polyketide biosynthesis." Angewandte Chemie International Edition 54.45 (2015): 13457-13461. https://doi.org/10.1002/anie.201505282

Peter, Dominik M., et al. "A chemo-enzymatic road map to the synthesis of CoA esters." Molecules 21.4 (2016): 517. https://doi.org/10.3390/molecules21040517

Plaitakis, Andreas, et al. "The glutamate dehydrogenase pathway and its roles in cell and tissue biology in health and disease." Biology 6.1 (2017): 11. https://doi.org/10.3390/biology6010011

Ploux, Olivier, Satoru Masamune, and Christopher T. Walsh. "The NADPH-linked acetoacetyl-CoA reductase from *Zoogloea ramigera*: Characterization and mechanistic studies of the cloned enzyme over-produced in *Escherichia coli*." European journal of biochemistry 174.1 (1988): 177-182. https://doi.org/10.1111/j.1432-1033.1988.tb14079.x

Ogita, Takeshi, and Jeremy R. Knowles. "On the intermediacy of carboxyphosphate in biotin-dependent carboxylations." Biochemistry 27.21 (1988): 8028-8033. Doi: 10.1021/bi00421a009

Riihelä, Aku, Ryan M. Bright, and Kati Anttila. "Recent strengthening of snow and ice albedo feedback driven by Antarctic sea-ice loss." Nature Geoscience 14.11 (2021): 832-836. https://doi.org/10.1038/s41561-021-00841-x

Ruetz, Markus, et al. "Itaconyl-CoA forms a stable biradical in methylmalonyl-CoA mutase and derails its activity and repair." Science 366.6465 (2019): 589-593. Doi: 10.1126/science.aay0934

Richardt, Arnd, et al. "Ebony, a novel nonribosomal peptide synthetase for β-alanine conjugation with biogenic amines in *Drosophila*." Journal of Biological Chemistry 278.42 (2003): 41160-41166. doi.org/10.1074/jbc.M304303200

Scheffen, Marieke, et al. "A new-to-nature carboxylation module to improve natural and synthetic CO_2 fixation." Nature Catalysis 4.2 (2021): 105-115. https://doi.org/10.1038/s41929-020-00557-y

Schousboe, A. W. J. Y., J. Y. Wu, and E. Roberts. "Purification and characterization of the 4-aminobutyrate-2-ketoglutarate transaminase from mouse brain." Biochemistry 12.15 (1973): 2868-2873.

Schwander, Thomas, et al. "A synthetic pathway for the fixation of carbon dioxide in vitro." Science 354.6314 (2016): 900-904. doi: 10.1126/science.aah5237

Schwander, Thomas. The design and realization of synthetic pathways for the fixation of carbon dioxide in vitro. Diss. Philipps-Universität Marburg, (2018a). https://doi.org/10.17192/z2018.0066

Schwander, Thomas, et al. "Structural basis for substrate specificity of methylsuccinyl-CoA dehydrogenase, an unusual member of the acyl-CoA dehydrogenase family." Journal of Biological Chemistry 293.5 (2018b): 1702-1712. https://doi.org/10.1074/jbc.RA117.000764

Sévin, Daniel C., et al. "Nontargeted in vitro metabolomics for high-throughput identification of novel enzymes in *Escherichia coli*." Nature methods 14.2 (2017): 187-194. https://doi.org/10.1038/nmeth.4103

Shaw, L., and Paul C. Engel. "The suicide inactivation of ox liver short-chain acyl-CoA dehydrogenase by propionyl-CoA. Formation of an FAD adduct." Biochemical Journal 230.3 (1985): 723-731. https://doi.org/10.1136/bmj.290.6484.1771

Sherwood, Steven C., Vishal Dixit, and Chryséis Salomez. "The global warming potential of near-surface emitted water vapour." Environmental Research Letters 13.10 (2018): 104006. http://dx.doi.org/10.1088/1748-9326/aae018

Shimomura, Yoshiharu, et al. "Purification and partial characterization of 3-hydroxyisobutyryl-coenzyme A hydrolase of rat liver." Journal of Biological Chemistry 269.19 (1994): 14248-14253. https://doi.org/10.1016/S0021-9258(17)36781-9

Sievers, Fabian, et al. "Fast, scalable generation of high-quality protein multiple sequence alignments using Clustal Omega." Molecular systems biology 7.1 (2011): 539. https://doi.org/10.1038/msb.2011.75

Simpson, J. "The interaction of dithiothreitol and acetyl coenzyme A in a radiochemical assay for rat brain ATP: citrate oxaloacetate lyase." Journal of Neurochemistry 37.1 (1981): 100-106. https://doi.org/10.1111/j.1471-4159.1981.tb05296.x

Song, Yoseb, et al. "Functional cooperation of the glycine synthase-reductase and Wood–Ljungdahl pathways for autotrophic growth of *Clostridium drakei*." Proceedings of the National Academy of Sciences 117.13 (2020): 7516-7523. https://doi.org/10.1073/pnas.1912289117

Takahashi-Íñiguez, Tóshiko, et al. "Protection and reactivation of human methylmalonyl-CoA mutase by MMAA protein." Biochemical and biophysical research communications 404.1 (2011): 443-447. https://doi.org/10.1016/j.bbrc.2010.11.141

Takahashi-Iñiguez, Tóshiko, et al. "Role of vitamin B_{12} on methylmalonyl-CoA mutase activity." Journal of Zhejiang University Science B 13.6 (2012): 423-437. https://doi.org/10.1631/jzus.B1100329

Tamiya, H., and H. Huzisige. "Effect of oxygen on the dark reaction of photosynthesis." Acta Phytochim 15 (1949): 83-104.

Thomä, Nicolas H., Philip R. Evans, and Peter F. Leadlay. "Protection of radical intermediates at the active site of adenosylcobalamin-dependent methylmalonyl-CoA mutase." Biochemistry 39.31 (2000): 9213-9221.

Tong, L. "Acetyl-coenzyme A carboxylase: crucial metabolic enzyme and attractive target for drug discovery." Cellular and Molecular Life Sciences CMLS 62.16 (2005): 1784-1803. https://doi.org/10.1007/s00018-005-5121-4

Tong, Liang. "Structure and function of biotin-dependent carboxylases." Cellular and Molecular Life Sciences 70.5 (2013): 863-891. https://doi.org/10.1007/s00018-012-1096-0

Usselman, Robert J., et al. "Impact of mutations on the midpoint potential of the [4Fe-4S]+ 1,+ 2 cluster and on catalytic activity in electron transfer flavoprotein-ubiquinone oxidoreductase (ETF-QO)." Biochemistry 47.1 (2008): 92-100. https://doi.org/10.1021/bi701859s

Wadler, Caryn, and John E. Cronan. "Dephospho-CoA kinase provides a rapid and sensitive radiochemical assay for coenzyme A and its thioesters." Analytical biochemistry 368.1 (2007): 17-23. https://doi.org/10.1016/j.ab.2007.05.031

Wagner, Gregory R., et al. "A class of reactive acyl-CoA species reveals the non-enzymatic origins of protein acylation." Cell metabolism 25.4 (2017): 823-837. https://doi.org/10.1016/j.cmet.2017.03.006

Walker, John M., ed. The proteomics protocols handbook. Humana press, 2005. https://doi.org/10.1385/1592598900

Wan, Fen, et al. "Oxidized OxyR up-regulates ahpCF expression to suppress plating defects of oxyR-and catalase-deficient strains." Frontiers in microbiology 10 (2019): 439. https://doi.org/10.3389/fmicb.2019.00439

Webb, Michael E., and Alison G. Smith. "Pantothenate biosynthesis in higher plants." Advances in botanical research. Vol. 58. Academic Press, 2011. 203-255. https://doi.org/10.1016/B978-0-12-386479-6.00001-9

Westin, Maria AK, Mary C. Hunt, and Stefan EH Alexson. "The identification of a succinyl-CoA thioesterase suggests a novel pathway for succinate production in peroxisomes." Journal of Biological Chemistry 280.46 (2005): 38125-38132. https://doi.org/10.1074/jbc.M508479200

Xu, Zhinan, et al. "High-level expression of recombinant glucose dehydrogenase and its application in NADPH regeneration." Journal of Industrial Microbiology and Biotechnology 34.1 (2007): 83-90. https://doi.org/10.1007/s10295-006-0168-2

Yonaha, Kazuo, Seizen Toyama, and Kenji Soda. "[20] Taurine-glutamate transaminase." Methods in Enzymology. Vol. 113. Academic Press, 1985. 102-108. https://doi.org/10.1016/S0076-6879(85)13023-5

Zarzycki, Jan, et al. "Identifying the missing steps of the autotrophic 3-hydroxypropionate CO2 fixation cycle in *Chloroflexus aurantiacus*." Proceedings of the National Academy of Sciences 106.50 (2009): 21317-21322. https://doi.org/10.1073/pnas.0908356106

Zarzycki, Jan, and Cheryl A. Kerfeld. "The crystal structures of the tri-functional *Chloroflexus aurantiacus* and bi-functional *Rhodobacter sphaeroides* malyl-CoA lyases and comparison with CitE-like superfamily enzymes and malate synthases." BMC structural biology 13.1 (2013): 1-19. https://doi.org/10.1186/1472-6807-13-28

Zeng, Xiaohua, et al. "Proteomic characterization of the *Rhodobacter sphaeroides* 2.4. 1 photosynthetic membrane: identification of new proteins." Journal of bacteriology 189.20 (2007): 7464-7474. https://doi.org/10.1128/JB.00946-07

Zhang, Jianbo, et al. "Creatine Phosphate– Creatine Kinase in Enzymatic Synthesis of Glycoconjugates." Organic Letters 5.15 (2003): 2583-2586. https://doi.org/10.1021/ol034319a

Zhong, Haohui, et al. "Novel insights into the *Thaumarchaeota* in the deepest oceans: their metabolism and potential adaptation mechanisms." Microbiome 8.1 (2020): 1-16. https://doi.org/10.1186/s40168-020-00849-2

Zhongming, Zhu, et al. "The Emissions Gap Report 2021." (2021).

Acknowledgements

First and foremost, I would like to thank my supervisor Prof. Tobias Erb for hosting me in his lab. For a project that could have progressed down countless different avenues, he granted me a great deal of freedom to explore what this cycle can be. As a result, I feel that I've learned not only a lot about the subject at hand, but also a lot about how to design and pursue different lines of experimentation, and maybe most importantly, when to change approaches if something isn't working.

I would like to thank my thesis advisory committee members, Prof. Gert Bange and Prof. Hannes Link for their insights and advice throughout my degree. Also, my examination committee members, Prof. Lennart Randau, Prof. Lars-Oliver Essen, and Prof. Martin Thanbichler for their time and expertise in critiquing my thesis.

A special thanks goes to Thomi Schwander for laying the groundwork for this project, helping me get my head around its scope, and settling me into the lab.

I am continually impressed by the breadth and depth of the knowledge in the lab, whenever I hit a dead end, there was someone with a strange new perspective to get me moving again. Thanks to Basti, Gabo, and Simon for useful insights after every presentation. Iria for her acrylyl-CoA as well as her help with Pcs. Marieke and Martina for their help with acyl-CoA synthetases and glyoxylate reductase. Lenny for his help with the β-hydroxyaspartate cycle. Alberto for his help planning future in vivo ventures. The entire in vitro subgroup for advice along the way, especially Chris for thoughtful conversations and commiserations. I'd also like to thank Dr. Timo Glatter and Witek for help with proteomic analysis as well as Kookie, Nicole, and Peter for running many thousands of samples through Heidi and Emmma, making this project possible. Finally, a big thanks to Jan for cracking the Mcd structure and useful insights along the way.

Last but not least, I'd like to thank my family. My parents, for their support and continued interest. Sutherland, for her endless support, keeping me on the rails, and picking up all of my slack during the late nights and early mornings, the last couple years have been crazy, and I couldn't have done it without you. Finally, to Liam and Finn, whose tiny hugs and giant smiles can remedy even the worst days in the lab.

Curriculum Vitae